

Copyright © 1989, by the author(s).  
All rights reserved.

Permission to make digital or hard copies of all or part of this work for personal or classroom use is granted without fee provided that copies are not made or distributed for profit or commercial advantage and that copies bear this notice and the full citation on the first page. To copy otherwise, to republish, to post on servers or to redistribute to lists, requires prior specific permission.

**KINEMATICS, PLANNING AND CONTROL  
OF DEXTROUS ROBOT HANDS**

by

Zexiang Li

Memorandum No. UCB/ERL M89/127

29 November 1989

COVER PAGE

**KINEMATICS, PLANNING AND CONTROL  
OF DEXTROUS ROBOT HANDS**

by

Zexiang Li

Memorandum No. UCB/ERL M89/127

29 November 1989

**ELECTRONICS RESEARCH LABORATORY**

College of Engineering  
University of California, Berkeley  
94720

TITLE PAGE

**KINEMATICS, PLANNING AND CONTROL  
OF DEXTROUS ROBOT HANDS**

by

Zexiang Li

Memorandum No. UCB/ERL M89/127

29 November 1989

**ELECTRONICS RESEARCH LABORATORY**

College of Engineering  
University of California, Berkeley  
94720

# Kinematics, Planning and Control of Dextrous Robot Hands

By  
Zexiang Li

---

Shankar Sastry  
Chairman

## ABSTRACT

An industrial manipulator we found today has a simple parallel-jaw gripper for interacting with the workpiece or the environment. Since the gripper can not impart small motions to the grasped object, tasks that can be executed are rather limited. This motivates a strong need for more flexible, versatile and multifingered robot hands.

In this dissertation, we use geometrical tools to formulate, analyze and solve problems related to the kinematics, planning and control of a dextrous robot hand.

Starting with a review of rigid body motions in  $\mathbf{R}^3$ , the basic velocity and force transformation relations under changes of coordinate frames are developed. Then, this dissertation uses the exponential notation to derive the forward kinematic map and the manipulator Jacobian. The results are then applied to derive the equations of motion of a manipulator in both the Newton-Euler formulation and the Lagrangian formulation.

The geometry of a surface, including the metric tensor, curvature form and connection form, is studied. These concepts are crucial to the development of contact equations for motion of two rigid bodies under contact. Three basic kinematic relations, *the kinematics of contact*, *the grip Jacobian* and *the hand Jacobian*, underlying a robot hand system are carefully examined and formulated. The operation of a robot hand system in terms of these kinematic relations is explained.

Two fundamental planning problems associated with task planning for a robot hand system, *grasp planning*, *motion planning for dextrous manipulation*,

are examined. It is argued that task requirement should be the primary consideration in grasp selection. Two grasp quality measures that incorporate the task models are proposed and a performance measure that balances the two is used as the objective function for optimization. The problem of dextrous manipulation is defined. This hopefully will set up the framework for future research in this area. To gain further insight of this problem, motion of two rigid bodies under rolling constraint is studied. First, the differential equations for rolling motion are derived using the contact equations. Then, Chow's theorem is invoked to determine the existence of motion between two contact configurations. Finally, the Gauss-Bonnet theorem is used to solve the path finding problem.

Two manipulation modes of a robot hand system are defined. Then, starting with a review of control strategies for a manipulator, a basic control scheme for coordinated manipulation by a robot hand system is presented. The scheme is then extended to robot hand system with redundant degrees of freedom and to rolling motion. Simulation results based on a two-fingered robot hand system are shown.

# Acknowledgement

Throughout my graduate studies at Berkeley, my research advisor, Professor Shankar Sastry has been a constant source of support, guidance and encouragement. He got me interested in control and then in robotics. He has also created an environment which I can freely work on many diversified problems. His broad knowledge and deep insight are of great importance to my research.

I am grateful to members of my qualifying committee, Professor Charles A. Desoer, Professor Masayoshi Tomizuka and Professor Lotfi A. Zadeh, and to Professor Felix Wu and Professor Jerry Marsden. The advices Professor Felix Wu offered to me during the first week of my graduate study have proven to be very valuable.

I would like to thank three friends here: Richard Montgomery, John Canny and Ronald Fearing. Professor Richard Montgomery from the Mathematics Department has been an inspiration to me, Professor John F. Canny has offered me many helps in sorting out confusing problems. It is also a great pleasure to share with Professor Ronald Fearing many interesting ideas regarding robot hands. (Ron, let's go to play badminton today!) I wish them good luck on their career.

I would like to thank Professor Marc Raibert from the Artificial Intelligence Laboratory, MIT, for offering me several opportunities to work in his laboratory. His deep insight into engineering problems has been an inspiration to me. I would also like to thank members of the Leg Laboratory at MIT for their friendship.

I have benefitted greatly from interactions with many friends and colleagues here at Berkeley. To name just a few, Er-Wei Bai, Li-Chen Fu, Ping Hsu, Yuxi Zheng, Andy Packard, Jeff Mason, John Hauser, Arlene Cole, A.K. Pradeep, Brad Paden, Richard Murray, Greg Heinzinger, Paul Jacobs, Dinesh Monocha, Saman Behtash, Niklas Nordstrom, Kris Pister, Matt Berkemeier, Raja Kadiyala and Curt Deno. I also like to thank Dr. Yu Wang and Professor Matt Mason from the Robotics Institute, CMU, for their friendship.

As one of the first undergraduate students coming from P.R. China to study in the U.S.A., I have been in this country for exactly 10 years. Over this long period of time,

I have received help and support from many people. First, The Alumnum Company of America (ALCOA) and the people of ALCOA, especially Mr. C.T. Young, Mr and Mrs G. Bates and Ms. C. Max, have helped me going through my undergraduate study at Carnegie-Mellon University. I would like to acknowledge the generous fellowship (1979-1983) from the ALCOA Foundation.

My graduate work has been funded in part by the National Science Foundation under grant DMC-8451129.

Dr. Michael Dunn and Dr. Joanne Dunn have always treated me like a member of their family. They have offered me what a family has to offer to its children. (Thanks, Joanne!)

I would like to express my deepest love and gratitude to Jiang Hua Lu. Her unfailing support and understanding through these years have been a source of great strength. I would like to dedicate this dissertation to my mother, Jiang Hua Lu, my brothers and my sister.

# Contents

<b>Table of Contents</b>	<b>vii</b>
<b>List of Figures</b>	<b>ix</b>
<b>1 Introduction</b>	<b>1</b>
1.1 Why Study Robot Hands . . . . .	1
1.2 Previous Work . . . . .	3
1.3 Preview . . . . .	4
<b>2 Manipulator Kinematics and Dynamics</b>	<b>8</b>
2.1 Introduction . . . . .	8
2.2 Rigid Motions . . . . .	9
2.3 Manipulator Kinematics . . . . .	17
2.4 Manipulator Dynamics . . . . .	24
2.4.1 Rigid Body Dynamics and Static Force Transformation . . . . .	25
2.4.2 Newton-Euler Formulation . . . . .	27
2.4.3 Lagrangian Formulation . . . . .	31
2.5 Conclusion . . . . .	34
<b>3 Robot Hand Kinematics</b>	<b>38</b>
3.1 Introduction . . . . .	38
3.2 The Geometry of a Surface . . . . .	40
3.3 The Kinematics of Contact . . . . .	46
3.4 The Kinematics of a Robot Hand System . . . . .	52
3.5 Conclusion . . . . .	63
<b>4 Planning</b>	<b>67</b>
4.1 Introduction . . . . .	67
4.2 Grasp Planning . . . . .	70
4.2.1 Task Modeling . . . . .	72
4.2.2 Structured Quality Measures for Grasp Planning . . . . .	77
4.3 What Is Dextrous Manipulation? . . . . .	82
4.4 Motion Planning with Nonholonomic Constraint . . . . .	86
4.4.1 Existence of Motion . . . . .	88

4.4.2	A Path Planning Algorithm . . . . .	95
4.5	Conclusion . . . . .	101
<b>5</b>	<b>Coordinated Control of Robot Hands</b>	<b>106</b>
5.1	Introduction . . . . .	106
5.2	Control of Robot Manipulators: A Review . . . . .	107
5.2.1	Computed Torque Method . . . . .	108
5.2.2	Cartesian Space Control . . . . .	110
5.3	Control Algorithms for Coordinated Manipulation by Robot Hands .	111
5.3.1	Control Laws for Coordinated Manipulation . . . . .	113
5.3.2	Control Laws for Rolling Motion . . . . .	120
5.3.3	Simulation . . . . .	122
5.4	Conclusion . . . . .	124
<b>6</b>	<b>Conclusions</b>	<b>129</b>
6.1	Review . . . . .	129
6.2	Future Work . . . . .	131

# List of Figures

2.1	Motion of a rigid body about a fixed point “o” . . . . .	11
2.2	Motion of a free rigid body . . . . .	13
2.3	Velocity transformation under change of coordinate . . . . .	15
2.4	(a) A one-link manipulator with revolute joint, (b) a one-link manipulator with prismatic joint. . . . .	19
2.5	A planar manipulator of three-degrees of freedom. . . . .	22
2.6	Motion of a free rigid body. . . . .	26
2.7	A 3R manipulator. . . . .	26
3.1	(a) A sphere of radius $\rho$ , (b) A football. . . . .	41
3.2	Holonomy angle of a closed path in $S$ . . . . .	45
3.3	Showing the definitions of the coordinate frames of two bodies in contact . . . . .	48
3.4	Motion of a unit ball over the plane. . . . .	51
3.5	A unit disk on the plane. . . . .	52
3.6	A hand manipulation system . . . . .	54
3.7	Force/velocity transformation for a robot hand system. . . . .	60
3.8	(a) A stable but not manipulable grasp, (b) a manipulable but not stable grasp. . . . .	63
4.1	A flow diagram for task execution by a robot hand . . . . .	69
4.2	Peg-in-hole task . . . . .	73
4.3	A scribing task . . . . .	74
4.4	A geometrical interpretation of $\mu_t(\Omega)$ . . . . .	77
4.5	A geometrical interpretation of $\mu_w(\Omega)$ . . . . .	78
4.6	Planar peg-in-hole task . . . . .	80
4.7	Performance measure, grasp quality measures versus $\theta_{11}$ . . . . .	82
4.8	A robot hand system . . . . .	83
4.9	A global view of dextrous manipulation . . . . .	85
4.10	Motion of an object with rolling constraints . . . . .	87
4.11	An interpretation of $[X_1, X_2]$ . . . . .	90
4.12	Motion of a unit ball over another ball . . . . .	92
4.13	A Lie bracket motion . . . . .	98
4.14	A (general) Lie bracket motion . . . . .	100

4.15	Another Lie bracket motion . . . . .	101
5.1	A block diagram of the computed torque method . . . . .	109
5.2	A block diagram of the Cartesian space control . . . . .	111
5.3	A robot hand system . . . . .	112
5.4	A two-fingered planar manipulation system . . . . .	123
5.5	Position error from simulation . . . . .	124
5.6	Simulation without internal grasping force . . . . .	125
5.7	Simulation with 10 units of internal grasping force . . . . .	125

# Chapter 1

## Introduction

### 1.1 Why Study Robot Hands

The *need for a more flexible manufacturing system* has been the driving force for the rapid development in robotics over the last three decades. The first industrial robot was introduced by Unimation Inc. in 1959. The key to this device was the use of a computer in conjunction with a manipulator to produce a machine that could be “taught” to carry out a variety of tasks automatically. To enhance the flexibility of these machines, sensory feedbacks, such as tactile, vision and force, were added in the 60’s and 70’s. At Stanford, Bolles and Paul ([BP73]) using both visual and force feedback, demonstrated a computer-controlled Stanford arm connected to a PDP-10 computer for assembling automotive water pumps. At the Drapper Laboratory Nevins et al ([NW74]) investigated sensing technologies based on compliance. This work developed into the instrumentation of a passive compliance device called *remote center of compliance* (RCC) which was attached to the mounting plate of the last joint of the manipulator for close parts-mating assembly. In 1988, Adept Inc. introduced a force-controlled industrial robot, which used direct-drive technology developed by H. Asada ([AY87]).

An industrial manipulator we found today has a simple parallel-jaw gripper (or end-effector) at the end for interacting with the environment. As a typical scenario when it performs a task, the gripper will first grasp the object and then the entire arm will move to achieve a desired motion of the object. Since the gripper can not impart small motions on the grasped object, tasks that can be executed

by an ordinary manipulator are very coarse, e.g., pick-and-place operations, spray paintings. To execute more sophisticated tasks such as scribing with a grasped pen, bolting a nut onto a screw, where small motions of the object are required, there is a strong need for a more flexible, versatile and multifingered robot hand (or dextrous robot hand).

The added functionality of a dextrous robot hand includes:

- The potential for increasing the number of contact points with the object, thereby yielding a more stable grasp. In addition, the ability to reach a wide range of grasp configurations will allow more types of objects to be grasped than with the simple gripper.
- The ability to adjust grasp configurations within the hand. This enables a task to be executed with some of the most efficient grasp configurations.
- The ability to impart displacements and large changes of orientation of the grasped objects. Observation of the human hand reveals that almost all manipulation of small objects is done entirely within the hand. In some cases, obstacles in the environment prevent the whole arm from moving along with the object, whereas fingers can reach into more restrictive environments to perform tasks arms can not reach.
- A potential for high fidelity control. A dextrous robot hand considered as a micro-manipulation system has high bandwidth while an arm, considered as a macro-manipulation system, has large workspace. A robot hand augmented with a proper manipulator can achieve high bandwidth while retaining large workspace.
- The ability to sense information about the environment. Hands equipped with tactile sensors or force sensors have the potential for locating and identifying parts. The information obtained can be used for guiding the operation of the hand or for modeling the world for autonomous manipulation systems.

All of these capabilities of a dextrous robot hand will be necessary for extending the classes of tasks possible with autonomous manipulation systems.

## 1.2 Previous Work

The last decade has seen a rapid growth of research activities in both mechanical design of robot hands and determining how to use the vast amount of flexibility resulting from the relatively simple structure of the hand.

Okada ([Oka79]), intending to emulate human functions, designed a three-fingered hand, with eleven joints, controlled by computers. Salisbury ([MS85]) designed a hand that has a thumb with two joints and two fingers with three joints each. Starting from contact models and kinematic analysis, Salisbury proposed a control algorithm, now known as Stiffness Control, for imparting motion to grasped objects. One of the most mechanically sophisticated hands, the Utah/MIT hand, was developed at University of Utah ([JWBI86]). The computer architecture multiprocessor serving the Utah/MIT hand was developed at MIT ([Nar88]). The Utah/MIT hand has four fingers with four joints each, and is pneumatically driven.

J. Kerr ([Ker85]) formally extended some of Salisbury's work identifying special grasp configurations with linear algebra. He also investigated the kinematic relations and the use of internal grasp force for fine motion control. A chapter of his thesis is devoted to hand workspace. J. Trinkle ([Tri87], M. Cutkosky ([Cut86]), V. Nguyen ([Ngu86]) and H. Hanafusa and H. Asada ([HA77]) have done works in grasp planning and fine motion manipulation.

D. Montana ([Mon86]) and Cai and Roth ([CR87]) studied the kinematics of contact between two rigid objects. They established similar sets of equations, called the contact equations, that govern motion of the contact points in response to relative motion of these objects.

P. Hsu ([Hsu88]), Nakamura et al ([NNY87]) and Zheng and Luh ([ZL85]) have studied control strategies for coordinated manipulation by multiple-robotic systems, which can be treated in the same framework as for robot hand system.

R. Fearing ([Fea87]) developed a robot finger mounted with tactile sensors.

The main deficiency with work in the field of hands is the lack of a unifying approach to the analysis and design of hands. There is very little work on the analysis of hands in general, or methodologies of design driven by some desired functionalities. This thesis endeavors to develop general methodologies applicable to a wide variety of hands.

## 1.3 Preview

This thesis covers three different topics relating to the analysis and operation of dextrous robot hands. They are kinematics, planning and coordinated control. The following is a summary of the contents of each chapter.

**Chapter 2 - Manipulator Kinematics and Dynamics.** This chapter starts with a review of rigid motions in  $\mathbb{R}^3$ . It develops basic transformation relations for velocity and force under change of coordinate frames. Then, it studies manipulator kinematics using the exponential notation. The results are then used to derive the equations of motion for a manipulator in both the Newton-Euler formulation and the Lagrangian formulation.

**Chapter 3 - Robot Hand Kinematics.** The geometry of a surface, including the metric tensor, curvature form and connection form, is studied. These concepts are then used to develop the contact equations for motion of two rigid bodies under contact. This is a summary of Montana's work on the kinematics of contact. Finally, the three basic kinematics relations in a robot hand system are formulated and then tabulated. The operation of a robot hand system using these kinematics relations is explained.

**Chapter 4 - Planning.** Two fundamental planning problems associated with task planning for a robot hand system, *grasp planning*, *motion planning for dextrous manipulation*, are examined. It is argued that task requirement should be the primary consideration in grasp selection. Two grasp quality measures that incorporate the task models are proposed and a performance measure that balances the two is used as the objective function for optimization. The problem of dextrous manipulation is defined. This hopefully will set up the framework for future research in this area. To gain further insight of this problem, motion of two rigid bodies under rolling constraint is studied. First, the differential equations for rolling motion are derived using the contact equations of Chapter 3. Then, Chow's theorem is invoked to determine the existence of motion between two contact configurations. Finally, the Gauss-Bonnet theorem is used to solve the path finding problem.

**Chapter 5 - Coordinated Control for Robot Hands.** Two manipulation modes of a robot hand system are defined. Then, starting with a review of control strategies for a manipulator, a basic control scheme for coordinated manipulation by a robot

hand system is presented. The scheme is then extended to robot hand system with redundant degrees of freedom and to rolling motion. Simulation results based on a two-fingered robot hand system are shown.

**Chapter 6 - Conclusion.** The entire thesis is reviewed and the major conclusions are presented. Limitations in this work, and areas for future work are discussed.

# Bibliography

- [AY87] H. Asada and K. Youcef-Toumi. *Direct Drive Robots: Theory and Practice*. MIT Press, 1987.
- [BP73] R. Bolles and R. Paul. *An Experimental System for Computer Controlled Mechanical Assembly*. Technical Report, Stanford Artificial Intelligence Laboratory Memo. AIM-220, Stanford University, 1973.
- [CR87] C. Cai and B. Roth. On the spatial motion of rigid bodies with point contact. In *IEEE International Conference on Robotics and Automation*, pages 686–695, 1987.
- [Cut86] M. Cutkosky. *Grasping and Fine Manipulation for Automated Manufacturing*. Kulware-Acadmeic Publisher, 1986.
- [Fea87] R. Fearing. *Tactile sensing, perception and shape interpretation*. PhD thesis, Electrical Engineering Department, Stanford University, 1987.
- [HA77] H. Hanafusa and H. Asada. *Stable prehension by a robot hand with elastic fingers*, chapter 5. *Robot Motion: Planning and Control*, MIT Press, 1977.
- [Hsu88] P. Hsu. *Control of Mechanical Manipulators*. PhD thesis, EECS Dept, University of California at Berkeley, 1988.
- [JWBI86] S. Jacobsen, J. Wood, K. Bigger, and E. Inversen. The utah/mit hand: works in progress. *International Journal of Robotics Research*, 4(3):221–250, 1986.
- [Ker85] J. Kerr. *An analysis of multifingered hand*. PhD thesis, Department of Mechanical Engineering, Stanford University, 1985.

- [Mon86] D. Montana. *Tactile sensing and kinematics of contact*. PhD thesis, Division of Applied Sciences, Harvard University, 1986.
- [MS85] M.T. Mason and J. K. Salisbury. *Robot Hands and the Mechanics of Manipulation*, chapter 1 - 10. MIT Press, 1985.
- [Nar88] S. Narasimhan. *Dexterous Robotic Hands: Kinematics and Control*. Technical Report, MIT Artificial Intelligence Laboratory, MIT, 1988.
- [Ngu86] V. Nguyen. *The synthesis of force-closure grasps*. Master's thesis, Department of Electrical Engineering and Computer Science, MIT, 1986.
- [NNY87] Y. Nakamura, K. Nagai, and T. Yoshikawa. Mechanics of coordinative manipulation by multiple robotic mechanisms. In *IEEE International Conference on Robotics and Automation*, pages 991-998, 1987.
- [NW74] J.L. Nevins and D.E. Whitney. *Exploratory Research in Industrial Modular Assembly*. Technical Report, C.C. Draper Laboratory, Cambridge, Mass., 1974.
- [Oka79] T. Okada. Object handling system for manual industry. *IEEE Transactions on System, man and Cybernetics*, SMC 12:289-299, 1979.
- [Tri87] J. Trinkle. *Mechanics and planning of enveloping grasps*. PhD thesis, Department of Computer and Information Science, University of Pennsylvania, 1987.
- [ZL85] Y.F. Zheng and J.Y.S. Luh. Control of two coordinated robots in motion. In *24th Control and Decision Conference*, pages 1761-1766, 1985.

## Chapter 2

# Manipulator Kinematics and Dynamics

### 2.1 Introduction

A robotic hand consists of a number of fingers which are open kinematic chains, or manipulators. Manipulator kinematics is the subject that studies motion of the manipulator without regard to the forces which cause it. The relationships between the motions of a manipulator and the forces and torques which cause them are subjects of manipulator dynamics.

This chapter reviews some of the fundamental concepts concerning manipulator kinematics and manipulator dynamics. The two goals which we want to achieve here are:

1. To provide a rigorous and yet concise treatment of these familiar and extensively studied subjects using geometric tools. The payoffs of undergoing this rigor are: (a) A better physical insight in the derivation procedures. (b) The results can be presented in a more compact and a more comprehensible form.
2. To introduce notation and preliminary concepts needed for the thesis.

#### Rigid Motions of $\mathbb{R}^3$

A common way to represent the motion of a workpiece, or the end-effector of a manipulator, is to affix a Cartesian frame to the object. This enables us to

identify the configuration space of the object with the group of Euclidean ( or rigid ) motions of  $\mathbb{R}^3$ , which is a well-known example of a Lie group - a topological group with added differentiable structures. Consequently, a trajectory of the object can be represented by a curve in the Euclidean group and we study motion of the object by studying flows on the Euclidean group, ... etc. The reader is referred to [War71], and Chapter 4 of [AM78] for further study of Lie groups and Lie algebra.

## Manipulator Kinematics

An important map in the study of manipulator kinematics is the forward kinematic map. Denavit-Hartenberg notation (see [Cra86]) is one of the traditional approaches of representing this map. More recently, R. Brockett ([Bro83]), uses the exponential mapping on a Lie group to introduce the exponential formula for the forward kinematic map. This notion is further developed by B. Paden ([Pad86]) for the study manipulator singularities and inverse kinematics. The simplicity and the geometric clarity of the exponential formula are explored here using the manipulator Jacobian as an example.

## Manipulator Dynamics

We further apply the exponential formula and the definition of the adjoint map to formulate the recursive Newton-Euler equations of motion for a manipulator. One will find that, the recursive relations for velocity and acceleration are much simpler and more intuitive in the exponential notation than in the Denavit-Hartenberg notation. Furthermore, it is straightforward to calculate the Lagrangian equations of motion for a 3R manipulator in closed-form.

## 2.2 Rigid Motions of $\mathbb{R}^3$

Consider the Euclidean space  $\mathbb{R}^3$  with the usual inner product  $\|\cdot\|$ .

**Definition 2.1** A rigid motion of  $\mathbb{R}^3$  is a map  $\psi : \mathbb{R}^3 \rightarrow \mathbb{R}^3$  such that  $|\psi(x) - \psi(y)| = |x - y|, \forall x, y \in \mathbb{R}^3$ .

**Example 2.1** For  $r \in \mathbb{R}^3$ , define  $\psi : \mathbb{R}^3 \rightarrow \mathbb{R}^3$  by  $\psi(x) = x + r$ . Then,  $\psi$  is a rigid motion, called translation by  $r$ . □

**Example 2.2** Let  $\psi : \mathbb{R}^3 \rightarrow \mathbb{R}^3$  be a linear transformation such that  $|\psi(x)| = |x| \forall x \in \mathbb{R}^3$ . Then,  $\psi$  is a rigid motion because  $|\psi(x) - \psi(y)| = |\psi(x - y)| = |x - y|$ .  $\psi$  is called an orthogonal transformation.  $\square$

Fix a Cartesian frame in  $\mathbb{R}^3$  with the origin at a point "o". Then a point  $x \in \mathbb{R}^3$  can be written as

$$x = \sum x^i e_i, i = 1, \dots, 3,$$

where  $e_i$  is the usual basis and  $x^i$  is the coordinate of  $x$  relative to the basis, or frame. Consequently, an orthogonal transformation can be represented by a 3 by 3 orthogonal matrix of determinant  $\pm 1$ . Denote by  $O(3)$  the group of such matrices and  $SO(3)$  the subgroup of  $O(3)$  whose determinant is +1.  $SO(3)$  is also called the *proper orthogonal group of  $\mathbb{R}^3$* .

The proper orthogonal group  $SO(3)$  has a special physical meaning as revealed by the following example.

**Example 2.3** Consider the motion of a rigid body about a fixed point "o" (Figure 2.1). Attach a Cartesian frame to the body with its origin at "o". Choose a reference configuration and identify it with the identity element,  $e$ , of  $O(3)$ . A configuration of the rigid body then is represented by an element,  $R$ , of  $O(3)$ .  $R$  transforms the coordinates of a point at the current configuration to the coordinates of the same point at the reference configuration. A trajectory of the rigid body thus can be represented by a curve,  $R(t) \in O(3), t \in [0, \infty)$ , with  $R(0) = e$ . Since the motion is assumed to be at least continuous, it follows that  $\det R(t) = 1$  and therefore  $R(t) \in SO(3)$ . In other words, the configuration space of a rigid body about a fixed point may be identified with  $SO(3)$ .  $\square$

Define for given  $A \in SO(3)$  the left translation by  $A$ ,  $\mathcal{L}_A$ , by

$$\mathcal{L}_A : SO(3) \rightarrow SO(3) : B \mapsto AB \quad (2.1)$$

Since  $\mathcal{L}_A \circ \mathcal{L}_{A^T} = \mathcal{L}_{A \cdot A^T} = \mathcal{L}_e$ , where  $e$  is the identity element of  $SO(3)$ ,  $\mathcal{L}_A$  is a diffeomorphism of  $SO(3)$  with the inverse given by  $\mathcal{L}_{A^T}$ . To evaluate the derivative of (2.1) with respect to  $B$  at the identity, we consider a curve  $B(t) \in SO(3), t \in [0, \infty)$ , with  $B(0) = e$ , and  $\frac{d}{dt}|_{t=0} B(t) = \xi$ . Then,

$$\frac{d}{dt}|_{t=0} \mathcal{L}_A(B(t)) = \frac{d}{dt}|_{t=0} A \cdot B(t) = A \cdot \xi \triangleq T_e \mathcal{L}_A \xi,$$

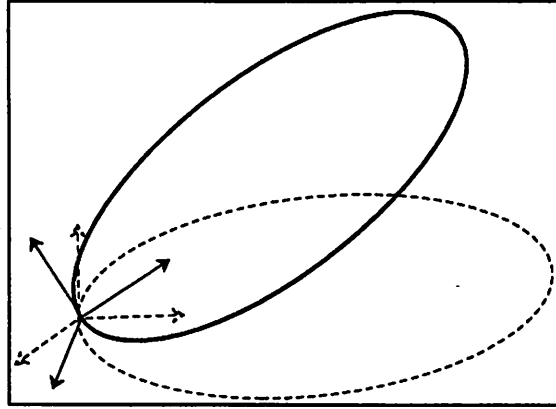


Figure 2.1: Motion of a rigid body about a fixed point “o”.

The map  $l_A \triangleq T_e \mathcal{L}_A$ , defined by

$$l_A : so(3) \longrightarrow T_A SO(3) : \xi \longmapsto A\xi, \quad (2.2)$$

is called the tangent map of  $\mathcal{L}_A$  at the identity, where  $T_A SO(3)$  is called the tangent space to  $SO(3)$  at  $A$ , and  $so(3) \triangleq T_e SO(3)$  the Lie algebra of  $SO(3)$ . Recall that a vector space  $\mathcal{V}$  over  $\mathbb{R}$  is a *Lie algebra* if in addition to its vector space structure it possesses a product, that is, a map  $\mathcal{V} \times \mathcal{V} \longrightarrow \mathcal{V}$ , taking the pair  $(\mathbf{v}, \mathbf{w})$  to the element  $[\mathbf{v}, \mathbf{w}]$  of  $\mathcal{V}$ , which has the following properties:

1. It is bilinear over  $\mathbb{R}$ :

$$[\alpha_1 \mathbf{v}_1 + \alpha_2 \mathbf{v}_2, \mathbf{w}] = \alpha_1 [\mathbf{v}_1, \mathbf{w}] + \alpha_2 [\mathbf{v}_2, \mathbf{w}],$$

$$[\mathbf{v}, \alpha_1 \mathbf{w}_1 + \alpha_2 \mathbf{w}_2] = \alpha_1 [\mathbf{v}, \mathbf{w}_1] + \alpha_2 [\mathbf{v}, \mathbf{w}_2];$$

2. It is skew commutative:

$$[\mathbf{v}, \mathbf{w}] = -[\mathbf{w}, \mathbf{v}];$$

3. It satisfies the *Jacobi identity*:

$$[\mathbf{u}, [\mathbf{v}, \mathbf{w}]] + [\mathbf{w}, [\mathbf{u}, \mathbf{v}]] + [\mathbf{v}, [\mathbf{w}, \mathbf{u}]] = 0.$$

**Proposition 2.1**  $so(3)$  consists of 3 by 3 skew symmetric matrices, and is a Lie algebra with the Lie algebra bracket given by

$$[\xi_1, \xi_2] = \xi_1 \cdot \xi_2 - \xi_2 \cdot \xi_1$$

i.e.,  $[\cdot, \cdot]$  is simply the matrix commutator.

**Proof.** Differentiating the expression

$$A(t)^T A(t) = e, \quad (2.3)$$

at the identity yields

$$\dot{A}^T(0) + \dot{A}(0) = 0,$$

Thus,  $\dot{A}(0) = -\dot{A}^T(0)$  is skew-symmetric. ■

We can identify  $so(3)$  with  $\mathbb{R}^3$  via the following isomorphism

$$\mathcal{S} : \mathbb{R}^3 \mapsto so(3) : \begin{bmatrix} w_1 \\ w_2 \\ w_3 \end{bmatrix} \mapsto \begin{bmatrix} 0 & -w_3 & w_2 \\ w_3 & 0 & -w_1 \\ -w_2 & w_1 & 0 \end{bmatrix}. \quad (2.4)$$

The ordinary cross product,  $\times$ , of  $\mathbb{R}^3$  becomes the Lie-algebra bracket,  $[ \ ]$ , of  $so(3)$  via the following identity.

$$\mathcal{S}(w \times v) = \mathcal{S}(w) \cdot \mathcal{S}(v) - \mathcal{S}(v) \cdot \mathcal{S}(w) \triangleq [\mathcal{S}(w), \mathcal{S}(v)].$$

**Definition 2.2** Let  $A(t) \in SO(3)$  be a curve representing a trajectory of a rigid body. Then,  $\dot{A}(t) \in T_{A(t)}SO(3)$  and the rotational velocity of the body is a 3-vector,  $w \in \mathbb{R}^3$ , obtained from  $\dot{A}(t)$  through the following procedure:

$$T_{A(t)}SO(3) \xrightarrow{l_{A^T}} so(3) \xrightarrow{\mathcal{S}^{-1}} \mathbb{R}^3 : \dot{A}(t) \mapsto A^T \cdot \dot{A}(t) \mapsto \mathcal{S}^{-1}(A^T \cdot \dot{A}) = w, \quad (2.5)$$

where

$$l_{A^T} : T_{A(t)}SO(3) \rightarrow so(3)$$

is the tangent map of  $\mathcal{L}_{A^T}$  evaluated at  $A$ .

**Theorem 2.1** Let  $\psi : \mathbb{R}^3 \rightarrow \mathbb{R}^3$  be a rigid motion. Then there exists a unique orthogonal transformation  $R$  and a unique translation by  $r$  such that

$$\psi(x) = Rx + r.$$

**Proof.** Let  $r = \psi(0)$ . It is straightforward to show that the map  $x \mapsto \psi(x) - r$ , preserves norm and is linear, thus is an orthogonal transformation. ■

It follows from Theorem 2.1 that, by writing an element  $x \in \mathbb{R}^3$  in the form

$$x = \begin{bmatrix} x^1 \\ x^2 \\ x^3 \\ 1 \end{bmatrix}, \quad (2.6)$$

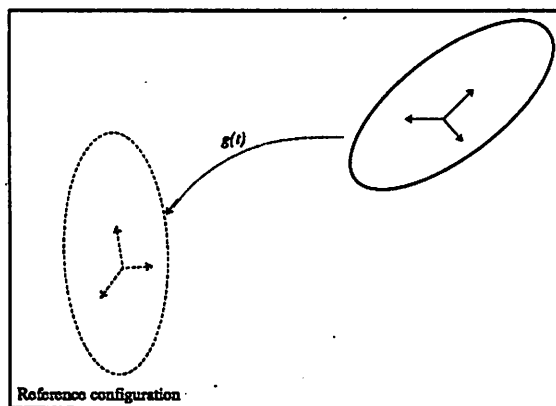


Figure 2.2: Motion of a free rigid body.

a rigid motion,  $g$ , assumes the form

$$g = \begin{bmatrix} R & r \\ 0 & 1 \end{bmatrix}, \quad R \in O(3), r \in \mathbb{R}^3. \quad (2.7)$$

(2.6) and (2.7) are known as the homogeneous representation of rigid transformation. Clearly the set of rigid transformations, under matrix multiplication, form a group, known as the Euclidean group of  $\mathbb{R}^3$  and is denoted by  $E(3)$ . Theorem 2.1 allows us to identify  $E(3)$  with the semi-direct product of  $O(3)$  with  $\mathbb{R}^3$ , i.e.,  $E(3) = O(3) \ltimes \mathbb{R}^3$ .

The subgroup of  $E(3)$  which consists of *proper* orthogonal transformation followed by translation is denoted by  $SE(3) (= SO(3) \ltimes \mathbb{R}^3)$ .

**Example 2.4** Consider motion of a rigid body shown in Figure 2.2. Attach a Cartesian frame to the body and choose a reference configuration. Identify the reference configuration with the identity element,  $e$ , of  $SE(3)$ . Then a trajectory of the rigid body can be represented by a curve  $g(t) \in SE(3)$ ,  $t \in [0, \infty)$ , and  $g(0) = e$ .  $SE(3)$  is the configuration space of the free rigid body.  $\square$

**Proposition 2.2** Let  $T_g SE(3)$  be the tangent space to  $SE(3)$  at  $g$ , and  $se(3) \triangleq T_e SE(3)$ , the Lie algebra of  $SE(3)$ . Then,  $se(3)$  consists of 4 by 4 matrices of the form

$$\xi = \begin{bmatrix} S(w) & v \\ 0 & 0 \end{bmatrix}, \quad \text{where } v, w \in \mathbb{R}^3.$$

**Proof.** This follows from differentiating the expression

$$g^{-1}(t) \cdot g(t) = e$$

at the identity. ■

We identify  $se(3)$  with  $\mathbf{R}^6$  via the following isomorphism.

$$\mathcal{T} : se(3) \longrightarrow \mathbf{R}^6 : \xi = \begin{bmatrix} \mathcal{S}(w) & v \\ 0 & 0 \end{bmatrix} \longmapsto \begin{bmatrix} v \\ w \end{bmatrix}. \quad (2.8)$$

For notational convenience we sometimes let  $\hat{\xi} \triangleq \mathcal{T}(\xi)$  denote the 6-vector extracted from  $\xi \in se(3)$ . The six vector  $\hat{\xi}$  is called the twist coordinates of  $\xi$ .

**Definition 2.3** Let  $g(t) \in SE(3)$ ,  $t \in [0, \infty)$ , be a curve representing a trajectory of a rigid body, then  $\dot{g}(t) \in T_{g(t)}SE(3)$  and the velocity of the rigid body is a 6-vector,

$\begin{bmatrix} v \\ w \end{bmatrix} \in \mathbf{R}^6$ , obtained from  $\dot{g}(t)$  through the following procedure:

$$\begin{aligned} T_{g(t)}SE(3) &\xrightarrow{l_{g^{-1}(t)}} se(3) \xrightarrow{\mathcal{T}} \mathbf{R}^6 \\ \dot{g} &\longmapsto g^{-1} \cdot \dot{g} = \begin{bmatrix} R^T \dot{R} & R^T \dot{r} \\ 0 & 0 \end{bmatrix} \longmapsto \begin{bmatrix} v \\ w \end{bmatrix} = \begin{bmatrix} R^T \dot{r} \\ \mathcal{S}^{-1}(R^T \dot{R}) \end{bmatrix} \end{aligned} \quad (2.9)$$

where  $l_{g^{-1}(t)}$  is the tangent map of the left translation  $\mathcal{L}_{g^{-1}(t)}$  evaluated at  $g(t)$ .

**Remark 2.1** We call  $w = \mathcal{S}^{-1}(R^T \dot{R})$  the rotational velocity and  $v = R^T \dot{r}$  the translational velocity, of the rigid body. □

We now study the effect on the velocity representation under change of coordinate frames. Consider again motion of a free rigid body in  $\mathbf{R}^3$  (see Figure 2.3). Fix two Cartesian frames  $C_1$  and  $C_2$  to the body and let  $C_2$  be related to  $C_1$  by a constant configuration  $h = (r, R) \in SE(3)$ . In other words,  $r \in \mathbf{R}^3$  and  $R \in SO(3)$  are the position and orientation of  $C_2$  relative to  $C_1$ . If  $g_1(t), g_2(t) \in SE(3)$ ,  $t \in [0, \infty)$ , are two representations of a trajectory of a rigid body relative to frame  $C_1$  and  $C_2$ , respectively, then the following relation exists

$$g_2(t) = h^{-1} \cdot g_1(t) \cdot h. \quad (2.10)$$

Let  $\begin{bmatrix} v_1 \\ w_1 \end{bmatrix} \in \mathbf{R}^6$  be the velocity of the rigid body obtained from  $\dot{g}_1(t)$ , and  $\begin{bmatrix} v_2 \\ w_2 \end{bmatrix} \in \mathbf{R}^6$  be the velocity of the rigid body obtained from  $\dot{g}_2(t)$ , then it follows from Eq. (2.10) that

$$\begin{bmatrix} v_2 \\ w_2 \end{bmatrix} = \underbrace{\begin{bmatrix} R^T & -R^T \mathcal{S}(r) \\ 0 & R^T \end{bmatrix}}_{Ad_{h^{-1}}} \begin{bmatrix} v_1 \\ w_1 \end{bmatrix}. \quad (2.11)$$

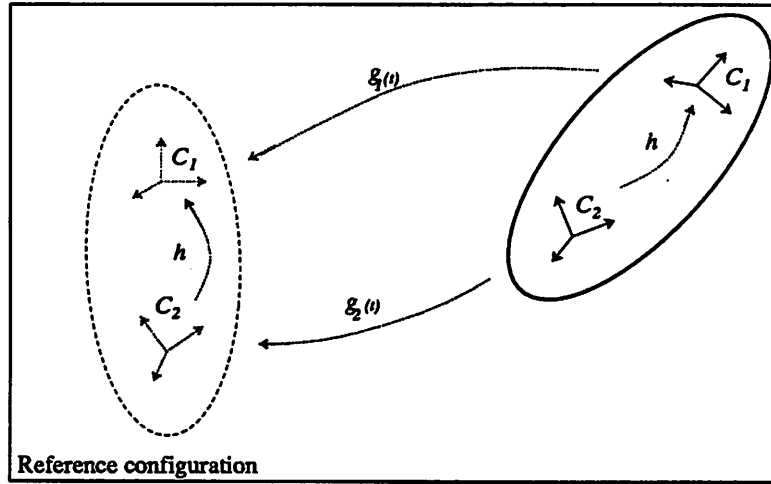


Figure 2.3: Velocity transformation under change of coordinate.

The 6 by 6 matrix given in Eq. (2.11) is a representation of the similarity transformation of (2.11), known as the adjoint map of  $SE(3)$ . For each  $g \in SE(3)$ , the adjoint map,  $Ad_g$ , defined by

$$Ad_g : se(3) \longrightarrow se(3) : \xi \longmapsto g \cdot \xi \cdot g^{-1} \quad (2.12)$$

is a Lie-algebra isomorphism with the inverse given by  $Ad_{g^{-1}}$ . The lie-algebra bracket,  $[\cdot, \cdot]$ , on  $se(3)$  is

$$[\xi_1, \xi_2] = \xi_1 \cdot \xi_2 - \xi_2 \cdot \xi_1. \quad (2.13)$$

After identifying  $se(3)$  with  $\mathbb{R}^6$  using (2.8), the Lie-algebra bracket (2.13) becomes, for  $\hat{\xi}_1 = \begin{bmatrix} v_1 \\ w_1 \end{bmatrix}$ ,  $\hat{\xi}_2 = \begin{bmatrix} v_2 \\ w_2 \end{bmatrix}$ ,

$$[\hat{\xi}_1, \hat{\xi}_2] = \begin{bmatrix} v_1 \times w_2 + w_1 \times v_2 \\ w_1 \times w_2 \end{bmatrix} \triangleq ad_{\hat{\xi}_1}(\hat{\xi}_2), \quad (2.14)$$

a generalized cross product to  $\mathbb{R}^6$ , and the matrix representation of  $Ad_{g^{-1}}$  is given by Eq. (2.11).

In studying manipulator kinematics and dynamics, there is a need to calculate relative velocities of more than two rigid bodies. The rest of the section is devoted to investigating the relations between velocities of multiple rigid bodies.

**Notation 2.1** Let  $C_i$  and  $C_j$  be two coordinate frames in  $\mathbb{R}^3$ , where  $i$  and  $j$  are arbitrary subscripts. Then,  $g_{i,j} = (r_{i,j}, R_{i,j})$  denote the position and orientation of  $C_i$  relative to  $C_j$ , and  $(v_{i,j}, w_{i,j})$  the corresponding velocity defined as in (2.9).

**Proposition 2.3** Consider motion of three coordinate frames  $C_1$ ,  $C_2$  and  $C_3$ . The following relation exists between their relative velocities.

$$\boxed{\begin{bmatrix} v_{3,1} \\ w_{3,1} \end{bmatrix} = Ad_{g_{3,2}}^{-1} \begin{bmatrix} v_{2,1} \\ w_{2,1} \end{bmatrix} + \begin{bmatrix} v_{3,2} \\ w_{3,2} \end{bmatrix}} \quad (2.15)$$

where  $Ad_{g_{3,2}}^{-1}$ , the adjoint map of  $SE(3)$ , is given by

$$Ad_{g_{3,2}}^{-1} = \begin{bmatrix} R_{3,2}^T & -R_{3,2}^T \mathcal{S}(r_{3,2}) \\ 0 & R_{3,2}^T \end{bmatrix}. \quad (2.16)$$

**Proof.** The configuration of  $C_3$  relative to  $C_1$  is composed according to

$$g_{3,1} = g_{2,1} \cdot g_{3,2} = \begin{bmatrix} R_{2,1} R_{3,2} & R_{2,1} r_{3,2} + r_{2,1} \\ 0 & 1 \end{bmatrix}.$$

Thus,

$$\xi_{3,1} = g_{3,1}^{-1} \cdot \dot{g}_{3,1} = g_{3,2}^{-1} \cdot g_{2,1}^{-1} (\dot{g}_{2,1} \cdot g_{3,2} + g_{2,1} \cdot \dot{g}_{3,2}) = g_{3,2}^{-1} \cdot \xi_{2,1} \cdot g_{3,2} + \xi_{3,2}.$$

Expanding the above equation into translational and rotational component, and noting that the operator  $\mathcal{S}$  satisfies

$$\mathcal{S}(w)v = w \times v, \forall w, v \in \mathbb{R}^3, \quad (2.17)$$

and

$$R\mathcal{S}(w)R^T = \mathcal{S}(Rw), \forall R \in SO(3), w \in \mathbb{R}^3, \quad (2.18)$$

yield

$$v_{3,1} = R_{3,2}^T v_{2,1} - R_{3,2}^T \mathcal{S}(r_{3,2}) w_{2,1} + v_{3,2} \quad (2.19)$$

and

$$w_{3,1} = R_{3,2}^T w_{2,1} + w_{3,2}. \quad (2.20)$$

Combining (2.19) and (2.20) gives the desired result.  $\blacksquare$

As a consequence of Proposition 2.3, we have

**Corollary 2.1** *Suppose that  $C_3$  is fixed relative to  $C_2$ . Then the velocity of  $C_3$  relative to  $C_1$  is related to that of  $C_2$  by the adjoint transformation.*

$$\begin{bmatrix} v_{3,1} \\ w_{3,1} \end{bmatrix} = \begin{bmatrix} R_{3,2}^T & -R_{3,2}^T \mathcal{S}(r_{3,2}) \\ 0 & R_{3,2}^T \end{bmatrix} \begin{bmatrix} v_{2,1} \\ w_{2,1} \end{bmatrix}. \quad (2.21)$$

This is simply a restatement of the result given in Eq. (2.11).

**Corollary 2.2** *Suppose that  $C_2$  is fixed relative to  $C_1$ . Then, the velocity of  $C_3$  relative to  $C_2$  is the same as the velocity of  $C_3$  relative to  $C_1$ , i.e.,*

$$v_{3,1} = v_{3,2}, \text{ and } w_{3,1} = w_{3,2}. \quad (2.22)$$

This shows that the velocity of a rigid body is independent of the choice of the inertia reference frame.

## 2.3 Manipulator Kinematics

A manipulator, or an open kinematic chain consists of a number of rigid bodies, called links, connected in a chain by joints. Each joint is either of revolute type or prismatic type. Manipulator kinematics studies motion of the end effector in response to motion of the joints. For example, the forward kinematic map relates position of the joints to configuration of the end effector, and manipulator Jacobian relates joint velocity to velocity of the end effector. This section explores these notions using tools from differential geometry. See ([Pad86], [Bro83] and [Cra86]) for further references.

**Definition 2.4** *An element  $\xi$  of  $se(3)$  is called a twist. Like a screw one finds in a hardware store, a twist has the attributes of pitch, magnitude and axis. Let  $\xi = \mathcal{T}^{-1} \begin{bmatrix} v \\ w \end{bmatrix}$  be a twist. Its pitch,  $\rho_\xi$ , magnitude,  $m_\xi$ , and axis  $l_\xi$  are defined by*

$$\rho_\xi = \begin{cases} \frac{w^T v}{|w|^2} & \text{if } w \neq 0, \\ \infty & \text{otherwise;} \end{cases}$$

$$m_\xi = \begin{cases} |w| & \text{if } w \neq 0, \\ |v| & \text{otherwise;} \end{cases}$$

and  $l_\xi$  is the line defined by

1. if  $w \neq 0$ , then,

$$l_\xi = \left\{ o + \frac{w \times v}{|w|^2} + \lambda w, \lambda \in \mathbf{R} \right\}$$

where  $o$  is the origin of the coordinate frame.

2. if  $w = 0$ , then  $l_\xi$  is any directed line with direction  $v$ .

**Example 2.5** 1.  $\xi = \mathcal{T}^{-1} \begin{bmatrix} 0 \\ w \end{bmatrix}$  is called a zero-pitch twist. It describes motion of a revolute joint.

2.  $\xi = \mathcal{T}^{-1} \begin{bmatrix} v \\ 0 \end{bmatrix}$  is called a  $\infty$ -pitch twist. It describes motion of a prismatic joint.

□

**Definition 2.5** The exponential mapping of  $SE(3)$  is defined by the following convergent series of matrices.

$$\exp : se(3) \longrightarrow SE(3) : \xi \longmapsto \sum_{n=0}^{\infty} \frac{\xi^n}{n!}. \quad (2.23)$$

Properties of the exponential mapping are summarized as follows (see [AM78] for the proof):

- It is a local diffeomorphism.
- It commutes with the adjoint map of Section 2.2 in the sense

$$\exp(Ad_{g^{-1}} \cdot \xi) = \exp(g^{-1} \cdot \xi \cdot g) = g^{-1} \cdot \exp \xi \cdot g, \forall g \in SE(3), \xi \in se(3). \quad (2.24)$$

- For  $\xi_1, \xi_2 \in se(3)$  and  $g \in SE(3)$  we have

$$Ad_g \cdot ad_{\hat{\xi}_1}(\hat{\xi}_2) = ad_{Ad_g \hat{\xi}_1}(Ad_g \hat{\xi}_2) \quad (2.25)$$

where  $ad_{\hat{\xi}_1}(\hat{\xi}_2)$ , the Lie-algebra bracket of  $se(3)$  is defined in Eq. (2.14).

- Using Eq. (2.25) and differentiating  $Ad_{(g \cdot \exp t \xi_1)^{-1}} \hat{\xi}_2$  with respect to time  $t$  yield

$$\frac{d}{dt} Ad_{(g \cdot \exp t \xi_1)^{-1}} \hat{\xi}_2 = Ad_{(g \cdot \exp t \xi_1)^{-1}} \cdot ad_{\hat{\xi}_2}(Ad_g \hat{\xi}_1). \quad (2.26)$$

Eq (2.24) is a key result for studying manipulator kinematics, while Eq. (2.26) is a frequently used identity in manipulator equations of motion.

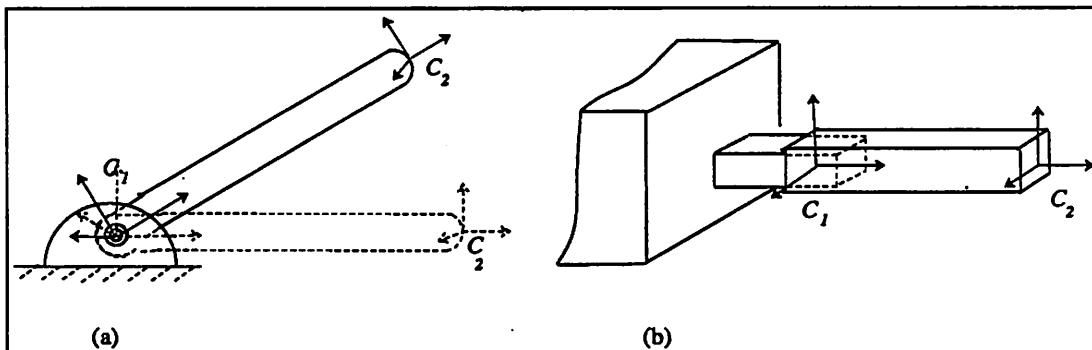


Figure 2.4: (a) A one-link manipulator with revolute joint, (b) a one-link manipulator with prismatic joint.

**Example 2.6 (1)** Consider the one-linked manipulator shown in Figure 2.4(a), where the link is connected to the base by a revolute joint and the joint axis points outward from the paper. To describe motion of the manipulator, we attach a Cartesian frame,  $C_1$ , to the link. The origin of  $C_1$  is at the joint axis and the  $z$ -axis of  $C_1$  coincides with the joint axis. Now, choose a reference configuration of the manipulator and identify the joint position,  $\theta$ , with zero. At a given value of  $\theta$ , the configuration of  $C_1$  relative to the reference configuration is given by

$$g_1(\theta) = \exp \xi_1 \theta, \quad \text{where } \xi_1 = \mathcal{T}^{-1} \begin{bmatrix} 0 \\ e_z \end{bmatrix} \text{ and } e_z = \begin{bmatrix} 0 \\ 0 \\ 1 \end{bmatrix}. \quad (2.27)$$

$\xi_1$  is the twist representing the joint axis relative to frame  $C_1$ . Expanding Eq. (2.27) using (2.23) yields

$$g_1(\theta) = \begin{bmatrix} \cos \theta & \sin \theta & 0 & 0 \\ -\sin \theta & \cos \theta & 0 & 0 \\ 0 & 0 & 1 & 0 \\ 0 & 0 & 0 & 1 \end{bmatrix}.$$

Note that  $\theta$  ranges from 0 to  $2\pi$ , and thus the joint space is  $S^1$ , the circle group.

(2) Suppose we wish to describe motion of the manipulator relative to a different frame, say  $C_2$ , which is displaced from  $C_1$  by a constant  $h \in SE(3)$ . Let  $g_2(\theta)$

be the configuration of  $C_2$  relative to the reference configuration at  $\theta$ . Then, the following relation holds between  $g_1(\theta)$  and  $g_2(\theta)$ .

$$g_2(\theta) = h^{-1} \cdot g_1(\theta) \cdot h.$$

Using Eqs (2.24) and (2.27) we have

$$g_2(\theta) = h^{-1} \cdot \exp \xi_1 \theta \cdot h = \exp(Ad_{h^{-1}} \xi_1 \theta) \triangleq \exp \xi_2 \theta,$$

where

$$\hat{\xi}_2 = Ad_{h^{-1}} \cdot \hat{\xi}_1 = \begin{bmatrix} R^T & -R^T \mathcal{S}(r) \\ 0 & R^T \end{bmatrix} \begin{bmatrix} 0 \\ e_z \end{bmatrix} = \begin{bmatrix} (R^T e_z) \times (R^T e_z) \\ R^T e_z \end{bmatrix} \triangleq \begin{bmatrix} \bar{e}_z \times \bar{r} \\ \bar{e}_z \end{bmatrix}.$$

$\bar{e}_z$  and  $\bar{r}$  are, respectively, the joint axis and the vector from the origin of  $C_2$  to the joint axis, expressed relative to  $C_2$  frame. In other words,  $\xi_2$  is the twist representing the joint axis relative to  $C_2$  frame. Readers who are familiar with line geometry should also recall the transformation of line vectors under change of coordinate frames ([BR79]).

- (3) Figure 2.4(b) shows an one-linked manipulator with prismatic joint. Attach a coordinate frame to the link so that its  $z$ -axis coinciding with the joint axis. Choose a reference configuration and identify the joint length,  $\theta$ , with zero. At a given value of  $\theta$ , the configuration of  $C_1$  relative to the reference configuration is given by

$$g_1(\theta) = \exp \xi_1 \theta, \text{ where } \xi_1 = T^{-1} \begin{bmatrix} e_z \\ 0 \end{bmatrix}.$$

Change coordinate frames from  $C_1$  to  $C_2$  and let  $g_2(\theta)$  be the configuration of  $C_2$  relative to the reference configuration at  $\theta$ . Then we have

$$g_2(\theta) = h^{-1} \cdot g_1 \cdot h = \exp(Ad_{h^{-1}} \xi_1 \theta) \triangleq \exp \xi_2 \theta,$$

where  $h$  is the configuration of  $C_2$  relative to  $C_1$  and

$$\xi_2 = \begin{bmatrix} R^T & -R^T \mathcal{S}(r) \\ 0 & R^T \end{bmatrix} \begin{bmatrix} e_z \\ 0 \end{bmatrix} = \begin{bmatrix} R^T e_z \\ 0 \end{bmatrix} \triangleq \begin{bmatrix} \bar{e}_z \\ 0 \end{bmatrix}.$$

Again,  $\xi_2$  is the twist representing the joint axis relative to  $C_2$  frame. Recall here, too, the transformation of a free vector under change of coordinate frames (see [BR79]).

□

Generalizing from these examples, we wish to define the forward kinematic map of a manipulator with  $n$ -degrees of freedom. Call the last link the end-effector, and let  $Q$  denote the joint space, which is the Cartesian product of the configuration space of the joints. The configuration space of a revolute joint is  $S^1$ , and the configuration space of a prismatic joint is  $\mathbb{R}^1$ . In other words,

$$Q = \underbrace{S^1 \times \dots \times S^1}_{n_1} \times \underbrace{\mathbb{R} \times \dots \times \mathbb{R}}_{n_2},$$

where  $n_1$  is the number of revolute joints, and  $n_2$  is the number of prismatic joints.

**Definition 2.6** Consider a manipulator with  $n$ -degrees of freedom. Attach a coordinate frame,  $C$ , to link  $n$  of the manipulator, and choose a reference configuration. Set the joint position,  $\theta_i, i = 1, \dots, n$ , to zero at the reference configuration. The forward kinematic map,  $\mathcal{F}$ , then assigns to each point in the joint space a point in the configuration space of the last link. The formula of  $\mathcal{F}$  is given by

$$\mathcal{F} : Q \longrightarrow SE(3) : (\theta_1, \dots, \theta_n) \longmapsto \exp(\xi_1 \theta_1) \cdot \dots \cdot \exp(\xi_n \theta_n), \quad (2.28)$$

where  $\xi_i, i = 1, \dots, n$ , is defined by:

$$\xi_i = \begin{cases} \mathcal{T}^{-1} \begin{bmatrix} e_i \times r_i \\ e_i \end{bmatrix} & \text{for revolute joint;} \\ \mathcal{T}^{-1} \begin{bmatrix} e_i \\ 0 \end{bmatrix} & \text{for a prismatic joint.} \end{cases} \quad (2.29)$$

**Remark 2.2** For both revolute and prismatic joints,  $e_i$  is the direction vector of the joint axis; while for a revolute joint  $r_i$  is the vector from the origin of  $C$  to the axis.  $\square$

**Example 2.7** Consider the planar manipulator shown in Figure 2.5. Each link is of unit length and its joint axis points outward from the paper. The joint space is the three-torus, i.e.,  $Q = S^1 \times S^1 \times S^1$ . Choose the configuration in dotted lines as the reference configuration. Then, the forward kinematic map is given by

$$\mathcal{F} : Q \longrightarrow SE(3) : (\theta_1, \theta_2, \theta_3) \longmapsto \exp(\xi_1 \theta_1) \cdot \exp(\xi_2 \theta_2) \cdot \exp(\xi_3 \theta_3), \quad (2.30)$$

where

$$\xi_3 = \mathcal{T}^{-1} \begin{bmatrix} -e_z \times e_x \\ e_z \end{bmatrix}, \quad \xi_2 = \mathcal{T}^{-1} \begin{bmatrix} -e_z \times 2e_x \\ e_z \end{bmatrix} \quad \text{and} \quad \xi_1 = \mathcal{T}^{-1} \begin{bmatrix} -e_z \times 3e_x \\ e_z \end{bmatrix},$$

$e_x$  and  $e_y$  are the usual basis vectors.  $\square$

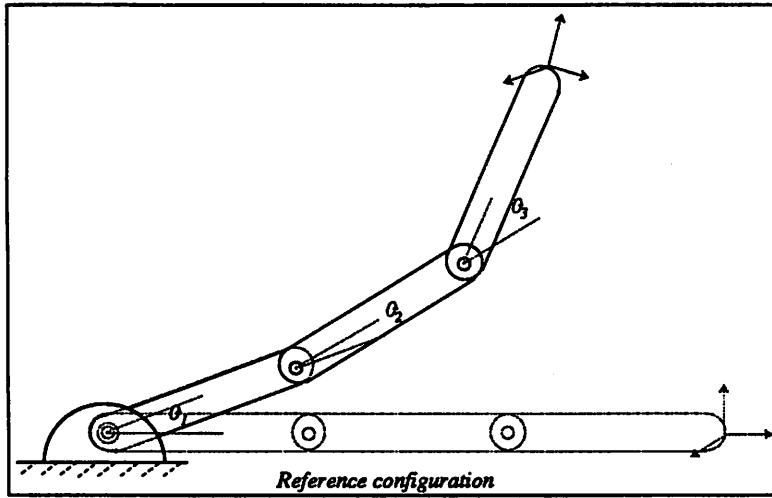


Figure 2.5: A planar manipulator of three-degrees of freedom.

Consider again a manipulator with  $n$ -degrees of freedom. Let  $\theta(t) = (\theta_1(t), \dots, \theta_n(t))^T \in Q, t \in [0, \infty)$ , be a trajectory of the manipulator in the joint space. The joint velocity is  $\dot{\theta}(t) \in T_{\theta(t)}Q$ . We wish to determine the velocity of the end effector as a function of the joint velocity.

Differentiating the forward kinematic map (2.30) with respect to time and using the chain rule, yields

$$\frac{d}{dt} \mathcal{F}(\theta(t)) = \sum_{i=1}^n \exp(\xi_1 \theta_1) \cdot \dots \cdot \exp(\xi_i \theta_i) \xi_i \dot{\theta}_i \cdot \exp(\xi_{i+1} \theta_{i+1}) \cdot \dots \cdot \exp(\xi_n \theta_n). \quad (2.31)$$

Eq. (2.31) can be rearranged in the form

$$\frac{d}{dt} \mathcal{F}(\theta(t)) = \mathcal{F}(\theta) \sum_{i=1}^n \bar{\xi}_i \dot{\theta}_i, \quad (2.32)$$

where

$$\bar{\xi}_i = \{\exp(\xi_{i+1} \theta_{i+1}) \cdot \dots \cdot \exp(\xi_n \theta_n)\}^{-1} \cdot \xi_i \cdot \{\exp(\xi_{i+1} \theta_{i+1}) \cdot \dots \cdot \exp(\xi_n \theta_n)\}. \quad (2.33)$$

If, we define,

$$\mathcal{F}_i(\theta) \triangleq (\exp(\xi_{i+1} \theta_{i+1}) \cdot \dots \cdot \exp(\xi_n \theta_n)), \quad i = 1, \dots, n-1, \quad (2.34)$$

to be the forward kinematic map of the manipulator with the first  $i$  joints locked at zero. Then,  $\bar{\xi}_i$  is the twist representing the  $i^{\text{th}}$  joint relative to the end effector frame

when the manipulator is at the configuration  $(0, \dots, 0, \theta_{i+1}, \dots, \theta_n)$ . Using Definition 2.3, the velocity of the end effector is a 6-vector,  $\begin{bmatrix} v \\ w \end{bmatrix} \in \mathbb{R}^6$ , given by

$$\begin{bmatrix} v \\ w \end{bmatrix} = \mathcal{T} \left( \sum_{i=1}^n \bar{\xi}_i \dot{\theta}_i \right) = \underbrace{[\mathcal{T}(\bar{\xi}_1), \dots, \mathcal{T}(\bar{\xi}_n)]}_n \begin{bmatrix} \dot{\theta}_1 \\ \vdots \\ \dot{\theta}_n \end{bmatrix}. \quad (2.35)$$

The  $n$  by 6 matrix

$$[\mathcal{T}(\bar{\xi}_1), \dots, \mathcal{T}(\bar{\xi}_n)] \triangleq J(\theta) \quad (2.36)$$

which relates the joint velocity to velocity of the end effector is called the manipulator Jacobian of the forward kinematic map. It is composed of the tangent map of  $\mathcal{F}$  and the left translation map  $l_{g^{-1}}$ , where  $g = \mathcal{F}(\theta)$ .

We summarize here a procedure for deriving the manipulator Jacobian,  $J(\theta)$ , at a configuration  $\theta \in Q$ .

#### Algorithm 2.1

**Step 1:** Choose a reference configuration of the manipulator and identify the joint position vector,  $\theta$ , with zero. Let  $\xi_i, i = 1, \dots, n$ , be the twist representing the  $i^{\text{th}}$  joint axis relative to the reference configuration.

**Step 2:** Evaluate  $\mathcal{F}_i(\theta), i = 1, \dots, n-1$ , using Eq. (2.34), where  $\mathcal{F}_n(\theta) = e$ .

**Step 3:** Compute  $\bar{\xi}_i = \mathcal{F}_i^{-1}(\theta) \cdot \xi_i \cdot \mathcal{F}(\theta), i = 1, \dots, n$ .

**Step 4:** Set  $J(\theta) = [\mathcal{T}^{-1}(\bar{\xi}_1), \dots, \mathcal{T}^{-1}(\bar{\xi}_n)]$ .

**Example 2.8** Recall the planar manipulator studied in Example 2.7. We wish to derive the manipulator Jacobian,  $J(\theta)$ , at  $\theta = (0, 15^\circ, 15^\circ)$ . Following Algorithm 2.1, we have

**Step 1:**  $\xi_1, \xi_2$  and  $\xi_3$  are given by Example 2.7.

**Step 2:**

$$\mathcal{F}_2(\theta) = \exp \xi_3 \theta_3 = \begin{bmatrix} 0.966 & 0.259 & 0 & -0.034 \\ -0.259 & 0.966 & 0 & 0.259 \\ 0 & 0 & 1 & 0 \\ 0 & 0 & 0 & 1 \end{bmatrix}$$

and

$$\mathcal{F}_1(\theta) = \exp \xi_2 \theta_2 \cdot \exp \xi_3 \theta_3 = \begin{bmatrix} 0.866 & 0.5 & 0 & -0.168 \\ -0.5 & 0.866 & 0 & 0.76 \\ 0 & 0 & 1 & 0 \\ 0 & 0 & 0 & 1 \end{bmatrix}.$$

**Step 3:**

$$\bar{\xi}_1 = \mathcal{F}_1^{-1}(\theta) \cdot \xi_1 \cdot \mathcal{F}_1(\theta) = \begin{bmatrix} 0 & -1 & 0 & -0.0742 \\ 1 & 0 & 0 & -1.3915 \\ 0 & 0 & 0 & 0 \\ 0 & 0 & 0 & 0 \end{bmatrix};$$

$$\bar{\xi}_2 = \mathcal{F}_2^{-1}(\theta) \cdot \xi_2 \cdot \mathcal{F}_2(\theta) = \begin{bmatrix} 0 & -1 & 0 & 0.2765 \\ 1 & 0 & 0 & -2.0314 \\ 0 & 0 & 0 & 0 \\ 0 & 0 & 0 & 0 \end{bmatrix};$$

and

$$\hat{\xi}_3 = \xi_3 = \begin{bmatrix} 0 & -1 & 0 & 0 \\ 1 & 0 & 0 & -1 \\ 0 & 0 & 0 & 0 \\ 0 & 0 & 0 & 0 \end{bmatrix}.$$

**Step 4:**

$$J(\theta) = \begin{bmatrix} -0.0742 & 0.2765 & 0 \\ -1.3915 & -2.0314 & -1 \\ 0 & 0 & 0 \\ 0 & 0 & 0 \\ 0 & 0 & 0 \\ 1 & 1 & 1 \end{bmatrix}.$$

□

## 2.4 Manipulator Dynamics

We now consider the equations of motion for a manipulator - the way in which motion of the manipulator arises from torques applied by the actuators or

from external forces applied to the manipulator. It is well known that the equations of motion can be formulated differently if different principles were used. Two formulations which are particularly suited for applications to manipulators and which we will consider in this section are the Newton-Euler formulation and the Lagrangian formulation.

We will start with the Newton-Euler equations of motion for a single rigid body and the relations for static force transformation. Then, we will derive iteratively the Newton-Euler equations of motion for a manipulator. Finally we formulate explicitly the Lagrangian equations of motion for a 3R manipulator (a 3-degrees of freedom manipulator with revolute joints).

### 2.4.1 Rigid Body Dynamics and Static Force Transformation.

Consider the rigid body shown in Figure 2.6. Fix a coordinate frame to the mass center of the body and choose a reference configuration. The copy of the coordinate frame at the reference configuration is labeled with  $C_r$ , which is called the inertia reference frame. The inertia tensor,  $\mathcal{I}$ , of the rigid body relative to the body frame is a 3 by 3 matrix given by

$$\mathcal{I}_{ij} = \begin{cases} -\int_{\mathcal{B}} \rho(X) X^i X^j d^3X, & \text{if } i \neq j; \\ \int_{\mathcal{B}} \rho(X) (|X|^2 - (X^i)^2) d^3X, & \text{if } i = j, \end{cases} \quad (2.37)$$

where  $\mathcal{B} \subset \mathbb{R}^3$  is the set of  $\mathbb{R}^3$  occupied by the body, and  $\rho(X)$  is the mass density function of the body. Integrating the density function over  $\mathcal{B}$  yields the total mass of the body

$$m = \int_{\mathcal{B}} \rho(X) d^3X.$$

Let  $\begin{bmatrix} f_b \\ n_b \end{bmatrix}$  be the net external force/torque pair exerted on the rigid body<sup>1</sup>.

Also, let  $g(t) \in SE(3)$ ,  $t \in [0, \infty)$ , be a curve representing the trajectory of the rigid

---

<sup>1</sup>In the rest of the thesis, *force or wrench* will mean both force and torque, whereas *a force relative to a coordinate frame* means (1) both the force and the torque vectors are expressed relative to this coordinate frame and (2) the origin of the coordinate frame is also the torque origin and the exerting point of the force vector.

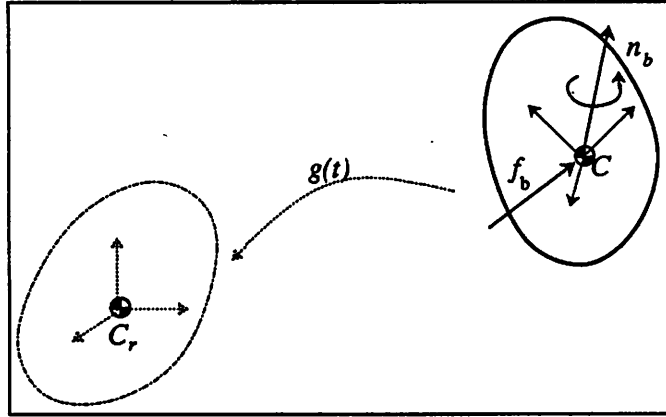


Figure 2.6: Motion of a free rigid body

body. Then the Newton-Euler equations of motion of the rigid body are

$$\begin{bmatrix} mI_d & 0 \\ 0 & \mathcal{I} \end{bmatrix} \begin{bmatrix} \dot{v} \\ \dot{w} \end{bmatrix} + \begin{bmatrix} w \times mI_d v \\ w \times \mathcal{I} w \end{bmatrix} = \begin{bmatrix} f_b \\ n_b \end{bmatrix}, \quad (2.38)$$

where as usual,  $v$ ,  $w$  are the translational and rotational velocity of the rigid body, and  $I_d$  is the  $3 \times 3$  identity matrix. Note that the first equation has a slightly different form from the usual Newton's equation of motion because  $v$  is expressed in a non-inertia frame.

We now study transformation relations for force under change of coordinate frames.

**Proposition 2.4** Consider two coordinate frames,  $C_1$  and  $C_2$ , which are related by a constant  $h \in SE(3)$  (see Figure 2.3). Let  $\begin{bmatrix} f_1 \\ n_1 \end{bmatrix}, \begin{bmatrix} f_2 \\ n_2 \end{bmatrix} \in \mathbb{R}^6$  be the expressions of the same force relative to  $C_1$  and  $C_2$ , respectively. Then the following relation exists.

$$\begin{bmatrix} f_1 \\ n_1 \end{bmatrix} = Ad_{h^{-1}}^T \cdot \begin{bmatrix} f_2 \\ n_2 \end{bmatrix} \triangleq \begin{bmatrix} R & 0 \\ S(r)R & R \end{bmatrix} \begin{bmatrix} f_2 \\ n_2 \end{bmatrix} \quad (2.39)$$

**Proof.** This follows from the Principle of Virtual Work. Let  $\begin{bmatrix} v_1 \\ w_1 \end{bmatrix}, \begin{bmatrix} v_2 \\ w_2 \end{bmatrix} \in \mathbb{R}^6$  be the virtual displacement per unit time of the rigid body relative to  $C_1$  and  $C_2$ .

Then, the virtual work,  $\delta W$ , per unit time is

$$\delta W = \left\langle \begin{bmatrix} v_1 \\ w_1 \end{bmatrix}, \begin{bmatrix} f_1 \\ n_1 \end{bmatrix} \right\rangle = \left\langle \begin{bmatrix} v_2 \\ w_2 \end{bmatrix}, \begin{bmatrix} f_2 \\ n_2 \end{bmatrix} \right\rangle.$$

Substituting the transformation relation (2.11) for the velocities yields the desired result. ■

## 2.4.2 Newton-Euler Formulation

Consider the manipulator shown in Figure 2.7. Without loss of generality we may assume that the manipulator lives in a gravity-free environment. To derive the Newton-Euler equations of motion, we need to calculate the velocities and accelerations of the links. For this, we fix a coordinate frame,  $C_i$ ,  $i = 1, \dots, 3$ , to the mass center of link  $i$  and choose a reference configuration of the manipulator, where the joint position,  $\theta_i$  is identified with zero. The copy of the link frame at the reference configuration is labeled with  $C_{ir}$ ,  $i = 1, \dots, 3$ , which is also called the inertia reference frame of link  $i$ .

**Notation 2.2** Let  $h_{i,j} \in SE(3)$ ,  $i > j$ , denote the configuration of  $C_{ir}$  relative to  $C_{jr}$ . Also, let  $\hat{\xi}_i^j = \begin{bmatrix} e_i^j \times r_i^j \\ e_i^j \end{bmatrix}$ ,  $j \geq i$ , be the twist representing the  $i^{\text{th}}$  joint axis relative to frame  $C_{jr}$ .

For example, assuming in Figure 2.7 that  $C_{ir}$  is positioned half way from the link axis and each link is of unit length, then

$$h_{2,1} = h_{3,2} = \begin{bmatrix} I_d & e_x \\ 0 & 1 \end{bmatrix}$$

and

$$\hat{\xi}_1^1 = \hat{\xi}_2^2 = \hat{\xi}_3^3 = \begin{bmatrix} -e_z \times \frac{1}{2}e_x \\ e_z \end{bmatrix}, \text{ and } \hat{\xi}_1^2 = \begin{bmatrix} -e_z \times \frac{3}{2}e_x \\ e_z \end{bmatrix}.$$

**Proposition 2.5** The following relation exists between the parameters defined above.

$$\xi_s^j = Ad_{h_{j,i}^{-1}} \cdot \xi_s^i, \text{ where } j > i. \quad (2.40)$$

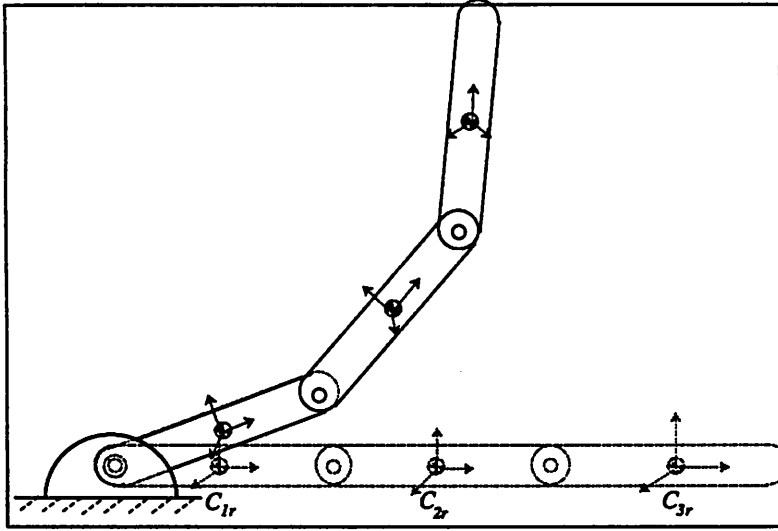


Figure 2.7: A 3R manipulator.

**Proof.** This follows from the figure and Example 2.6. ■

At a point  $\theta = (\theta_1, \theta_2, \theta_3)$  in the joint space, the forward kinematic map of link  $i$  is Link 1:

$$\mathcal{F}_1 = \exp \xi_1^1 \theta_1. \quad (2.41)$$

Link 2:

$$\mathcal{F}_2 = \exp \xi_1^2 \theta_1 \cdot \exp \xi_2^2 \theta_2. \quad (2.42)$$

Link 3:

$$\mathcal{F}_3 = \exp \xi_1^3 \theta_1 \cdot \exp \xi_2^3 \theta_2 \cdot \exp \xi_3^3 \theta_3. \quad (2.43)$$

Thus, the velocity of link  $i$ ,  $i = 1, \dots, 3$ , can be computed using Eqs (2.41) ~ (2.43) and we claim that the results can be rearranged into the following recursive formulae

$$\begin{bmatrix} v_1 \\ w_1 \end{bmatrix} = \hat{\xi}_1^1 \dot{\theta}_1; \quad (2.44)$$

$$\begin{bmatrix} v_2 \\ w_2 \end{bmatrix} = \hat{\xi}_2^2 \dot{\theta}_2 + Ad_{(h_{2,1} \cdot \exp \xi_2^2 \theta_2)^{-1}} \cdot \begin{bmatrix} v_1 \\ w_1 \end{bmatrix}; \quad (2.45)$$

and

$$\begin{bmatrix} v_3 \\ w_3 \end{bmatrix} = \hat{\xi}_3^3 \dot{\theta}_3 + Ad_{(h_{3,2} \cdot \exp \xi_3^3 \theta_3)^{-1}} \cdot \begin{bmatrix} v_2 \\ w_2 \end{bmatrix}. \quad (2.46)$$

In other words, the velocity of link  $i$  is simply the sum of the velocities of joint  $i$  and link  $i - 1$ . We prove (2.45) for example. First, by definition and the chain rule, we have

$$\mathcal{F}_2^{-1} \cdot \dot{\mathcal{F}}_2 = (\exp \xi_2^2 \theta_2)^{-1} \xi_1^2 \dot{\theta}_1 \exp \xi_2^2 \theta_2 + \xi_2^2 \dot{\theta}_2.$$

Now substitute Eq. (2.40) into the above equation and note that  $Ad_{gh} = Ad_g \cdot Ad_h$ , the desired result follows.

The Newton-Euler equations of motion for link  $i$  are

$$\begin{bmatrix} m_i I_d & 0 \\ 0 & \mathcal{I}_i \end{bmatrix} \begin{bmatrix} \dot{v}_i \\ \dot{w}_i \end{bmatrix} + \begin{bmatrix} w_i \times m_i v_i \\ w_i + \mathcal{I}_i w_i \end{bmatrix} = \begin{bmatrix} f_i \\ n_i \end{bmatrix} \quad (2.47)$$

where  $m_i$  and  $\mathcal{I}_i$  are, respectively, the mass and the inertia tensor of link  $i$ , and  $\begin{bmatrix} f_i \\ n_i \end{bmatrix}$  is the net force exerted on the link.

To obtain the link acceleration, we simply differentiate the velocity with respect to time and use the properties of the exponential mapping. This leads to the following recursive formulae.

$$\begin{bmatrix} \dot{v}_1 \\ \dot{w}_1 \end{bmatrix} = \hat{\xi}_1^1 \ddot{\theta}_1; \quad (2.48)$$

$$\begin{bmatrix} \dot{v}_2 \\ \dot{w}_2 \end{bmatrix} = \hat{\xi}_2^2 \ddot{\theta}_2 + Ad_{(h_{2,1} \cdot \exp \xi_2^2 \theta_2)^{-1}} \cdot \begin{bmatrix} \dot{v}_1 \\ \dot{w}_1 \end{bmatrix} + Ad_{(\exp \xi_2^2 \theta_2)^{-1}} \cdot ad_{-\hat{\xi}_2^2} (Ad_{h_{2,1}^{-1}} \cdot \begin{bmatrix} v_1 \\ w_1 \end{bmatrix}); \quad (2.49)$$

and

$$\begin{bmatrix} \dot{v}_3 \\ \dot{w}_3 \end{bmatrix} = \hat{\xi}_3^3 \ddot{\theta}_3 + Ad_{(h_{3,2} \cdot \exp \xi_3^3 \theta_3)^{-1}} \cdot \begin{bmatrix} \dot{v}_2 \\ \dot{w}_2 \end{bmatrix} + Ad_{(\exp \xi_3^3 \theta_3)^{-1}} \cdot ad_{-\hat{\xi}_3^3} (Ad_{h_{3,2}^{-1}} \cdot \begin{bmatrix} v_2 \\ w_2 \end{bmatrix}). \quad (2.50)$$

**Remark 2.3** • Link velocities and accelerations are calculated recursively starting from the first link outward to the last link.

- The acceleration of link  $i$  is the sum of the accelerations of joint  $i$  and link  $i - 1$  and a cross-product like term.

□

We now use inward iterations to compute the net force exerted on the links and the required joint torques for the Newton Euler equations of motion.

**Notation 2.3** Let  $\begin{bmatrix} F_i \\ N_i \end{bmatrix} \in \mathbb{R}^6$  denote the force exerted on link  $i$  by link  $i - 1$  relative to  $C_i$ ; and  $\tau_i$  denote the required joint torque.

We start with link 3 of the manipulator. Let  $\begin{bmatrix} f_{ext} \\ n_{ext} \end{bmatrix} \in \mathbb{R}^6$  be the force the manipulator applied to the environment, then the net force exerted on the link is given by

$$\begin{bmatrix} f_3 \\ n_3 \end{bmatrix} = \begin{bmatrix} F_3 \\ N_3 \end{bmatrix} - \begin{bmatrix} f_{ext} \\ n_{ext} \end{bmatrix}.$$

Rearranging the equation we get

$$\begin{bmatrix} F_3 \\ N_3 \end{bmatrix} = \begin{bmatrix} f_3 \\ n_3 \end{bmatrix} + \begin{bmatrix} f_{ext} \\ n_{ext} \end{bmatrix}. \quad (2.51)$$

The required joint torque,  $\tau_3$ , for a revolute joint is found by taking the projection of  $N_3$  along joint axis,  $e_3^3$ , i.e.,

$$\tau_3 = \langle e_3^3, N_3 \rangle. \quad (2.52)$$

The net force exerted on link 2 is the sum of forces exerted by link 1 and link 3. Expressing these forces relative to  $C_2$ , we have

$$\begin{bmatrix} f_2 \\ n_2 \end{bmatrix} = \begin{bmatrix} F_2 \\ N_2 \end{bmatrix} - Ad_{g_{3,2}}^T \cdot \begin{bmatrix} F_3 \\ N_3 \end{bmatrix},$$

where  $g_{3,2} \in SE(3)$  denotes the configuration of  $C_3$  relative to  $C_2$  and is given by

$$\begin{aligned} g_{3,2} &= (\exp \xi_1^2 \theta_1 \cdot \exp \xi_2^2 \theta_2)^{-1} \cdot h_{3,2} \cdot (\exp \xi_1^3 \theta_1 \cdot \exp \xi_2^3 \theta_2 \cdot \exp \xi_3^3 \theta_3) \\ &= h_{3,2} \cdot \exp \xi_3^3 \theta_3. \end{aligned}$$

Thus, the recursive formula for force computation of link 2 is

$$\begin{bmatrix} F_2 \\ N_2 \end{bmatrix} = \begin{bmatrix} f_2 \\ n_2 \end{bmatrix} - Ad_{(h_{3,2} \cdot \exp \xi_3^3)^{-1}}^T \cdot \begin{bmatrix} F_3 \\ N_3 \end{bmatrix}, \quad (2.53)$$

and the required joint torque,  $\tau_2$ , is

$$\tau_2 = \langle e_2^2, N_2 \rangle. \quad (2.54)$$

Finally for link 1 we have

$$\begin{bmatrix} F_1 \\ N_1 \end{bmatrix} = \begin{bmatrix} f_1 \\ n_1 \end{bmatrix} - Ad_{(h_{2,1} \cdot \exp \xi_2^2)^{-1}}^T \cdot \begin{bmatrix} F_2 \\ N_2 \end{bmatrix} \quad (2.55)$$

and

$$\tau_1 = \langle e_1^1, N_1 \rangle. \quad (2.56)$$

This completes the derivation of the Newton Euler equations of motion.

### 2.4.3 Lagrangian Formulation

The Newton-Euler Equations of motion derived in the previous subsection are in iterative form. For numerical simulations these results are very convenient to use. However, when it comes to control the manipulator, we are often more interested in closed form expressions. One approach is through combining Eqs (2.48) ~ (2.56). Another approach, which we will consider here, is to derive the equations of motion using the Lagrangian formulation.

The Lagrangian formulation starts with the derivation of the kinetic energy. At a point  $(\theta, \dot{\theta})$  in the velocity space, the kinetic energy of the 3R manipulator has the form

$$K = \sum_{i=1}^3 K_i(\theta, \dot{\theta}), \quad (2.57)$$

where  $K_i$ , the kinetic energy of link  $i$  is calculated as follows: Let

$$M_i = \begin{bmatrix} m_i I_d & 0 \\ 0 & \mathcal{I}_i \end{bmatrix}$$

be the inertia tensor of link  $i$ . Then,

$$K_i = \frac{1}{2} \left\langle \begin{bmatrix} v_i \\ w_i \end{bmatrix}, M_i \begin{bmatrix} v_i \\ w_i \end{bmatrix} \right\rangle. \quad (2.58)$$

Substitute the velocity Eqs. (2.44) ~ (2.46) into Eq. (2.58), we have

$$K_1 = \frac{1}{2} \langle \hat{\xi}_1^1 \dot{\theta}_1, M_1 \hat{\xi}_1^1 \dot{\theta}_1 \rangle; \quad (2.59)$$

$$\begin{aligned} K_2 &= \frac{1}{2} \langle \hat{\xi}_2^2 \dot{\theta}_2, M_2 \hat{\xi}_2^2 \dot{\theta}_2 \rangle + \langle \hat{\xi}_2^2 \dot{\theta}_2, M_2 Ad_{(h_{2,1} \exp \xi_2^2 \theta_2)^{-1}} \hat{\xi}_1^1 \dot{\theta}_1 \rangle \\ &+ \frac{1}{2} \langle Ad_{(h_{2,1} \exp \xi_2^2 \theta_2)^{-1}} \hat{\xi}_1^1 \dot{\theta}_1, M_2 Ad_{(h_{2,1} \exp \xi_2^2 \theta_2)^{-1}} \hat{\xi}_1^1 \dot{\theta}_1 \rangle; \end{aligned} \quad (2.60)$$

and

$$K_3 = \frac{1}{2} \langle \hat{\xi}_3^3 \dot{\theta}_3, M_3 \hat{\xi}_3^3 \dot{\theta}_3 \rangle + \langle \hat{\xi}_3^3 \dot{\theta}_3, M_3 Ad_{(h_{3,2} \exp \xi_3^3 \theta_3)^{-1}} \hat{\xi}_2^2 \dot{\theta}_2 \rangle$$

$$\begin{aligned}
& + \langle \hat{\xi}_3^3 \dot{\theta}_3, M_3 Ad_{(h_{3,1} \exp \xi_2^2 \theta_2 \exp \xi_3^3 \theta_3)^{-1}} \hat{\xi}_1^1 \dot{\theta}_1 \rangle \\
& + \frac{1}{2} \langle Ad_{(h_{3,2} \exp \xi_3^3 \theta_3)^{-1}} \hat{\xi}_2^2 \dot{\theta}_2, M_3 Ad_{(h_{3,2} \exp \xi_3^3 \theta_3)^{-1}} \hat{\xi}_2^2 \dot{\theta}_2 \rangle \\
& + \langle Ad_{(h_{3,2} \exp \xi_3^3 \theta_3)^{-1}} \hat{\xi}_2^2 \dot{\theta}_2, M_3 Ad_{(h_{3,1} \exp \xi_2^2 \theta_2 \exp \xi_3^3 \theta_3)^{-1}} \hat{\xi}_1^1 \dot{\theta}_1 \rangle \quad (2.61) \\
& + \frac{1}{2} \langle Ad_{(h_{3,1} \exp \xi_2^2 \theta_2 \exp \xi_3^3 \theta_3)^{-1}} \hat{\xi}_1^1 \dot{\theta}_1, M_3 Ad_{(h_{3,1} \exp \xi_2^2 \theta_2 \exp \xi_3^3 \theta_3)^{-1}} \hat{\xi}_1^1 \dot{\theta}_1 \rangle.
\end{aligned}$$

The calculation of the kinetic energy expression for a manipulator with many degrees of freedom can be facilitated by using data structures such as labeled trees. See [GL87] for further details.

Define

$$M_2^1 = Ad_{(h_{2,1} \exp \xi_2^2 \theta_2)^{-1}}^T \cdot M_2 \cdot Ad_{(h_{2,1} \exp \xi_2^2 \theta_2)^{-1}},$$

$$M_3^1 = Ad_{(h_{3,1} \exp \xi_2^2 \theta_2 \exp \xi_3^3 \theta_3)^{-1}}^T \cdot M_3 \cdot Ad_{(h_{3,1} \exp \xi_2^2 \theta_2 \exp \xi_3^3 \theta_3)^{-1}},$$

and

$$M_3^2 = Ad_{(h_{3,2} \exp \xi_3^3 \theta_3)^{-1}}^T \cdot M_3 \cdot Ad_{(h_{3,2} \exp \xi_3^3 \theta_3)^{-1}},$$

where  $M_j^i, j = 2, 3, i = 1, 2$ , is the inertia tensor of link  $j$  reflected to link  $i$ .

Now summing Eqs (2.59) ~ (2.61) the total kinetic energy can be written

as

$$K = \frac{1}{2} \sum_{i,j}^3 m_{i,j} \dot{\theta}_i \dot{\theta}_j \triangleq \frac{1}{2} \dot{\theta}^T \cdot M(\theta) \cdot \dot{\theta} \quad (2.62)$$

where  $M(\theta) \in \mathbb{R}^{3 \times 3}$  is called the inertia matrix of the manipulator and its entries are given by

$$m_{11} = \langle \hat{\xi}_1^1, (M_1 + M_2^1 + M_3^1) \hat{\xi}_1^1 \rangle;$$

$$m_{22} = \langle \hat{\xi}_2^2, (M_2 + M_3^2) \hat{\xi}_2^2 \rangle;$$

$$m_{33} = \langle \hat{\xi}_3^3, M_3 \hat{\xi}_3^3 \rangle;$$

and

$$m_{12} = m_{21} = \langle \hat{\xi}_2^2, (M_2 + M_3^2) Ad_{(h_{2,1} \exp \xi_2^2 \theta_2)^{-1}} \hat{\xi}_1^1 \rangle;$$

$$m_{13} = m_{31} = \langle \hat{\xi}_3^3, M_3 Ad_{(h_{3,1} \exp \xi_2^2 \theta_2 \exp \xi_3^3 \theta_3)^{-1}} \hat{\xi}_1^1 \rangle;$$

$$m_{23} = m_{32} = \langle \hat{\xi}_3^3, M_3 Ad_{(h_{3,2} \exp \xi_3^3 \theta_3)^{-1}} \hat{\xi}_2^2 \rangle.$$

The Lagrangian equations of motion for the manipulator, in the absence of gravity, are

$$\frac{d}{dt} \frac{\partial K}{\partial \dot{\theta}} - \frac{\partial K}{\partial \theta} = \tau, \quad (2.63)$$

where  $\theta = \begin{bmatrix} \theta_1 \\ \theta_2 \\ \theta_3 \end{bmatrix}$ ,  $\tau = \begin{bmatrix} \tau_1 \\ \tau_2 \\ \tau_3 \end{bmatrix}$  are the joint position and joint torque vector, respectively.

Apply Eq. (2.62) to Eq. (2.63) and rearrange the results, the equations of motion have the form

$$\boxed{M(\theta)\ddot{\theta} + N(\theta, \dot{\theta}) = \tau} \quad (2.64)$$

where

$$N(\theta, \dot{\theta}) = \left( \frac{d}{dt} M(\theta) \right) \dot{\theta} - \frac{1}{2} \dot{\theta}^T \frac{\partial M(\theta)}{\partial \theta} \dot{\theta} \quad (2.65)$$

and its entries are calculated as follows:

$$\begin{aligned} N_1(\theta, \dot{\theta}) &= \sum_i \left( \frac{d}{dt} m_{1i}(\theta) \right) \dot{\theta}_i - \frac{1}{2} \dot{\theta}^T \frac{\partial}{\partial \theta_1} M(\theta) \dot{\theta} \\ &= \sum_i \left( \frac{d}{dt} m_{1i}(\theta) \right) \dot{\theta}_i \quad (\text{since } M(\theta) \text{ is independent of } \theta_1) \end{aligned}$$

and

$$\begin{aligned} \frac{d}{dt} m_{11}(\theta) &= \langle \hat{\xi}_1^1, 2M_2^1 \cdot ad_{\hat{\xi}_1^1}(Ad_{h_{2,1}} \hat{\xi}_2^2 \dot{\theta}_2) \rangle \\ &\quad + \langle \hat{\xi}_1^1, 2M_3^1 \cdot ad_{\hat{\xi}_1^1}(Ad_{h_{3,1}} \exp \xi_2^2 \theta_2 \hat{\xi}_2^2 \dot{\theta}_3 + Ad_{h_{2,1}} \hat{\xi}_2^2 \dot{\theta}_2) \rangle \\ &\triangleq \frac{\partial m_{11}}{\partial \theta_2} \dot{\theta}_2 + \frac{\partial m_{11}}{\partial \theta_3} \dot{\theta}_3; \end{aligned} \quad (2.66)$$

$$\begin{aligned} \frac{d}{dt} m_{12}(\theta) &= \langle \hat{\xi}_2^2, M_3^2 Ad_{(h_{2,1} \exp \xi_2^2 \theta_2)^{-1}} \cdot ad_{\hat{\xi}_1^1}(2Ad_{h_{3,1}} \exp \xi_2^2 \theta_2 \hat{\xi}_3^3 \dot{\theta}_3 + Ad_{h_{2,1}} \hat{\xi}_2^2 \dot{\theta}_2) \rangle \\ &\triangleq \frac{\partial m_{12}}{\partial \theta_2} \dot{\theta}_2 + \frac{\partial m_{12}}{\partial \theta_3} \dot{\theta}_3; \end{aligned} \quad (2.67)$$

$$\begin{aligned} \frac{d}{dt} m_{13}(\theta) &= \langle \hat{\xi}_3^3, M_3 Ad_{(h_{3,1} \exp \xi_2^2 \theta_2 \exp \xi_3^3 \theta_3)^{-1}} \cdot ad_{\hat{\xi}_1^1}(Ad_{h_{3,1}} \exp \xi_2^2 \theta_2 \hat{\xi}_3^3 \dot{\theta}_3 + Ad_{h_{2,1}} \hat{\xi}_2^2 \dot{\theta}_2) \rangle \\ &\triangleq \frac{\partial m_{13}}{\partial \theta_2} \dot{\theta}_2 + \frac{\partial m_{13}}{\partial \theta_3} \dot{\theta}_3. \end{aligned} \quad (2.68)$$

$$\begin{aligned} N_2(\theta, \dot{\theta}) &= \sum_i^3 \frac{d}{dt} m_{2i}(\theta) \dot{\theta}_i - \frac{1}{2} \dot{\theta}^T \left( \frac{\partial}{\partial \theta_2} M(\theta) \right) \dot{\theta} \\ &= \frac{dm_{22}}{dt} \dot{\theta}_2 + \frac{dm_{23}}{dt} \dot{\theta}_3 - \frac{1}{2} \frac{\partial m_{11}}{\partial \theta_2} \dot{\theta}_1^2 + \left( \frac{\partial m_{12}}{\partial \theta_3} - \frac{\partial m_{13}}{\partial \theta_2} \right) \dot{\theta}_1 \dot{\theta}_3 \end{aligned} \quad (2.69)$$

where we have used the fact that

$$\frac{dm_1}{dt} = \frac{\partial m_{12}}{\partial \theta_2} \dot{\theta}_2 + \frac{\partial m_{12}}{\partial \theta_3} \dot{\theta}_3. \quad (2.70)$$

From Eqs (2.66) ~ (2.68),  $\frac{\partial m_{1i}}{\partial \theta_j}$ ,  $i = 1, 2, 3$ ,  $j = 2, 3$ , can be obtained by comparing the coefficients. Thus, we only need to calculate  $\frac{d}{dt}m_{22}(\theta)$  and  $\frac{d}{dt}m_{23}(\theta)$ . But,

$$\frac{d}{dt}m_{22}(\theta) = \langle \hat{\xi}_2^2, M_3^2 \cdot ad_{\hat{\xi}_2^2}(2Ad_{h_{3,2}}\hat{\xi}_3^3\dot{\theta}_3) \rangle;$$

and

$$\frac{d}{dt}m_{23}(\theta) = \langle \hat{\xi}_3^3, M_3 \cdot ad_{\hat{\xi}_2^2}(Ad_{h_{3,2}}\hat{\xi}_3^3\dot{\theta}_3) \rangle.$$

Finally, we have

$$\begin{aligned} N_3(\theta, \dot{\theta}) &= \sum_i^3 \frac{d}{dt}m_{3i}(\theta)\dot{\theta}_i - \frac{1}{2}\dot{\theta}^T \left( \frac{\partial}{\partial \theta_3} M(\theta) \right) \dot{\theta} \\ &= \left( \frac{\partial m_{13}}{\partial \theta_2} - \frac{\partial m_{12}}{\partial \theta_3} \right) \dot{\theta}_1 \dot{\theta}_2 - \frac{1}{2} \frac{\partial m_{22}}{\partial \theta_3} \dot{\theta}_2^2 - \frac{1}{2} \frac{\partial m_{11}}{\partial \theta_3} \dot{\theta}_1^2 \end{aligned} \quad (2.71)$$

whereas

$$\frac{d}{dt}m_{33}(\theta) = 0.$$

This completely specifies all entries of  $N(\theta, \dot{\theta})$ , which is sometimes called the vector of centrifugal and Coriolis forces.

## 2.5 Conclusion

This chapter studied some of the fundamental concepts concerning rigid motions of  $\mathbb{R}^3$ , manipulator kinematics and manipulator dynamics.

Since the configuration space of the end-effector of a manipulator forms a Lie group, it is natural to apply Lie group theory to study manipulator kinematics. In particular, left translation is used to define the body velocity of a rigid body. If right translation were used, we would have obtained the spatial velocity of a rigid body (See [MW87] for further details). The adjoint map serves as a similarity transformation for velocities under change of coordinate frames. Further details about the Euclidean group can be found in ([Lon85] and [Li87]).

The forward kinematic map is written as a product of exponentials, where the exponents are the twists representing the joint axes of the manipulator. This

notation, in our view, is more intuitive and geometric than the Denavit-Hartenberg notation. Using the exponential formula to solve the inverse kinematics and study manipulator singularities have been discussed in [Pad86]. We have used the exponential formula and left translation to define the manipulator Jacobian, where the columns of the Jacobian matrix are twists representing the joint axes viewed by an observer sitting at the end-effector frame. Thus, the Jacobian matrix can be constructed using a camera at the end-effector.

The exponential notation is also used to formulate the Newton-Euler equations of motion for a manipulator. The infinitesimal generator,  $ad$ , of the adjoint map (or action),  $Ad$ , gives the Coriolis and centrifugal forces in the dynamics equations. Thus, it can be viewed as the generalized cross product to  $\mathbb{R}^6$ .

We conjecture from Section 2.4.3 that the use of the exponential formula may facilitate deriving symbolically the equations of motion because the terms involved are the inertia tensors, the adjoint map and its infinitesimal generator instead of the *sine* and *cosine* functions. We are currently considering this possibility along with the work of T. Kane ([KL83]), R. Featherstone ([Fea84]) and R. Grossman ([GL87]).

# Bibliography

- [AM78] R. Abraham and J. Marsden. *Foundations of Mechanics*. Benjamin/Cummings Publishing Company, 2nd edition edition, 1978.
- [BR79] O. Bottema and B. Roth. *Theoretical Kinematics*. North-Holland Publishing Co., 1979.
- [Bro83] R. W. Brockett. Robotic manipulators and the product of exponentials formula. In *Proceedings of the MTNS-83 International Symposium*, pages 120–129, 1983.
- [Cra86] J. Craig. *Introduction to Robotics, Mechanics and Control*. Addison-Wesley Publishing Company, 1986.
- [Fea84] R. Featherstone. *Robot Dynamics Algorithms*. Kluwer Academic Publishers, 1984.
- [GL87] R. Grossman and R. Larson. *Labeled Trees and Algebra of Differential Operators*. Technical Report, Math Dept., University of California at Berkeley, 1987.
- [KL83] T. R. Kane and D.A. Levinson. The use of kane's dynamical equations in robotics. *International Journal of Robotics Research*, 2(3), 1983.
- [Li87] Z.X. Li. *Geometrical Considerations of Robot Kinematics*. Technical Report, EECS Dept., University of California at Berkeley, preprint, 1987.
- [Lon85] J. Loncaric. *Geometric analysis of compliant mechanism in robotics*. PhD thesis, Division of Applied Sciences, Harvard University, 1985.

- [MW87] J.E. Marsden and A. Weinstein. *Reduction and semi-direct product*, page .  
AMS Publishing Co., 1987.
- [Pad86] B. Paden. *Kinematics and control of robot manipulators*. PhD thesis,  
Department of Electrical Engineering and Computer Science, University  
of California, Berkeley, 1986.
- [War71] F. Warner. *Foundations of Differentiable Manifolds and Lie Groups*. Scott,  
Foresman, Glenview, Ill., 1971.

## Chapter 3

# Robot Hand Kinematics

### 3.1 Introduction

In the second chapter we have defined a robot hand as a set of open kinematic chains, or fingers, connected in parallel to a common base, called the palm. We now define a robot hand system (or a hand manipulation system) to be a robot hand together with an object to be manipulated. We assume that whenever a finger contacts the object the contact occurs at the fingertip (i.e., the surface of the last link) only.

Given a robot hand system where the object is in grasp by the fingers, a typical task requires the object to be manipulated so that either a prescribed trajectory can be followed or a new grasp configuration can be attained. To fully understand this manipulation process, we need to explore the basic kinematic relations underlying a robot hand system. A kinematic relation describes the dependence of one set of motion parameters on another such set due to the geometry and mechanics of the physical world. Two prominent examples of a kinematic relation we have encountered so far are the *forward kinematic map* of a manipulator which relates the position and orientation of the end-effector to the joint angles of the manipulator, and the *manipulator Jacobian* which arises from the forward kinematic map and relates the end-effector velocity to the joint velocity.

There are three basic kinematic relations within a robot hand system: (1) *The hand Jacobian* which relates the velocity of the finger joints to the velocity of the fingertips. Since each finger is an open kinematic chain, the hand Jacobian

arises naturally from the forward kinematic map of the fingers; (2) *the transpose of the grip Jacobian* which relates the velocity of the object to the velocity of the contact points and (3) *the kinematics of contact* which describes the motion of the contact points over the surface of the object and the fingertips in response to relative motions of the fingers and the object.

Using the machinery developed in the previous chapter and methods from differential geometry, this chapter attempts to give a detailed account of these basic kinematic relations.

## **The Geometry of a Surface**

A robot hand is designed to handle objects of varied shapes and the fingertips themselves may have different shapes. When a finger is brought into contact with an object, the geometry of the fingertip and the object may affect, in a significant way, the contact forces that can be transmitted and the relative motions that can be constrained. In order to systematically analyze these effects, we need to study the geometry of a surface, one of the most extensively studied topics in differential geometry. The readers are referred to ([Spi74], [Kli78]) for further references. To describe a surface, we first cover it with local coordinate charts. Then locally a surface is characterized by the metric tensor, curvature form and the connection form.

## **The Kinematics of Contact**

The kinematics of contact describes the motion of a point of contact over the surface of two contacting objects in response to a relative motion of these objects. The contact equations, derived independently by D. Montana ([Mon86]) and C. Cai and B. Roth ([CR87]), embody this relationship. Early work in this subject with simplifying assumptions include J. Kerr ([Ker85]), J. Trinkle ([Tri87]) and M. Cutkosky ([Cut86]). We present the results of D. Montana in Section 3.3.

## **The Kinematics of a Robot Hand System**

In addition to the contact equations derived by D. Montana, the grip Jacobian, introduced by K. Salisbury ([MS85]) constitutes another basic kinematic

relation in a robot hand system. We derive in Section 3.4 the grip Jacobian and the hand Jacobian. We argue, using our understanding of contact constraints, that the contact velocity determined by the transpose of the grip Jacobian must equal to the contact velocity determined by the hand Jacobian in order to maintain a grasp. We also use the dual notion to explain how forces are transmitted in a robot hand system. Finally, we summarize all these kinematic relations in a table and use them to explain the operation of a robot hand system.

### 3.2 The Geometry of a Surface

This section reviews briefly the geometry of a surface. The notation used here closely follows that of ([Kli78] and [MP78]).

**Definition 3.1** *A space curve is the image of a  $C^2$  map  $c : I \rightarrow \mathbb{R}^3$ , where  $I$  is an interval. The pair  $(c, I)$  is called a parameterization of the space curve.  $c$  is regular if  $\dot{c}(t) \neq 0, \forall t \in I$ .*

**Notation 3.1**  *$U$  will always denote an open subset of  $\mathbb{R}^2$ . A point in  $U$  will be denoted by  $u \in \mathbb{R}^2$ , or by  $(u_1, u_2) \in \mathbb{R} \times \mathbb{R}$ , or  $(u, v) \in \mathbb{R} \times \mathbb{R}$ . Let  $f : U \rightarrow \mathbb{R}^3$  be a differentiable map,  $df_u : T_u\mathbb{R}^2 \rightarrow T_{f(u)}\mathbb{R}^3$  denotes the tangent map of  $f$ , and  $f_u, f_v$  denote the partial derivatives of  $f$  with respect to  $u$  and  $v$ , respectively.*

**Definition 3.2** *An embedded surface (or an embedded 2 manifold) in  $\mathbb{R}^3$  is a subset  $S \subset \mathbb{R}^3$  such that for every point  $s \in S$ , there exists an open subset  $S_s$  of  $S$  with the property (1)  $s \in S_s$ , (2)  $S_s$  is the image of a  $C^3$  map  $f : U \rightarrow \mathbb{R}^3$ , where  $f_u \times f_v \neq 0, \forall (u, v) \in U$ , and (3)  $f : U \rightarrow S_s \subset \mathbb{R}^3$  is a diffeomorphism.*

$S_s$  is called a coordinate patch and the pair  $(f, U)$  is called a (local) coordinate system of  $S$ . The coordinates of a point  $s \in S_s$  are given by  $(u, v) = f^{-1}(s)$ . The vectors  $E_1 = f_u, E_2 = f_v$  are called the coordinate vector fields of  $S$ , and they together form a basis for  $T_{f(u)}S$ . The collection of coordinate patches  $\{S_s\}$  which covers  $S$ , i.e.,  $S = \cup S_s$ , is called an atlas of  $S$ . By a curve in  $S$  we mean a curve  $c : I \rightarrow \mathbb{R}^3$ , which can be expressed as  $f \circ u(t)$  for some curve  $u : I \rightarrow U$  in  $U$ .

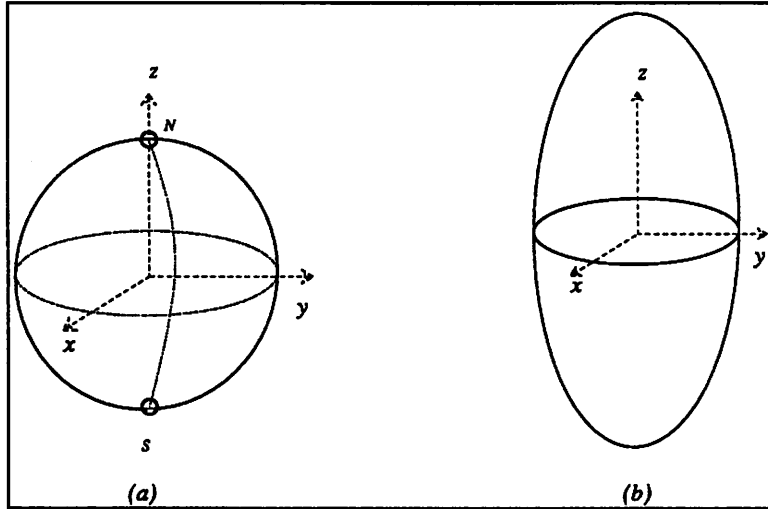


Figure 3.1: (a) A sphere of radius  $\rho$ , (b) A football.

**Example 3.1** The sphere  $S$  of radius  $\rho$  is an embedded surface. To prove this, let  $U = \{(u, v) \in \mathbb{R}^2, -\frac{\pi}{2} < u < \frac{\pi}{2}, -\pi < v < \pi\}$  and consider the following coordinate systems

$$f : U \longrightarrow \mathbb{R}^3 : (u, v) \longmapsto (\rho \cos u \cos v, -\rho \cos u \sin v, \rho \sin u) \quad (3.1)$$

and

$$\hat{f} : U \longrightarrow \mathbb{R}^3 : (u, v) \longmapsto (-\rho \cos u \cos v, \rho \sin u, \rho \cos u \sin v).$$

The image of  $f$  is the sphere minus the south pole, north pole and an arc of the great circle connecting them (see Figure 3.1(a)), i.e.,

$$f(U) = S - \{0, 0, \pm\rho\} \cup \{-\rho \cos u, 0, \rho \sin u\}, -\pi/2 < u < \pi/2.$$

Similarly, the image of  $\hat{f}$  is

$$\hat{f}(U) = S - \{0, \pm\rho, 0\} \cup \{\rho \cos u, \rho \sin u, 0\}, -\pi/2 < u < \pi/2.$$

The partial derivatives of  $f$  and  $\hat{f}$  are

$$f_u = (-\rho \sin u \cos v, \rho \sin u \sin v, \rho \cos u)$$

$$f_v = (-\rho \cos u \sin v, -\rho \cos u \cos v, 0)$$

and

$$\hat{f}_u = (\rho \sin u \cos v, \rho \cos u, -\rho \sin u \sin v)$$

$$\hat{f}_v = (\rho \cos u \sin v, 0, \rho \cos u \cos v)$$

Clearly,  $f_u \times f_v \neq 0$  and  $\hat{f}_u \times \hat{f}_v \neq 0$ ,  $\forall (u, v) \in U$ . Moreover,  $S_1 = f(U)$  and  $S_2 = \hat{f}(U)$  cover  $S$ . Thus,  $S$  is an embedded surface.  $\square$

We denote by  $S^2$  the unit sphere (i.e.,  $\rho = 1$ ) of  $\mathbb{R}^3$ .

**Example 3.2** The football  $x^2 + y^2 + \frac{z^2}{c^2} = 1$  (Figure 3.1(b)) can be parametrized by the following coordinate system

$$f : U \longrightarrow \mathbb{R}^3 : (u, v) \longmapsto (\cos u \cos v, -\cos u \sin v, c \sin u)$$

and

$$\hat{f} : U \longrightarrow \mathbb{R}^3 : (u, v) \longmapsto (-\cos u \cos v, \sin u, c \cos u \sin v)$$

where  $U$  is given by the previous example.  $\square$

**Definition 3.3** Let  $S$  be an embedded surface and  $f : U \longrightarrow \mathbb{R}^3$  a coordinate system. The inner product on  $\mathbb{R}^3$  induces a quadratic form on  $T_{f(u)}S$  by restriction. This form is called the first fundamental form and is denoted by  $I$  or  $I_u$ . Relative to the coordinate basis  $\{E_1, E_2\}$ ,  $I_u$  is represented by the following  $2 \times 2$  matrix

$$I_u = \begin{bmatrix} f_u \cdot f_u & f_u \cdot f_v \\ f_v \cdot f_u & f_v \cdot f_v \end{bmatrix} \triangleq \begin{bmatrix} g_{11} & g_{12} \\ g_{21} & g_{22} \end{bmatrix}.$$

$(f, U)$  is called an orthogonal coordinate system if  $g_{12} = g_{21} = 0$ ,  $\forall (u, v) \in U$ .

The following proposition shows that a surface admits an orthogonal coordinate system.

**Proposition 3.1** Suppose that  $X_1$  and  $X_2$  are tangential vector fields on  $f : U \longrightarrow \mathbb{R}^3$  which are linearly independent at each  $u \in U$ . Then, in a neighborhood  $U_0$  of each  $u_0$  we can change variables  $\psi : V_0 \longrightarrow U_0$  so that  $f \circ \psi = \tilde{f}$  has coordinate vector fields  $\tilde{E}_i$  propositional to  $X_i$ .

**Remark 3.1** (1) Let  $X_1 = E_1$  and  $X_2 = E_2 - \langle E_2, E_1 \rangle \frac{E_1}{|E_1|^2}$ , then  $\{\tilde{E}_1, \tilde{E}_2\}$  gives an orthogonal coordinate system for  $S$ . (2) If  $U$  is simply connected, it is possible to find a globally defined change of variables  $\psi : V \longrightarrow U$ , satisfying the theorem.

**Proof.** (1) Consider the vector fields  $\bar{X}_i(\mathbf{u}) = df_u^{-1}X_i(\mathbf{u})$  defined for each  $\mathbf{u} \in U$ . Suppose we could find a change of variables  $\eta : U \rightarrow V$ ,  $\eta(\mathbf{u}) = (v^1(\mathbf{u}), v^2(\mathbf{u}))$  for which

$$dv^1(\bar{X}_2) = 0, \quad dv^2(\bar{X}_1) = 0. \quad (3.2)$$

Then, in terms of the canonical basis vector fields  $(\bar{e}_1, \bar{e}_2)$  on  $V$ ,  $d\eta_u(\bar{X}_1) = dv^1(\bar{X}_1)\bar{e}_1 + 0$  and  $d\eta_u(\bar{X}_2) = 0 + dv^2(\bar{X}_2)\bar{e}_2$ . Consequently, if  $\psi = \eta^{-1} : V \rightarrow U$ , then  $\bar{f} = f \circ \psi$  satisfies  $\bar{E}_i = d\bar{f}_v(\bar{e}_i) = df_{\psi(v)} \circ d\psi_v(\bar{e}_i) = \alpha_i(v)X_i$ , where  $\alpha_i = (dv^i(\bar{X}_i))^{-1}$ . Thus,  $\psi$  is the required change of variables. Note that since  $\{\bar{X}_1, \bar{X}_2\}$  are linearly independent,  $\alpha_i$  is well defined.

(2). Let  $\{e_1, e_2\}$  be the canonical basis vector fields on  $U$  and write  $\bar{X}_i(\mathbf{u}) = \sum_{k=1}^2 \xi_i^k e_k$ . By the standard existence theorem for ordinary differential equations, we may assert the existence, locally, of integral curves  $c_i(t)$  of  $\bar{X}_i(\mathbf{u})$ . That is, for  $|t|$  sufficiently small, we may find curves  $c_1(t), c_2(t)$  in  $V$  with  $c_i(0) = \mathbf{u}_0$  and  $\dot{c}_i(t) = \bar{X}_i(c_i(t))$ . We wish to solve (3.2) which is equivalent to

$$\frac{\partial v^1}{\partial u^1} \xi_2^1(\mathbf{u}) + \frac{\partial v^1}{\partial u^2} \xi_2^2(\mathbf{u}) = 0, \quad (3.3)$$

$$\frac{\partial v^2}{\partial u^1} \xi_1^1(\mathbf{u}) + \frac{\partial v^2}{\partial u^2} \xi_1^2(\mathbf{u}) = 0, \quad (3.4)$$

with the initial conditions  $v^i(c_i(t)) = t$ . A standard result in partial differential equations allows us to do this in a neighborhood of  $\mathbf{u}_0$ , provided that for (i)  $\dot{c}_1(t)$  and  $\bar{X}_2(c_1(t))$  are linearly independent and for (ii)  $\dot{c}_2(t)$  and  $\bar{X}_1(c_2(t))$  are linearly independent. But  $\dot{c}_i(t) = \bar{X}_i(c_i(t))$ , so these conditions are satisfied by hypothesis. Also,  $t = v^i(c_i(t))$ ,  $i \neq j$ , implies that

$$1 = \frac{d}{dt}(v^i(c_i(t))) = dv^i(\dot{c}_i(t)) = dv^i(\bar{X}_i(c_i(t))).$$

Therefore  $dv^i \neq 0$ ,  $i = 1, 2$ . ■

One can check that the coordinate systems of the sphere given by Example 3.1 and that of the football given by Example 3.2 are both orthogonal. From now on, we will assume, without loss of generality, that the surface in consideration is covered by orthogonal coordinate systems.

**Definition 3.4** A Gauss map of a surface  $S$  is a continuous map  $n : S \rightarrow S^2$ , such that  $n(s)$  is normal to  $S$ . We say that  $S$  is orientable if a Gauss map exists.

We will also use  $n$  to denote the composition map  $n \circ f : U \rightarrow S^2$  and  $d_u n : T_u \mathbb{R}^2 \rightarrow T_{f(u)} \mathbb{R}^3$  the tangent map of  $n$ . The quadratic form

$$-d_u n \cdot df_u : T_u \mathbb{R}^2 \times T_u \mathbb{R}^2 \rightarrow \mathbb{R}$$

is called the second fundamental form of  $f$  at  $\mathbf{u}$ , and is denoted by  $\Pi$  (or  $\Pi_u$ ). The matrix representation of  $\Pi_u$  with respect to the canonical basis  $\{e_1, e_2\}$  of  $T_u \mathbb{R}^2$  and the coordinate basis  $\{E_1, E_2\}$  of  $T_{f(u)} S$  is

$$\Pi_u = - \begin{bmatrix} n_u \cdot f_u & n_u \cdot f_v \\ n_v \cdot f_u & n_v \cdot f_v \end{bmatrix} \triangleq \begin{bmatrix} h_{11} & h_{12} \\ h_{21} & h_{22} \end{bmatrix}.$$

Note that  $n \cdot f_u = 0$  implies that  $h_{11} = n \cdot f_{uu}$  and etc.

**Example 3.3** Consider the sphere  $S$  of Example 3.1. Choose the outward Gauss map

$$n : S \rightarrow S^2 : s \mapsto s/\rho.$$

Thus, relative to the coordinate system  $(f, U)$  given by (3.1), the first and the second fundamental forms are

$$I = \begin{bmatrix} \rho^2 & 0 \\ 0 & \rho^2 \cos^2 u \end{bmatrix} \quad \text{and} \quad II = \begin{bmatrix} \rho & 0 \\ 0 & \rho \cos^2 u \end{bmatrix}.$$

**Definition 3.5** Consider a surface  $S$  with Gauss map  $n$ , and a coordinate system  $(f, U)$ . We define the normalized Gauss frame at a point  $\mathbf{u} \in U$  as the coordinate frame with origin at  $f(\mathbf{u})$  and coordinate axes

$$\mathbf{x}(\mathbf{u}) = \frac{E_1}{|E_1|}, \quad \mathbf{y}(\mathbf{u}) = \frac{E_2}{|E_2|}, \quad \mathbf{z}(\mathbf{u}) = n \circ f(\mathbf{u}). \quad (3.5)$$

Since  $\{\mathbf{x}(\mathbf{u}), \mathbf{y}(\mathbf{u})\}$  forms an orthonormal basis for  $T_{f(\mathbf{u})} S$  at each  $\mathbf{u} \in U$ , the second fundamental form can be expressed with respect to this basis and the result, denoted by  $K(\mathbf{u})$ , is given by

$$K(\mathbf{u}) = M^{-t} II_u M^{-1} \quad (3.6)$$

where

$$M = \begin{bmatrix} |f_u| & 0 \\ 0 & |f_v| \end{bmatrix} = I_u^{1/2} \quad (3.7)$$

is called the metric tensor. Note that

$$K(\mathbf{u}) = [\mathbf{x}(\mathbf{u}), \mathbf{y}(\mathbf{u})]^T [\mathbf{z}_u / \|f_u\|, \mathbf{z}_v / \|f_v\|].$$

E. Cartan ([Car47]) calls  $K(\mathbf{u})$  the curvature form of  $S$  at  $\mathbf{u}$ .

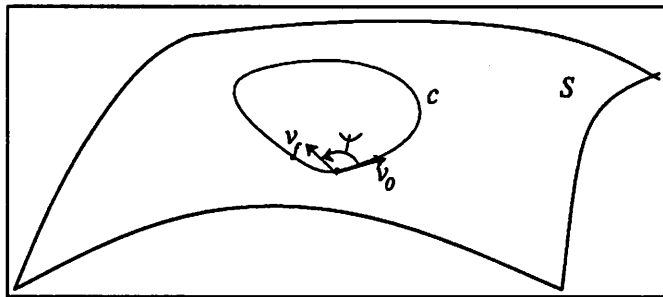


Figure 3.2: Holonomy angle of a closed path in  $S$

**Definition 3.6** Let  $S_o$  be a coordinate patch of  $S$ , with an orthogonal coordinate system  $(f, U)$ . At a point  $s_o \in S_o$ , the connection form  $T$  is a  $1 \times 2$  matrix defined by

$$T = \mathbf{y}(\mathbf{u})^t [\mathbf{x}_u(\mathbf{u})/|\mathbf{f}_u|, \mathbf{x}_v(\mathbf{u})/|\mathbf{f}_v|],$$

Consider Figure 3.2. Let  $c(t) = f \circ u(t)$ ,  $t \in [0, t_f]$ , be a closed path in  $S_o$ . Pick a tangent vector,  $v_0$ , to  $S$  at  $c(0)$  and parallel translate it along  $c$  back to the starting point.<sup>1</sup> Call the new vector  $v_f$ . If  $S_o$  is not flat then  $v_f$  is usually rotated from  $v_0$  by an angle  $\psi$ .  $\psi$  is called the holonomy angle of the path  $c$ . The following formula shows that the holonomy angle is given by the line integral of the connection form (see [Li89] for the proof.).

$$\psi = \int_c T M \dot{u} dt.$$

Gauss-Bonnet Theorem ([Tho78]) indicates that  $\psi$  not only depends on the path  $c$ , but also on the area enclosed by  $c$ .

To summarize, a surface  $S$  locally is described by the metric tensor,  $M$ , curvature form,  $K$ , and connection form,  $T$ . These geometric quantities can be explicitly obtained once a coordinatization of the surface is given.

**Example 3.4** Embed the plane in  $\mathbb{R}^3$  by the following parameterization

$$f : U \subset \mathbb{R}^2 \longrightarrow \mathbb{R}^3 : (u, v) \longmapsto (u, v, 0).$$

The axes of the Gaussian frame are

$$\mathbf{x}(\mathbf{u}) = \begin{bmatrix} 1 \\ 0 \\ 0 \end{bmatrix}, \mathbf{y}(\mathbf{u}) = \begin{bmatrix} 0 \\ 1 \\ 0 \end{bmatrix} \text{ and } \mathbf{z}(\mathbf{u}) = \begin{bmatrix} 0 \\ 0 \\ 1 \end{bmatrix}.$$

<sup>1</sup>Recall from [Kli78], that to parallel translate a vector along a curve one has to solve the geodesic equation.

The curvature form, connection form and metric tensor are

$$K = \begin{bmatrix} 0 & 0 \\ 0 & 0 \end{bmatrix}, T = [0, 0], M = \begin{bmatrix} 1 & 0 \\ 0 & 1 \end{bmatrix}.$$

□

**Example 3.5** Consider the sphere  $S$  of radius  $\rho$ . Let  $S_1 = f(U)$  be the coordinate patch of  $S$  studied in Example 3.1. The Gaussian frame at a point  $s \in S_1$  is given by

$$\mathbf{x}(\mathbf{u}) = \begin{bmatrix} -\sin u \cos v \\ \sin u \sin v \\ \cos u \end{bmatrix}, \mathbf{y}(\mathbf{u}) = \begin{bmatrix} -\sin v \\ -\cos v \\ 0 \end{bmatrix} \text{ and } \mathbf{z}(\mathbf{u}) = \begin{bmatrix} \cos u \cos v \\ -\cos u \sin v \\ \sin u \end{bmatrix}.$$

The curvature form, connection form and metric tensor are given by

$$K = \begin{bmatrix} 1/\rho & 0 \\ 0 & 1/\rho \end{bmatrix}, T = [0 - \tan u/\rho], \text{ and } M = \begin{bmatrix} \rho & 0 \\ 0 & \rho \cos u \end{bmatrix}.$$

□

### 3.3 The Kinematics of Contact

This section studies the kinematics of contact. The kinematics of contact describes the motion of a point of contact over the surface of two contacting objects in response to a relative motion of these two objects. Using concepts from the previous section, we derive a set of equations, called the contact equations, that embody this relationship. The results of this section are due primarily to Montana ([Mon86]).

We now consider the two objects that move while maintaining contact with each other (see Figure 3.3). Choose reference frames  $C_{r1}$  and  $C_{r2}$  fixed relative to *obj1* and *obj2*, respectively. Let  $S_1 \subset \mathbb{R}^3$  and  $S_2 \subset \mathbb{R}^3$  be the embeddings of the surfaces of *obj1* and *obj2* relative to  $C_{r1}$  and  $C_{r2}$ , respectively. Let  $n_1$  and  $n_2$  be the Gauss maps (outward normal) for  $S_1$  and  $S_2$ . Choose atlases  $\{S_{1,i}\}_{i=1}^{m_1}$  and  $\{S_{2,i}\}_{i=1}^{m_2}$  for  $S_1$  and  $S_2$ . Let  $(f_{1,i}, U_{1,i})$  be an orthogonal right handed coordinate system for  $S_{1,i}$  with Gauss map  $n_1$ . Similarly, let  $(f_{2,i}, U_{2,i})$  be an orthogonal, right-handed coordinate system for  $S_{2,i}$  with  $n_2$ .

Let  $c_1(t) \in S_1$  and  $c_2(t) \in S_2$  be the positions at time  $t$  of the point of contact relative to  $C_{r,1}$  and  $C_{r,2}$ , respectively. We will restrict our attention to an interval  $I$  such that  $c_1(t) \in S_{1,i}$  and  $c_2(t) \in S_{2,j}$  for all  $t \in I$  and some  $i$  and some  $j$ . The coordinate systems  $(f_{1,i}, U_{1,i})$  and  $(f_{2,j}, U_{2,j})$  induce a normalized Gaussian frame at all points in  $S_{1,i}$  and  $S_{2,j}$ . We define the contact frames,  $C_{c_1}$  and  $C_{c_2}$  as the coordinate frames that coincide with the normalized Gauss frames at  $c_1(t)$  and  $c_2(t)$ , respectively, for all  $t \in I$ . We also define a continuous family of coordinate frames, two for each  $t \in I$ , as follows. Let the local frames at time  $t$ ,  $C_{l_1}$  and  $C_{l_2}$ , be coordinate frames fixed relative to  $C_{r,1}$  and  $C_{r,2}$ , respectively, that coincide at time  $t$  with the normalized Gaussian frames at  $c_1(t)$  and  $c_2(t)$  (see Figure 3.3).

We now define the parameters that describe the 5 degrees of freedom for the motion of the point of contact. The coordinates of the point of contact relative to the coordinate system  $(f_{1,i}, U_{1,i})$  and  $(f_{2,j}, U_{2,j})$  are given by  $u_1(t) = f_{1,i}^{-1}(c_1(t)) \in U_{1,i}$  and  $u_2(t) = f_{2,j}^{-1}(c_2(t)) \in U_{2,j}$ . These account for 4 degrees of freedom. The final parameter is the angle of contact  $\psi(t)$ , which is defined as the angle between the  $x$ -axes of  $C_{l_1}$  and  $C_{l_2}$ . We choose the sign of  $\psi$  so that a rotation of  $C_{l_1}$  through  $-\psi$  around its  $z$  axis aligns the  $x$ -axis.

We describe the motion of *obj1* relative to *obj2* at time  $t$ , using the local coordinate frames  $C_{l_1}$  and  $C_{l_2}$ . Let  $v_x, v_y$  and  $v_z$  be the components of translation velocity of  $C_{l_1}$  relative to  $C_{l_2}$  at time  $t$ . Similarly, let  $w_x, w_y$  and  $w_z$  be the components of rotational velocity.

The symbols  $K_1, T_1$  and  $M_1$  represent, respectively, the curvature form, connection form and metric tensor at time  $t$  at the point  $c_1(t)$  relative to the coordinate system  $(f_{1,i}, U_{1,i})$ . We can analogously define  $K_2, T_2$  and  $M_2$ . We also let

$$R_\psi = \begin{bmatrix} \cos \psi & -\sin \psi \\ -\sin \psi & -\cos \psi \end{bmatrix}, \quad \tilde{K}_2 = R_\psi^T K_2 R_\psi.$$

Note that  $\tilde{K}_2$  is the curvature of *obj2* at the point of contact relative to the  $x$ - and  $y$ -axes of  $C_{l_1}$ . Call  $K_1 + \tilde{K}_2$  the relative curvature form.

The following contact equations that describe motion of the point of contact over the surface of *obj1* and *obj2* in response to a relative motion between these objects are due to Montana ([Mon86]).

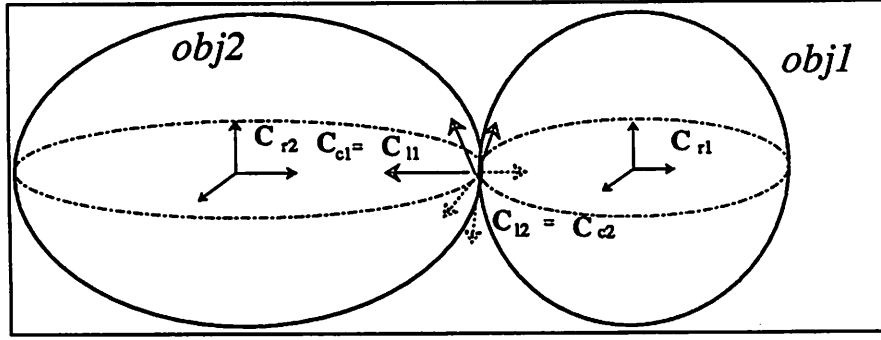


Figure 3.3: Showing the definitions of the coordinate frames of two bodies in contact.

**Theorem 3.1** (*Kinematic equations of contact*) *At a point of contact, if the relative curvature form is invertible, then the point of contact and angle of contact evolve according to*

$$\dot{u}_1 = M_1^{-1}(K_1 + \tilde{K}_2)^{-1} \left( \begin{bmatrix} -w_y \\ w_x \end{bmatrix} - \tilde{K}_2 \begin{bmatrix} v_x \\ v_y \end{bmatrix} \right), \quad (3.8)$$

$$\dot{u}_2 = M_2^{-1}R_\psi(K_1 + \tilde{K}_2)^{-1} \left( \begin{bmatrix} -w_y \\ w_x \end{bmatrix} + K_1 \begin{bmatrix} v_x \\ v_y \end{bmatrix} \right), \quad (3.9)$$

$$\dot{\psi} = w_z + T_1 M_1 \dot{u}_1 + T_2 M_2 \dot{u}_2, \quad (3.10)$$

$$0 = v_z. \quad (3.11)$$

**Proof.** Since  $C_{l1}(t)$  is fixed relative to  $C_{r1}$ , the velocity of  $C_{c1}$  relative to  $C_{r1}$ , according to Corollary 2.2, is the same as the velocity of  $C_{c1}$  relative to  $C_{l1}$ .

$$\begin{bmatrix} v_{c1,r1} \\ w_{c1,r1} \end{bmatrix} = \begin{bmatrix} v_{c1,l1} \\ w_{c1,l1} \end{bmatrix}. \quad (3.12)$$

Similarly, we have

$$\begin{bmatrix} v_{c2,r2} \\ w_{c2,r2} \end{bmatrix} = \begin{bmatrix} v_{c2,l2} \\ w_{c2,l2} \end{bmatrix}. \quad (3.13)$$

At time  $t$  the position and orientation of  $C_{c1}$  relative to  $C_{l1}(t)$  are  $r_{c1,l1} = 0$  and  $R_{c1,l1} = Id$ . Proposition 2.3 states that

$$\begin{bmatrix} v_{c1,l2} \\ w_{c1,l2} \end{bmatrix} = \begin{bmatrix} v_{c1,l1} \\ w_{c1,l1} \end{bmatrix} + \begin{bmatrix} v_{l1,l2} \\ w_{l1,l2} \end{bmatrix}. \quad (3.14)$$

Since  $r_{c1,c2} = 0$ , we have

$$\begin{bmatrix} v_{c1,l2} \\ w_{c1,l2} \end{bmatrix} = \begin{bmatrix} R_{c1,c2}^T & 0 \\ 0 & R_{c1,c2}^T \end{bmatrix} \begin{bmatrix} v_{c2,l2} \\ w_{c2,l2} \end{bmatrix} + \begin{bmatrix} v_{c1,c2} \\ w_{c1,c2} \end{bmatrix}. \quad (3.15)$$

Combining Eqs. (3.12) ~ (3.15) yields

$$\begin{bmatrix} v_{c1,r1} \\ w_{c1,r1} \end{bmatrix} + \begin{bmatrix} v_{l1,l2} \\ w_{l1,l2} \end{bmatrix} = \begin{bmatrix} R_{c1,c2}^T & 0 \\ 0 & R_{c1,c2}^T \end{bmatrix} \begin{bmatrix} v_{c2,r2} \\ w_{c2,r2} \end{bmatrix} + \begin{bmatrix} v_{c1,c2} \\ w_{c1,c2} \end{bmatrix}. \quad (3.16)$$

We now calculate the terms in Equation (3.16). First, observe that

$$R_{c1,c2} = \begin{bmatrix} R_\psi & 0 \\ 0 & -1 \end{bmatrix}, \quad r_{c1,c2} = 0.$$

Therefore,

$$v_{c1,c2} = 0, \quad \mathcal{S}(w_{c1,c2}) = \begin{bmatrix} 0 & -\dot{\psi} & 0 \\ \dot{\psi} & 0 & 0 \\ 0 & 0 & 0 \end{bmatrix}. \quad (3.17)$$

Also, by definition

$$v_{l1,l2} = \begin{bmatrix} v_x \\ v_y \\ v_z \end{bmatrix}, \quad w_{l1,l2} = \begin{bmatrix} w_x \\ w_y \\ w_z \end{bmatrix}. \quad (3.18)$$

To examine the motion of  $C_{c1}$  relative to  $C_{r1}$ , let  $x_1(\mathbf{u}_1)$ ,  $y_1(\mathbf{u}_1)$  and  $z_1(\mathbf{u}_1)$  be the axes of the Gaussian frame for *obj1* at the point of contact  $\mathbf{u}_1 \in U_{1i}$ . Then

$$r_{c1,r1} = c_1(t) = f_{1i}(\mathbf{u}_1(t)), \quad R_{c1,r1} = [x_1(\mathbf{u}_1(t)), y_1(\mathbf{u}_1(t)), z_1(\mathbf{u}_1(t))] \quad (3.19)$$

and

$$v_{c1,r1} = R_{c1,r1}^T \cdot \dot{r}_{c1,r1} = [x_1, y_1, z_1]^T [(f_{1i})_{u_1}, (f_{1i})_{v_1}] \dot{\mathbf{u}}_1 = \begin{bmatrix} M_1 \dot{\mathbf{u}}_1 \\ 0 \end{bmatrix}. \quad (3.20)$$

We also claim that

$$\begin{aligned} w_{c1,r1} &= \mathcal{S}^{-1}(R_{c1,r1}^T \cdot \dot{R}_{c1,r1}) \\ &= \mathcal{S}^{-1} \left( [x_1, y_1, z_1]^T [[(x_1)_{u_1}, (x_1)_{v_1}] \dot{\mathbf{u}}_1, [(y_1)_{u_1}, (y_1)_{v_1}] \dot{\mathbf{u}}_1, [(z_1)_{u_1}, (z_1)_{v_1}] \dot{\mathbf{u}}_1] \right) \\ &= \mathcal{S}^{-1} \left( \begin{bmatrix} 0 & -T_1 M_1 \dot{\mathbf{u}}_1 \\ T_1 M_1 \dot{\mathbf{u}}_1 & 0 & K_1 M_1 \dot{\mathbf{u}}_1 \\ -(K_1 M_1 \dot{\mathbf{u}}_1)^T & & 0 \end{bmatrix} \right). \end{aligned} \quad (3.21)$$

To see this, note that the 1-1 entry of (3.21) is given by

$$x_1^T \cdot [(x_1)_{u_1}, (x_1)_{v_1}] \dot{u}_1 = \frac{1}{2} \frac{d}{dt} \|x_1\|^2 = 0;$$

the 2-1 entry by

$$y_1^T \cdot [(x_1)_{u_1}, (x_1)_{v_1}] \dot{u}_1 = T_1 M_1 \dot{u}_1;$$

and the 1-3 and 2-3 entries by

$$\begin{bmatrix} x_1^T \\ y_1^T \end{bmatrix} \cdot [(z_1)_{u_1}, (z_1)_{v_1}] \dot{u}_1 = K_1 M_1 \dot{u}_1.$$

We similarly find that

$$v_{c2,r2} = \begin{bmatrix} M_2 \dot{u}_2 \\ 0 \end{bmatrix}, \quad (3.22)$$

$$w_{c2,r2} = S^{-1} \left( \begin{bmatrix} 0 & -T_2 M_2 \dot{u}_2 & \\ T_2 M_2 \dot{u}_2 & 0 & K_2 M_2 \dot{u}_2 \\ -(K_2 M_2 \dot{u}_2)^T & & 0 \end{bmatrix} \right). \quad (3.23)$$

Substitute Eqs. (3.17) ~ (3.23) into Equation (3.16), we get

$$M_1 \dot{u}_1 + \begin{bmatrix} v_x \\ v_y \end{bmatrix} = M_1 \dot{u}_2, \quad (3.24)$$

$$v_z = 0, \quad (3.25)$$

$$K_1 M_1 \dot{u}_1 + \begin{bmatrix} w_y \\ -w_x \end{bmatrix} = -R_\psi K_2 M_2 \dot{u}_2, \quad (3.26)$$

$$T_1 M_1 \dot{u}_1 + w_z = \dot{\psi} - T_2 M_2 \dot{u}_2. \quad (3.27)$$

Rearranging the above set of equations gives us the desired results. ■

Eqs. (3.8) ~ (3.10) are called the first, second and third contact equations, and Eq. (3.12) is called the constraint equation because it expresses the constraint on the relative motion necessary to maintain contact.

**Example 3.6** Let *obj1* be the flat surface of Example 3.4, and *obj2* be the unit ball studied in Example 3.5 (see Figure 3.4). Use the coordinate patches studied in these examples and reorient the objects, if necessary, so that  $\psi = 0$  at 0. The contact equations are

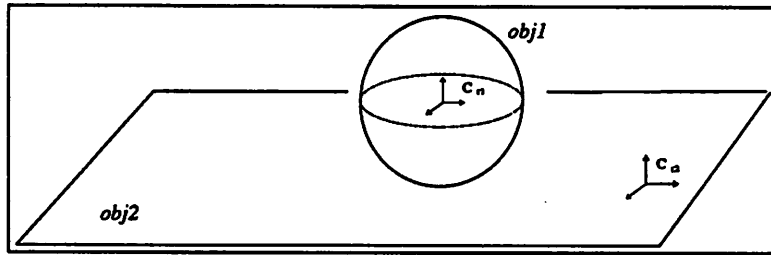


Figure 3.4: Motion of a unit ball over the plane

$$\begin{bmatrix} \dot{u}_1 \\ \dot{v}_1 \\ \dot{u}_2 \\ \dot{v}_2 \\ \dot{\psi} \end{bmatrix} = \begin{bmatrix} -w_y - v_x \\ w_x - v_y \\ -w_y \\ w_x \sec u_2 \\ w_z - w_x \tan u_2 \end{bmatrix}, \text{ where } \mathbf{u}_1 = \begin{bmatrix} u_1 \\ v_1 \end{bmatrix}, \mathbf{u}_2 = \begin{bmatrix} u_2 \\ v_2 \end{bmatrix}. \quad (3.28)$$

**Definition 3.7** Sliding contact is defined by

$$\begin{bmatrix} w_x \\ w_y \\ w_z \end{bmatrix} = 0; \quad (3.29)$$

Substituting Eq. (3.29) into Eq. (3.28) we get the contact equations for sliding motion

$$\begin{bmatrix} \dot{u}_1 \\ \dot{v}_1 \\ \dot{u}_2 \\ \dot{v}_2 \\ \dot{\psi} \end{bmatrix} = \begin{bmatrix} -1 \\ 0 \\ 0 \\ 0 \\ 0 \end{bmatrix} v_x + \begin{bmatrix} 0 \\ -1 \\ 0 \\ 0 \\ 0 \end{bmatrix} v_y. \quad (3.30)$$

**Definition 3.8** Rolling contact is defined by

$$\begin{bmatrix} v_x \\ v_y \end{bmatrix} = 0. \quad (3.31)$$

Similarly, substituting Eq. (3.31) into Eq. (3.28) we get the contact equations for

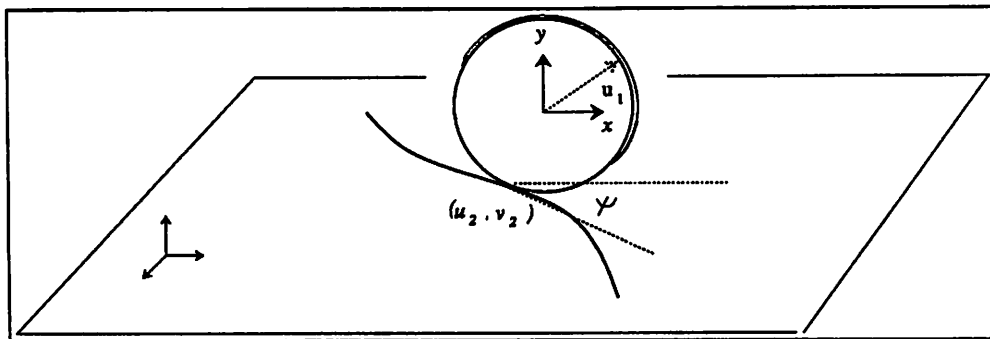


Figure 3.5: A unit disk on the plane

rolling motion

$$\begin{bmatrix} \dot{u}_1 \\ \dot{v}_1 \\ \dot{u}_2 \\ \dot{v}_2 \\ \dot{\psi} \end{bmatrix} = \begin{bmatrix} 0 \\ 1 \\ 0 \\ -\sec u_2 \\ \tan u_2 \end{bmatrix} w_x + \begin{bmatrix} -1 \\ 0 \\ -1 \\ 0 \\ 0 \end{bmatrix} w_y. \quad (3.32)$$

**Definition 3.9** When the relative motion is rotation around the common normal,

$$\begin{bmatrix} w_x \\ w_y \end{bmatrix} = 0, \text{ and } \begin{bmatrix} v_x \\ v_y \end{bmatrix} = 0. \quad (3.33)$$

Then, Eq. (3.28) becomes

$$\dot{u}_1 = 0, \dot{u}_2 = 0, \dot{\psi} = w_x. \quad (3.34)$$

For such motion the point of contact is fixed on both surfaces and only the angle of contact changes.  $\square$

**Example 3.7** (*The classical example re-visited*) Let's consider the classical example of a unit disk rolling on the plane, as shown in Figure 3.5 (See [Gol80], and [Gre77]). The point of contact has coordinates  $(u_2, v_2)$  over the plane and coordinates  $u_1$  over the disk. Embed the disk into  $\mathbb{R}^3$  with the following parameterization

$$f : U_1 \subset \mathbb{R} \longrightarrow \mathbb{R}^3 : u_1 \longmapsto (\cos u_1, \sin u_1, 0).$$

We define the Gaussian frame of the disk by the frame with origin at  $f(u_1)$  and coordinate axes

$$\mathbf{x}(u_1) = f', \mathbf{z}(u_1) = f'', \text{ and } \mathbf{y}(u_1) = \mathbf{z} \times \mathbf{x}.$$

Let  $\psi$  be the angle of the disk relative to the  $v_2$ -axis. Also let  $(v_x, v_y, v_z)$  be the components of translational velocity of  $C_{l1}$  relative to  $C_{l2}$ , and  $(0, w_y, w_z)$  be the components of rotational velocity. Following the proof of Theorem 3.1, we derive the following contact equations for the disk.

$$\begin{bmatrix} \dot{u}_1 \\ \dot{u}_2 \\ \dot{v}_2 \\ \dot{\psi} \end{bmatrix} = \begin{bmatrix} -1 \\ -\cos \psi \\ \sin \psi \\ 0 \end{bmatrix} w_y + \begin{bmatrix} 0 \\ 0 \\ 0 \\ 1 \end{bmatrix} w_z + \begin{bmatrix} 0 \\ \cos \psi \\ \sin \psi \\ 0 \end{bmatrix} v_x + \begin{bmatrix} 0 \\ -\sin \psi \\ \cos \psi \\ 0 \end{bmatrix} v_y \quad (3.35)$$

$$v_z = 0.$$

□

### 3.4 The Kinematics of A Robot Hand System

Analogous to manipulator kinematics, the kinematics of a robotic hand studies the relations between motion of the object being manipulated and the motion of the finger joints. For example, like the manipulator Jacobian and its transpose, *the hand Jacobian* and the transpose of the *grip Jacobian* relate the velocity of the object to the velocity of the finger joints; while the grip Jacobian relates applied finger forces to the net force on the object and the transpose of the hand Jacobian relates the applied finger force to the equivalent joint torque necessary for maintaining static equilibrium. But, unlike the manipulator Jacobian which arises from position constraints specified by the forward kinematic map, the constraints on the hand Jacobian and the grip Jacobian arise from contacts between the fingertips and the object. Contact constraints are usually unidirectional in nature, are nonholonomic and more difficult to work with than simple position constraints (holonomic). Moreover, the parameters specifying the hand Jacobian and the grip Jacobian evolve according to the contact equations of Section 3.3. Thus, it takes a great deal more effort to understand robot hand kinematics than manipulator kinematics.

**Definition 3.10** *A robot hand system consists of a set of open kinematics chains, called fingers, and an object to be manipulated. The 0<sup>th</sup> links of all the fingers are attached to a common base, called the hand palm. The surface of the last link of a finger is called the fingertip.*

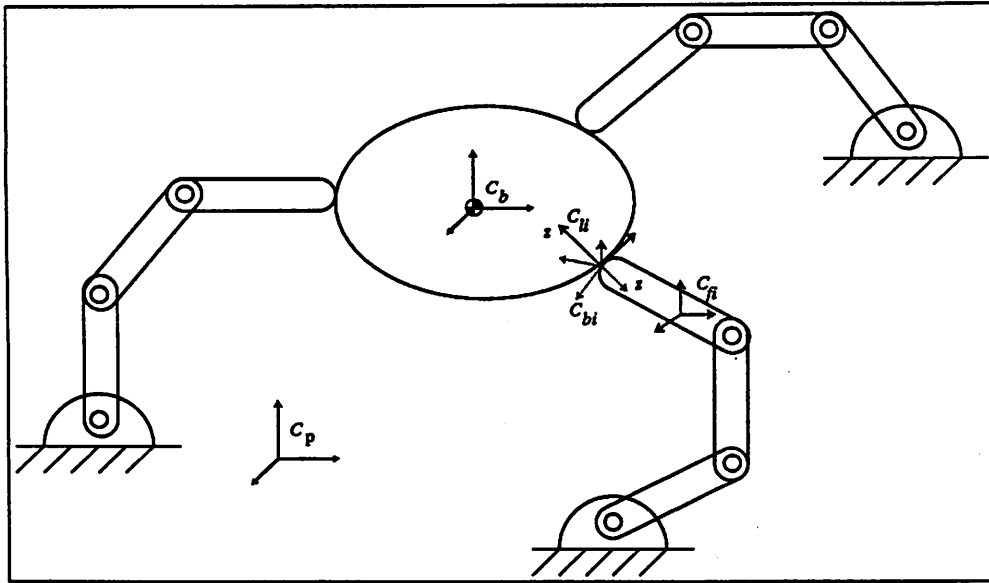


Figure 3.6: A hand manipulation system

**Assumption 3.1** *We assume that*

1. *Each finger contacts the object over its most distal link, or the fingertip, only.*
2. *Both the object and the fingertips are rigid and convex so that contacts occur over isolated points rather than over areas of their surfaces.*

Figure 3.36 illustrates a three-fingered robot hand system that satisfies the above assumption.

Consider a  $k$ -fingered robot hand system.

**Notation 3.2** *For  $i = 1, \dots, k$ , let  $m_i$  denote the number of joints of finger  $i$ , and  $\theta_i = (\theta_{i,1}, \dots, \theta_{i,m_i})^T$ ,  $\tau_i = (\tau_{i,1}, \dots, \tau_{i,m_i})^T \in \mathbb{R}^{m_i}$  denote the joint position and the joint torque vectors, respectively.*

We fix a set of coordinate frames to the system as follows. The reference frame of the system,  $C_p$ , is fixed to the hand palm, it is also called the palm frame; the body coordinate frame,  $C_b$ , is fixed to the mass center of the object, it is also called the body frame; for  $i = 1, \dots, k$ , the finger frame,  $C_{fi}$ , is fixed to the last link of finger  $i$ .

Choose a reference configuration of finger  $i$ , and identify  $\theta_i$  with zero at the reference configuration. Let  $\mathcal{F}_i(\theta_i)$  be the forward kinematic map of finger  $i$  relative

to the palm frame,  $C_p$ . Then the velocity of  $C_{fi}$  relative to the palm is related to the joint velocity by the Jacobian of  $\mathcal{F}_i(\theta_i)$ .

$$\begin{bmatrix} v_{fi,p} \\ w_{fi,p} \end{bmatrix} = J_i(\theta_i)\dot{\theta}_i. \quad (3.36)$$

Eq. (3.36) gives the first kinematic relation of the robot hand system.

Let  $S_o$  be the embedding of the surface of the object relative to  $C_b$ , and  $S_i$  be the embedding of the fingertip of finger  $i$  relative to  $C_{fi}$ . Choose coordinate charts for  $S_o$  and  $S_i$ . Let  $c_{oi}(t) \in S_o$  and  $c_{fi}(t) \in S_i$  be the position at time  $t$  of the contact point between the object and finger  $i$  relative to  $C_b$  and  $C_{fi}$ , respectively. We will restrict attention to a time interval  $I$  so that  $c_{oi}(t)$  belongs to a single coordinate system of  $S_o$  and  $c_{fi}(t)$  belongs to a single coordinate system of  $S_i$ .

At time  $t$ ,  $C_{bi}(t)$  denotes the local frame of the object at the point of contact with finger  $i$ . By our early definition,  $C_{bi}(t)$  is fixed relative to  $C_b$ . Similarly,  $C_{fi}$  denotes the local frame of finger  $i$  at the point of contact, and is fixed relative to  $C_{fi}$ .

Let  $(v_x^i, v_y^i, v_z^i)$  be the components of translational velocity of  $C_{bi}(t)$  relative to  $C_{li}(t)$ , and  $(w_x^i, w_y^i, w_z^i)$  the components of rotational velocity. Since the local frames  $C_{bi}(t)$  and  $C_{li}(t)$  share a common origin (i.e.,  $r_{bi,li} = 0$ ), according to Proposition 2.3, the following relation exists between the velocities of  $C_{bi}$  and  $C_{fi}$ .

$$\begin{bmatrix} v_{bi,p} \\ w_{bi,p} \end{bmatrix} = \begin{bmatrix} R_{\phi_i} & 0 \\ 0 & R_{\phi_i} \end{bmatrix} \begin{bmatrix} v_{li,p} \\ w_{li,p} \end{bmatrix} + \begin{bmatrix} v_x^i \\ v_y^i \\ v_z^i \\ w_x^i \\ w_y^i \\ w_z^i \end{bmatrix} \quad (3.37)$$

where

$$R_{\phi_i} = \begin{bmatrix} \cos \phi_i & \sin \phi_i & 0 \\ -\sin \phi_i & -\cos \phi_i & 0 \\ 0 & 0 & -1 \end{bmatrix}$$

is the orientation matrix of  $C_{bi}$  relative to  $C_{li}$ .

On the other hand, by Corollary 2.1, the velocity of  $C_{bi}$  is related to the velocity of  $C_b$  by a constant transformation

$$\begin{bmatrix} v_{bi,p} \\ w_{bi,p} \end{bmatrix} = Ad_{g_{bi,b}^{-1}} \begin{bmatrix} v_{b,p} \\ w_{b,p} \end{bmatrix}, \quad (3.38)$$

where  $g_{bi,b}$  is the configuration of  $C_{bi}$  relative to the object frame,  $C_b$ . Similarly we have for finger  $i$  that

$$\begin{bmatrix} v_{li,p} \\ w_{li,p} \end{bmatrix} = Ad_{g_{li,fi}^{-1}} \begin{bmatrix} v_{fi,p} \\ w_{fi,p} \end{bmatrix}, \quad (3.39)$$

where  $g_{li,fi}$  is the configuration of  $C_{li}$  relative to  $C_{fi}$ .

Combining Eqs. (3.36), (3.38) and (3.39) with Eq. (3.37) yields

$$Ad_{g_{bi,b}^{-1}} \begin{bmatrix} v_{b,p} \\ w_{b,p} \end{bmatrix} = J_{fi} \dot{\theta}_i + \begin{bmatrix} v_x^i \\ v_y^i \\ v_z^i \\ w_x^i \\ w_y^i \\ w_z^i \end{bmatrix}, \quad (3.40)$$

where

$$J_{fi} \triangleq \begin{bmatrix} R_{\phi_i} & 0 \\ 0 & R_{\phi_i} \end{bmatrix} \cdot Ad_{g_{li,fi}^{-1}} \cdot J_i(\theta_i). \quad (3.41)$$

When a robot finger grips the object with a prespecified contact model (see [MS85] and [Ker85] for a detailed account of contact models) certain components of the relative velocity are constrained to zero. For example, for a frictional point contact we have

$$\begin{bmatrix} v_x^i \\ v_y^i \\ v_z^i \end{bmatrix} = 0, \quad (3.42)$$

for a frictionless point contact we have

$$v_z^i = 0, \quad (3.43)$$

and for a *soft-finger* contact (see [MS85] for its definition) we have

$$\begin{bmatrix} v_x^i \\ v_y^i \\ v_z^i \end{bmatrix} = 0 \text{ and } w_z^i = 0. \quad (3.44)$$

The general form of constraint given by a particular contact model is

$$B_i^T \begin{bmatrix} v_x^i \\ v_y^i \\ v_z^i \\ w_x^i \\ w_y^i \\ w_z^i \end{bmatrix} = 0, \quad (3.45)$$

where  $B_i^T \in \mathbb{R}^{n_i \times 6}$  is called the selection matrix, or the basis matrix by J. Kerr ([Ker85]). For example, for a frictional point contact,

$$B_i^T = \begin{bmatrix} 1 & 0 & 0 & 0 & 0 & 0 \\ 0 & 1 & 0 & 0 & 0 & 0 \\ 0 & 0 & 1 & 0 & 0 & 0 \end{bmatrix}.$$

Assuming that a contact model in the form of Eq. (3.45) has been given, we now apply it to Eq. (3.40) and obtain a constraint equation that relates the velocity of the object to the velocity of the finger joints.

$$B_i^T Ad_{g_{bi,b}^{-1}} \begin{bmatrix} v_{b,p} \\ w_{b,p} \end{bmatrix} = B_i^T J_{fi} \dot{\theta}_i. \quad (3.46)$$

Define  $m = \sum_{i=1}^k m_i$ ,  $n = \sum_{i=1}^k n_i$  and

$$\theta = \begin{bmatrix} \theta_1 \\ \cdot \\ \cdot \\ \theta_k \end{bmatrix} \in \mathbb{R}^m, \quad B^T = \text{Diag}\{B_1^T, \dots, B_k^T\}.$$

Then, Eq. (3.45) can be concatenated for  $i = 1, \dots, k$  into the form

$$G^T \begin{bmatrix} v_{b,p} \\ w_{b,p} \end{bmatrix} = J_h \dot{\theta}, \quad (3.47)$$

where

$$J_h = B^T \cdot \text{Diag}\{J_{f1}, \dots, J_{fk}\} \in \mathbb{R}^{n \times m} \quad (3.48)$$

is called the *hand Jacobian*, and

$$G^T = B^T \begin{bmatrix} Ad_{g_{b1,b}}^{-1} \\ \cdot \\ \cdot \\ \cdot \\ Ad_{g_{bk,b}}^{-1} \end{bmatrix} \in \mathbb{R}^{n \times 6} \quad (3.49)$$

is called the transpose of the *grip Jacobian*.

Eq. (3.47), which relates the velocity of the object to the joint velocity of the fingers, is called the *fundamental constraint equation* for the robot hand system. Violation of the fundamental constraint equation may cause the object to drop. Thus, an important objective of the robot hand controller design is to enforce this constraint relation.

The contact constraint can also be viewed in terms of the number of independent wrenches, or forces, that one object is able to apply on the other. For example, under a frictional point contact, a robot finger can exert a pushing force along the contact normal and two components of frictional forces in the tangent directions on the gripped object. On the other hand, under a soft finger contact, a robot finger can apply in addition to the three contact wrenches under a frictional point contact a torque about the contact normal to an object. Let  $n_i$  be the number of independent contact wrenches applicable by finger  $i$  to the object. Then the resulting contact wrench can be expressed, relative to the local frame  $C_{bi}$ , as

$$\begin{bmatrix} f_{bi} \\ m_{bi} \end{bmatrix} = B_i x_i \quad (3.50)$$

where  $B_i \in \mathbb{R}^{6 \times n_i}$  is the basis matrix, and  $x_i = (x_{i,1}, \dots, x_{i,n_i})^T \in \mathbb{R}^{n_i}$  is the magnitude vector of applied contact wrenches along the directions of  $B_i$ . Note that for a frictional point contact,  $x_i$  is constrained to the friction cone,  $K_i$ , specified by

$$K_i = \{x_i \in \mathbb{R}^{n_i}, x_{i,3} \leq 0, x_{i,1}^2 + x_{i,2}^2 \leq \mu^2 x_{i,3}^2\}$$

where  $\mu$  is the coefficient of static Coulomb friction.

Transforming (3.50) to the object frame gives the contribution of finger forces from finger  $i$

$$\begin{bmatrix} f_b \\ m_b \end{bmatrix} = Ad_{g_{bi,b}}^T \cdot B_i x_i \quad (3.51)$$

On the other hand, the required joint torque for maintaining static equilibrium in the presence of contact wrench  $B_i x_i$ , is given by

$$\tau_i = J_{f_i}^t B_i x_i. \quad (3.52)$$

Finally, summing Eq. (3.51) for  $i = 1, \dots, k$  yields the net force on the object

$$\begin{bmatrix} f_b \\ m_b \end{bmatrix} = \sum_{i=1}^k Ad_{g_{bi,b}}^{T_{-1}} \cdot B_i x_i = Gx \quad (3.53)$$

where

$$G = [Ad_{g_{b1,b}}^{T_{-1}}, \dots, Ad_{g_{bk,b}}^{T_{-1}}] \cdot \text{Diag}\{B_1, \dots, B_k\} \in \mathbb{R}^{6 \times n}$$

is the grip Jacobian, and

$$x = [x_1^T, \dots, x_k^T]^T \in \mathbb{R}^n$$

is the vector of applied finger forces.

Define  $K = K_1 \oplus \dots \oplus K_k$  be the force cone. Then it is necessary that the magnitude vector  $x$  lie in  $K$  in order to maintain contact. Also, concatenate Eq. (3.52) for  $i = 1, \dots, k$  to yield the required joint torque vector for static equilibrium.

$$\tau = J_h^T \cdot x, \text{ where } \tau = \begin{bmatrix} \tau_1 \\ \cdot \\ \cdot \\ \cdot \\ \tau_k \end{bmatrix}. \quad (3.54)$$

We summarize the velocity and force transformation relations in Table 1, see also Figure 3.7 for a more intuitive picture. The vector  $\lambda \in \mathbb{R}^n$  is called the contact velocity.

	Force Torque Relations	Velocity Relations
Body to Fingertip	$\begin{bmatrix} f_b \\ m_b \end{bmatrix} = Gx$	$\lambda = G^t \begin{bmatrix} v_{b,p} \\ w_{b,p} \end{bmatrix}$
Fingertip to Joints	$\tau = J_h^t(\theta)x$	$J_h(\theta)\dot{\theta} = \lambda$

Table 1. Force/velocity transformation for a robot hand system.

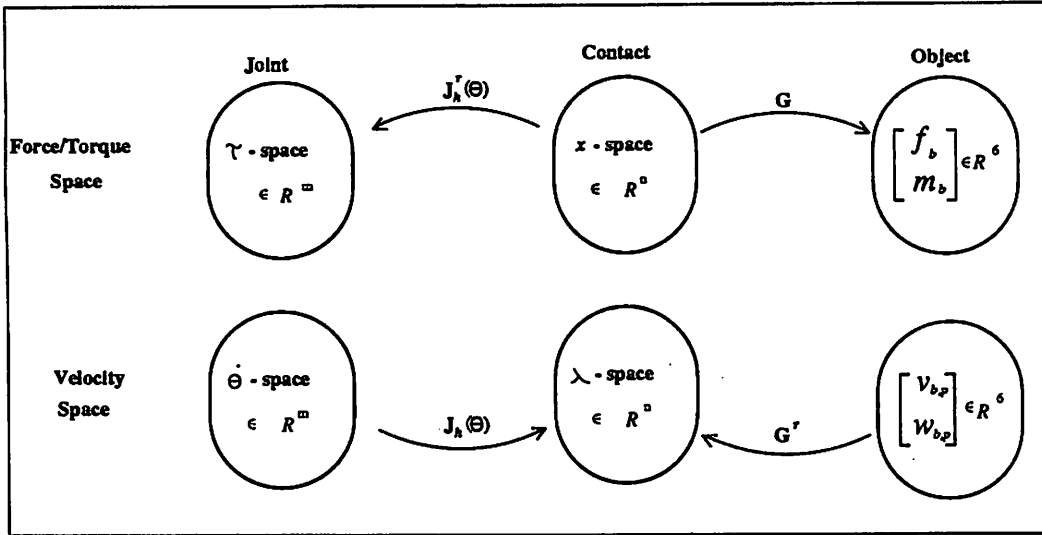


Figure 3.7: Force/velocity transformation for a robot hand system.

The operation of the robot hand system can be most effectively explained using Figure 3.7:

In the velocity domain, the hand Jacobian transforms velocity of the finger joints to velocity of the contact points. On the other hand, the transpose of the grip Jacobian transforms velocity of the object to velocity of the contact points. In order to maintain contact, the contact velocity specified by these two transformations must be the same. Thus, the fundamental constraint relation arises.

In the force domain, the grip Jacobian transforms the applied finger forces to the object frame. On the other hand, the required joint torque for maintaining static equilibrium is given by the transpose of the hand Jacobian.

The parameters specifying the transformation matrices,  $G$  and  $J_h$ , however, evolve according to the contact equations of Section 3.3. To be more specific, we distinguish two types of frictional point contact:

(1) Fixed frictional point contact

$$\begin{bmatrix} v_x^i \\ v_y^i \\ v_z^i \end{bmatrix} = 0 \text{ and } \begin{bmatrix} w_x^i \\ w_y^i \end{bmatrix} = 0; \quad (3.55)$$

(2) rolling contact

$$\begin{bmatrix} v_x^i \\ v_y^i \\ v_z^i \end{bmatrix} = 0 \text{ and } w_z^i = 0. \quad (3.56)$$

Let  $u_{oi}(t) \in \mathbb{R}^2$  be the coordinates of  $c_{oi}(t) \in \mathbb{R}^3$  relative to the chosen coordinate chart of  $S_o$ , and  $u_{fi}(t) \in \mathbb{R}^2$  be the coordinates of  $c_{fi}(t) \in \mathbb{R}^3$  relative to the chosen coordinate chart of  $S_i$ . Then, for a fixed frictional point of contact we have

$$\begin{bmatrix} \dot{u}_{oi} \\ \dot{u}_{fi} \\ \dot{\psi} \end{bmatrix} = \begin{bmatrix} 0 \\ 0 \\ w_z^i \end{bmatrix}, \quad (3.57)$$

where  $w_z^i$  is the rotational rate of finger  $i$  about the contact normal. It is clear from Eq (3.49) that the grip Jacobian,  $G$ , is constant for a fixed frictional point contact. But,  $J_h$  implicitly depends on  $\psi$ , as indicated by Eq. (3.41).

For rolling contact, the coordinates of contact involve according to

$$\begin{bmatrix} \dot{u}_{oi} \\ \dot{u}_{fi} \\ \dot{\psi} \end{bmatrix} = \begin{bmatrix} M_{oi}^{-1} \\ M_{fi}^{-1} \\ T_{oi} + T_{fi}R_{\psi_i} \end{bmatrix} (K_{oi} + \tilde{K}_{fi})^{-1} \begin{bmatrix} -w_y^i \\ w_x^i \end{bmatrix}. \quad (3.58)$$

where  $(w_y^i, w_x^i)$  are the components of rolling velocity.  $G$  and  $J_h$  depend implicitly on the rolling velocity, as revealed by Eqs. (3.58), (3.48) and (3.49).

To manipulate an object often requires solution of the following inverse problems.

**Problem 3.1 (a)** Given a body wrench  $\begin{bmatrix} f_b \\ m_b \end{bmatrix} \in \mathbb{R}^6$ , find a contact wrench  $x \in \mathbb{R}^n$  that lies in  $K$  and solves the equation

$$Gx = \begin{bmatrix} f_b \\ m_b \end{bmatrix}. \quad (3.59)$$

**(b)** Given an object velocity  $\begin{bmatrix} v_{b,p} \\ w_{b,p} \end{bmatrix} \in \mathbb{R}^6$ , find a joint velocity  $\dot{\theta}$  that solves the equation

$$J_h \dot{\theta} = G^T \begin{bmatrix} v_{b,p} \\ w_{b,p} \end{bmatrix}. \quad (3.60)$$

**Remark 3.2** We also call  $\tau = J_h^T x$ , where  $x$  is a solution to Eq. (3.59), the joint torque that solves Problem 3.1 (a).  $\square$

Denote by  $\Omega$  the triplet  $(G, K, J_h)$  and call it a grasp. We have

**Definition 3.11** A grasp  $\Omega \triangleq (G, K, J_h)$  is said to be stable if Eq. (3.59) has a solution for every body wrench, and manipulable if Eq. (3.60) has a solution for every object velocity.

**Remark 3.3** (1) A stable grasp has been called a force-closure grasp ([MS85]). It is important to note that stability is not to be understood in the sense of Lyapunov since we are not discussing stability of a differential equation. (2) A manipulable grasp is also called a grasp with full mobility (see [Kob85] and [MS85]).  $\square$

If  $K = \mathbb{R}^n$ , grasp stability and manipulability are easily characterized.

**Proposition 3.2** (1) A grasp is stable if and only if  $G$  is onto. (2) A grasp is manipulable if and only if  $R(J_h) \supset R(G^t)$ , where  $R(\cdot)$  denotes the range space.

We remark that the conditions (1) and (2) superficially appear to be distinct, but they are related. In particular, a stable grasp which requires zero joint torque to balance a non-zero body wrench will not be manipulable. Conversely, a manipulable grasp which requires zero joint motion to accommodate a non-zero body motion will not be stable. Figure 3.8 (a) shows a planar two-fingered grasp, where each finger is one-jointed and contacts the object with a point contact with friction. Clearly the grasp is stable and a force  $f_y$  can be resisted with no joint torques. But the grasp is not manipulable, since a  $y$ -direction velocity on the body cannot be accommodated. Figure 3.38 (b) shows a grasp of a body in  $\mathbb{R}^3$  by two three jointed fingers. The contacts are point contacts with friction. The grasp is manipulable, though the object can spin around the  $y$ -axis with zero joint velocities  $\dot{\theta}$ . However the grasp is not stable since a body torque  $\tau_n$  about the  $y$ -axis cannot be resisted by any combination of joint torques.

In view of the preceding remarks, we will require a grasp to be both manipulable and stable, i.e.,

$$R(G) = \mathbb{R}^6 \text{ and } R(J_h) \supset R(G^t). \quad (3.61)$$

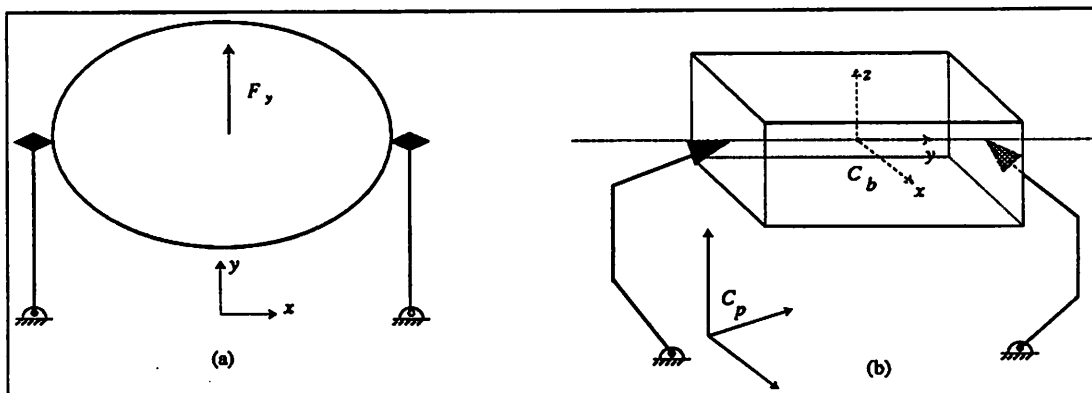


Figure 3.8: (a) A stable but not manipulable grasp, (b) a manipulable but not stable grasp.

The first condition suffers from the drawback that the force domain is left completely unconstrained. As we have seen earlier that the forces are constrained to lie in the force cone  $K$ , taking into account the unidirectionality of the contact forces and finite frictional forces, in which case the image of  $K \cap R(J_h)$  under  $G$  should cover all of  $\mathbb{R}^6$ . Thus, we have

**Corollary 3.1** *A grasp under unisense and finite frictional forces is both stable and manipulable if and only if*

$$G(K \cap R(J_h)) = \mathbb{R}^6, \text{ and } R(J_h) \supset R(G^t). \quad (3.62)$$

When a grasp is stable, the solution contact wrench has the form

$$x = G^T(GG^T)^{-1} \begin{bmatrix} f_b \\ m_b \end{bmatrix} + x_0 \quad (3.63)$$

where  $G^T(GG^T)^{-1} \begin{bmatrix} f_b \\ m_b \end{bmatrix}$  is the minimal norm solution to the inverse problem, and  $x_0 \in \mathbb{R}^n$  is any vector in the null space of  $G$  that renders  $x$  into the force cone  $K$ . Let  $\eta(G)$  be the null space of  $G$ . It is important to observe that a vector  $x \in \eta(G)$  contributes no net wrench upon the object. But, it reflects how hard the object is squeezed. Hence,  $\eta(G)$  is called the internal grasp force space. It is critical during the course of manipulation that a proper set of internal grasp forces be realized. This ensures the fundamental constraint relation.

Similarly, when a grasp is manipulable the solution joint velocity has the form

$$\dot{\theta} = J_h^T (J_h J_h^T)^{-1} G^T \begin{bmatrix} v_{b,p} \\ w_{b,p} \end{bmatrix} + \dot{\theta}_0 \quad (3.64)$$

where the first term is the minimal norm solution to the inverse problem and  $\dot{\theta}_0 \in \eta(J_h)$  is any joint velocity that causes no motion of the contact points.  $\eta(J_h)$  is called the internal motion space, which arises from robot fingers with redundant degrees of freedom.

### 3.5 Conclusion

Robot hand kinematics is perhaps one of the most complicated subjects in robotics: not only does the system have many degrees of freedom, holonomic and nonholonomic as well as unidirectional constraints are involved. This makes a robot hand system nonholonomic. There are three basic kinematic relations in a robot hand system: *the contact equations, the grip Jacobian, and the hand Jacobian*. These kinematic relations have been summarized in Table 3.1.

For quasi-static manipulation, solvability of the two *inverse problems* is of critical importance. It determines if a robot hand can impart motions to the grasped object.

# Bibliography

- [Car47] E. Cartan. *Lecons sur la geometrie de Riemann*. Paris:Gauthier-Wesley, 1947.
- [CR87] C. Cai and B. Roth. On the spatial motion of rigid bodies with point contact. In *IEEE International Conference on Robotics and Automation*, pages 686–695, 1987.
- [Cut86] M. Cutkosky. *Grasping and Fine Manipulation for Automated Manufacturing*. Kulware-Academic Publisher, 1986.
- [Gol80] H. Goldstein. *Classic Mechanics*. Addison-Wesley, 2nd edition edition, 1980.
- [Gre77] D. Greenwood. *Classical Dynamics*. Prentice-Hall, Inc., Englewood Cliffs, N.J., 1977.
- [Ker85] J. Kerr. *An analysis of multifingered hand*. PhD thesis, Department of Mechanical Engineering, Stanford University, 1985.
- [Kli78] W. Klingenberg. *A course in differential geometry*. Springer-Verlag, 1978.
- [Kob85] H. Kobayashi. Geometric considerations for a multifingerd robot hand. *International Journal of Robotics Research*, 4(1):3–12, 1985.
- [Li89] Z.X. Li. *Motion Planning with Nonholonomic Constraints*. Master's thesis, Mathematics Department, University of California at Berkeley, Berkeley, Ca. 94720 (to appear in *IEEE Transaction on Robotics and Automation*), 1989.
- [Mon86] D. Montana. *Tactile sensing and kinematics of contact*. PhD thesis, Division of Applied Sciences, Harvard University, 1986.

- [MP78] R.S. Millman and G.D. Parker. *Elements of differential geometry*. Prentice-Hall, Inc., Englewood Cliffs, N.J. 07632, 1978.
- [MS85] M.T. Mason and J. K. Salisbury. *Robot Hands and the Mechanics of Manipulation*, chapter 1 - 10. MIT Press, 1985.
- [Spi74] M. Spivak. *A Comprehensive Introduction to Differential Geometry*. Volume I and II, Publish or Perish, Boston, Mass., 1974.
- [Tho78] J.A. Thorpe. *Elementary topics in differential geometry*. Springer-Verlag, 1978.
- [Tri87] J. Trinkle. *Mechanics and planning of enveloping grasps*. PhD thesis, Department of Computer and Information Science, University of Pennsylvania, 1987.

## Chapter 4

# Planning

### 4.1 Introduction

Consider a typical task (for specificity, consider scribing with a grasped pen) to be executed by a robot hand system. The entire operation can be carried out in three consecutive phases: (1) *The robot hand grasps the object subject to a set of accessibility constraints.* For example, if the pencil is initially lying on the desk then the bottom face of the pencil is not accessible. (2) *If the initial grasp configuration is not satisfactory for executing the task, the object may be dropped for regrasp otherwise it is manipulated within the hand to an new grasp configuration.* Note that regrasping creates new constraints and is not likely to achieve a satisfying grasp. (3) *When a final grasp configuration is achieved, the object is manipulated to follow a desired trajectory while exerting a set of contact forces on the environment until the task is completed.* During the final phase, the fingers may contact the object with either a fixed point of contact or rolling contact.

We call the three phases the *initial grasp* phase, *dextrous manipulation* phase and *coordinated manipulation* phase. A flow diagram which illustrates the execution of a typical task is shown in Figure 4.1.

Task planning for a robot hand system, according to T. Lozano-Perez ([Loz82]), is to transform task-level specifications, such as scribing or peg-in-hole, into finger/object-level specifications, such as a desired trajectory of the object or a desired sequence of motions of the fingers. As suggested by the flow diagram of Figure 4.1, task planning for a robot hand system can also be divided into three

consecutive phases: (1) *(Task oriented) grasp planning*, (2) *motion planning for dextrous manipulation* and (3) *trajectory planning for coordinated manipulation*. Each of these planning phases are defined as follows:

**Grasp planning:** A task has certain favored grasp configurations which are most efficient for executing the task. Grasp planning is to transform the task requirement into criteria for selecting a grasp. **Motion planning for dextrous manipulation:** An initial grasp configuration may not be the optimal grasp. Thus, the object has to be manipulated within the hand to the optimal grasp configuration. This process is called dextrous manipulation. **Motion planning for dextrous manipulation** amounts to planning a sequence of finger motions so that dextrous manipulation can be carried out. **Trajectory planning for coordinated manipulation:** Assume that the fingers contact the object by either fixed points of contact or rolling contacts, trajectory planning for coordinated manipulation is to plan a trajectory of the object so that (1) the task gets executed and (2) the contact constraints are maintained.

This chapter studies several problems associated with task planning for a robot hand system.

## Grasp Planning

By reviewing early works in grasp planning, we argue that the only criterion for grasp planning should be the task requirement. Then, we propose a procedure for task modeling. Using the task model, we develop two quality measures for evaluating a grasp, and the optimal grasp is the one that maximizes the quality measures. Consequently, grasp planning is transformed into an optimization problem.

## What Is Dextrous Manipulation?

We formulate precisely in mathematical terms the dextrous manipulation problem and provide a guideline for future works in this area. The work of Section 4.3 constitutes an important step towards a full understanding of the dextrous manipulation problem.

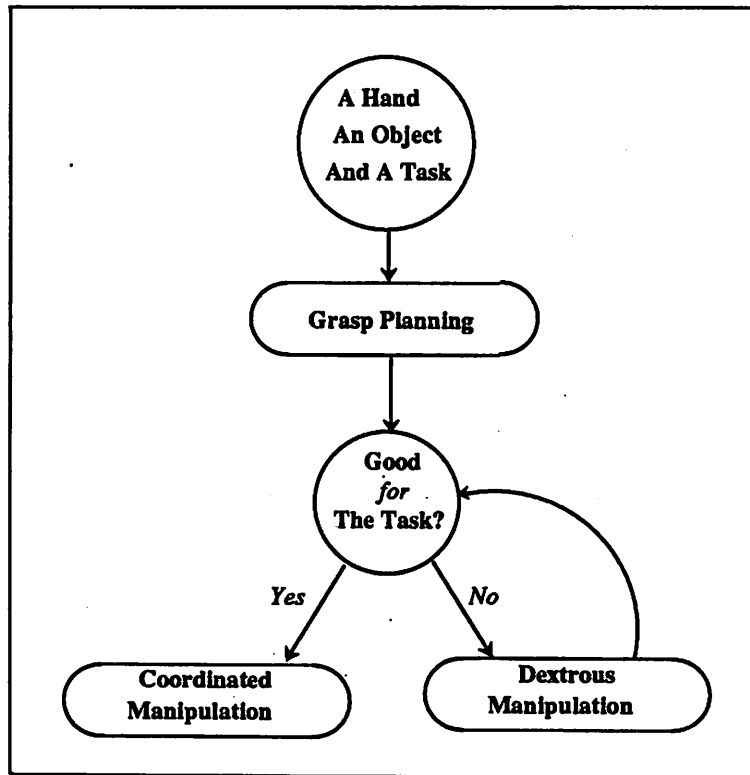


Figure 4.1: A flow diagram for task execution by a robot hand

## Motion Planning with Rolling Constraint

The two types of nonholonomic constraints involved in a robot hand system are: Rolling constraint and constraints due to finger relocation. *These constraints are what make dextrous manipulation possible.* To explore the use of nonholonomic constraints in dextrous manipulation we study motion of two objects under rolling constraint. In particular, we address the following two problems: (1) Given two contact configurations determine if an admissible path exists between them. (2) Assuming that a path exists, find such a path. Using the contact equations of Montana and methods from differential geometry we solve the first problem by computing the Lie algebra generated by the constrained vector fields. We then show that the path planning problem can be solved either using results from nonlinear control or using the notion of path lifting. We explicitly construct a solution when one of the object is flat.

## 4.2 Grasp Planning

The problem of *grasp planning* has not been clearly defined in the literature. It means differently when spoken by different people. For example, according to Reuleaux ([Reu75]) over a century ago, and to Lakshminarayna ([Lak78]) more recently, “grasp planning” is to *find a set of contact points upon the surface of a given object so that the induced grip Jacobian, under the assumption of a frictionless point contact model, is stable.* A somewhat related problem to this is, *how many contact points (or fingers) are necessary to achieve a stable grasp?* These problems have been extensively studied by many others, including J. K. Salisbury ([MS85]), V.D. Nguyen ([Ngu86]), J. Trinkle ([Tri87]), and B. Mishra, J. Schwartz and S. Sharir ([MSS86]).

In both [MSS86] and [Lak78], it was shown that the minimal number of contact points needed to achieve a stable is 4 for a 2-dimensional object and 7 for a 3-dimensional object. When the object is polyhedral, Mishra et al gave an algorithm that find a stable grasp and run in time linear in the complexity of the object (i.e., number of faces/sides).

In [MS85] and [Ngu86], the assumption was relaxed to allow frictional point contact and even soft finger contact. Nguyen ([Ngu86]) also discussed a procedure

for positioning two fingers around the object surface to achieve a stable grasp.

According to H. Hanafusa and H. Asada ([HA77]), to Cutkosky et al ([CAHK87]) and to V.D. Nguyen ([Ngu86]), where a finger is modeled by line springs, “grasp planning” is to find a set of contact points upon the surface of a given object so that the resulting potential function of the object has a local minimum. They presented examples to illustrate the derivation of the object potential function by reflecting from that of the fingers. The results, however, are valid only when the contact constraints are *holonomic*. In other words, when there is rolling contact the object potential function derived using the *reflection technique* is ambiguous. Furthermore, rolling contact is inevitable in dextrous manipulation.

There are three drawbacks associated with the first definition of “grasp planning”. First, the kinematics of the robot hand has not been taken into account. Thus, a set of contact points generated according to the *stable grasp criterion* may not be realizable by the robot fingers. Second, even if the contact points are realizable many choices of stable grasps to a given object exist. When the task is specified, some of these grasps may still not be satisfactory for executing the task. One may recall the grasp given by Figure 3.8, which is not manipulable while is stable. Third, it is always desirable from an engineering stand point that the grasp chosen should be “optimal” with respect to some acceptable criterion. Based on these considerations, Cutkosky ([Cut86]) and Li and Sastry ([LS88]) have suggested that the *task requirement should be the only criterion for selecting a grasp, while a grasp should consist of the contact configurations as well as the kinematic configurations of the robot fingers*. In other words, a *grasp should be judged based only on how efficiently the task can be executed*. This constitutes our philosophy for grasp planning.

The following questions then naturally arise.

1. *What should the definition of a grasp be?*
2. *How is a task to be modeled?*
3. *How is the task model incorporated into grasp planning?*

For the first question, let's examine our early definition of a grasp, which consists of the triplet  $\Omega \triangleq (G, K, J_h)$ . Given the friction properties of the object

and the robot fingers, the force cone  $K$  is determined (assuming uniform friction forces across the object surface). The grip Jacobian,  $G$ , is a function of the contact configurations, and the hand Jacobian,  $J_h$ , is a function of the finger joint variables,  $\theta$ , as well as the contact locations relative to the fingertips. The *objective of grasp planning is to specify the variables which determine  $G$  and  $J_h$* . For the remaining questions, we present a procedure for task modeling in Section 4.2.1. Then in Section 4.2.2 we introduce an objective function which incorporates the task model and can be used to formulate the optimization problem for grasp planning. We hope that new techniques can be developed to solve this optimization problem.

#### 4.2.1 Task Modeling

Consider a typical task such as grinding. First, in the wrench space of the object forces are required to manipulate the object or to act on the environment through contact with the object. Associated with the task are several special directions which require more forces than the others, e.g., the normal and the tangential directions for the grinding task. Second, in the twist space of the object, it is necessary to command motion of the object. In particular, a task has certain directions which require faster and larger range of motions than the others, e.g., the tangential directions of the grinding task. In each space, these special directions are called the preferred task directions. The relations between the preferred and the less or non-preferred task directions constitute the intrinsic features of a task. Task modeling is to determine, in each space, the task directions and the relationship between the preferred and the non-preferred task directions.

A methodology for task modeling was first developed by Z. Li and S. Sastry ([LS88]) and latter generalized by Z. Li, P. Hsu and S. Sastry ([LHS89]). According to [LHS89], one associates with each task an ellipsoid,  $A_\alpha$ , in the wrench space and another ellipsoid,  $B_\beta$ , in the twist space. In each space, the principal axes of the ellipsoid coincide with the task directions, and the length of a principal axis is determined by the weight assigned to that task direction. In particular, the longest axis of the ellipsoid coincides with the most preferred task direction, the second longest axis coincides with the second most preferred task direction and so on, and the shortest axis coincides with the least preferred task direction. In other words, the shape of the ellipsoid reflects the task requirement. To demonstrate the

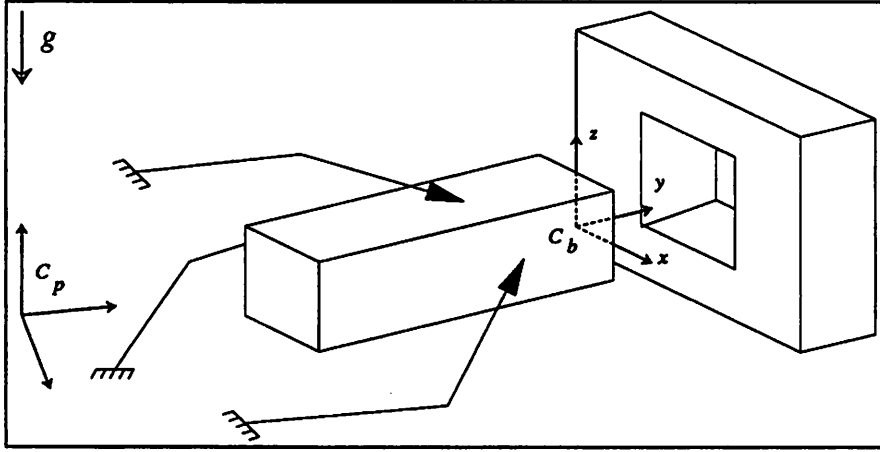


Figure 4.2: Peg-in-hole task

precise implications of this methodology we study task modeling for the following two tasks.

**Example 4.1** Consider the peg insertion task depicted in Figure 4.2 where the robot hand grasps the workpiece and inserts it into the hole.

In order to execute the task, a nominal trajectory is planned before grasping. After grasping the hand follows the planned trajectory until some misalignment of the peg causes the object to deviate from the nominal trajectory and collide with the environment.

With the body coordinate frame chosen as shown, the likelihood of collision forces in each force direction of decreasing probability would be  $-f_y$ ,  $\pm\tau_z$ ,  $\pm\tau_x$ ,  $\pm f_z$ ,  $\pm f_x$ ,  $\pm\tau_y$  and  $+f_y$ . If we denote by  $(r_i)_{i=1}^6$  the ratio of maximum expected collision forces in each direction, we obtain a set  $A_\alpha$ , parametrized by  $\alpha \in [0, \infty)$ , in the wrench space by

$$A_\alpha = \left\{ (f_x, \dots, \tau_z) \in \mathbb{R}^6, \frac{(f_y + c_1)^2}{r_1^2} + \frac{\tau_z^2}{r_2^2} + \frac{\tau_x^2}{r_3^2} + \frac{(f_z - c_2)^2}{r_4^2} + \frac{\tau_x^2}{r_5^2} + \frac{\tau_y^2}{r_6^2} \leq \alpha^2 \right\} \quad (4.1)$$

where the constant  $c_1$  reflects the offset of maximum expected collision force between  $+f_y$  and  $-f_y$  directions, and  $c_2$  reflects the gravitational force on the object. The set  $A_\alpha$  is an ellipsoid centered at  $(0, c_1, c_2, 0, 0, 0)$ , with the principal axes given by the generalized force directions, and axes lengths by the corresponding ratios  $r_i$ . The size of the ellipsoid is scaled by the parameter  $\alpha$ .

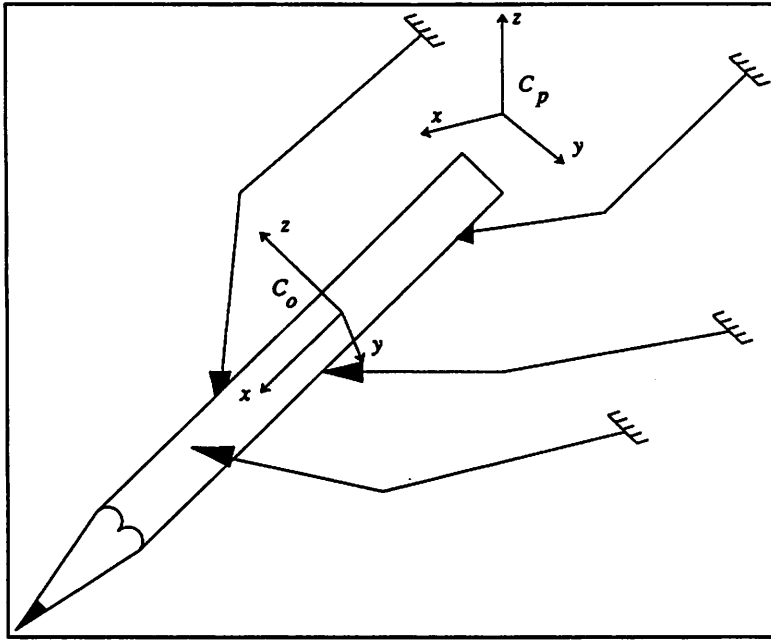


Figure 4.3: A scribing task

By appropriately assigning a set of values to the constants ( $r_i, i = 1, \dots, 6$ ) and ( $c_i, i = 1, 2$ ) we can decide on the shape of the ellipsoid so that it reflects the task requirement in the wrench space. In particular, the peg insertion task requires that ( $r_i \geq r_j$ ) whenever  $i \geq j$  and  $c_1$  to be large when collision forces in  $+f_y$  direction are very unlikely.

On the other hand, since the peg insertion task requires precise positioning the grasp should provide good manipulation capability (or dexterity) in certain directions. First, relatively large motion is needed in the  $v_y$  direction, and then follow  $w_y, v_x$  and  $v_z$  directions. If we model by  $(\delta_i)_{i=1}^6$  the ratio of relative maximum motion requirement among the six generalized velocity directions we obtain an ellipsoid  $B_\beta$  in the twist space, parametrized by  $\beta \in [0, \infty)$ , by

$$B_\beta = \left\{ (v_x, \dots, \omega_z) \in \mathbb{R}^6, \frac{v_x^2}{\delta_1^2} + \frac{v_y^2}{\delta_2^2} + \frac{v_z^2}{\delta_3^2} + \frac{\omega_x^2}{\delta_4^2} + \frac{\omega_y^2}{\delta_5^2} + \frac{\omega_z^2}{\delta_6^2} \leq \beta^2 \right\} \quad (4.2)$$

The shape of  $B_\beta$  reflects the task requirement in the twist space. In this case  $\delta_2$  is the largest of all, and then follow  $\delta_5, \delta_3$  and  $\delta_1$ . Precise values of these constants can be obtained from experiments or experience through error-and-trial procedures.  $\square$

**Example 4.2** Consider the scribing task shown in Figure 4.2.1. Human experience

tells us that, in order to execute the task efficiently, the grasp should provide, (1) good dexterity at the lead and (2) sufficient normal forces. With the body coordinate frame shown, the task requirements can be translated into requirements on the two task ellipsoids by (a) the task ellipsoid  $B_\beta$  in the twist space should have longer axes in  $\omega_y$  and  $\omega_z$  directions than in the other directions, and (b) the task ellipsoid  $A_\alpha$  in the wrench space should have longer axis in  $f_x$  direction than in the other directions. Applying this reasoning we obtain in (4.3) and (4.4) two task ellipsoids  $A_\alpha$  and  $B_\beta$  that describe the relative force and velocity ratios of the task.

$$A_\alpha = \left\{ (f_x, \dots, \tau_z) \in \mathbb{R}^6, \frac{(f_x + c)^2}{r_1^2} + \frac{f_y^2}{r_2^2} + \frac{f_z^2}{r_3^2} + \frac{\tau_x^2}{r_4^2} + \frac{\tau_y^2}{r_5^2} + \frac{\tau_z^2}{r_6^2} \leq \alpha^2 \right\} \quad (4.3)$$

*Wrench Space Task Ellipsoid*

$$B_\beta = \left\{ (v_x, \dots, \omega_z) \in \mathbb{R}^6, \frac{v_x^2}{\delta_1^2} + \frac{v_y^2}{\delta_2^2} + \frac{v_z^2}{\delta_3^2} + \frac{\omega_x^2}{\delta_4^2} + \frac{\omega_y^2}{\delta_5^2} + \frac{\omega_z^2}{\delta_6^2} \leq \beta^2 \right\} \quad (4.4)$$

*Twist Space Task Ellipsoid*

□

To conclude these examples, we emphasize that to each task we can associate two task ellipsoids, one in the wrench space that represents the relative force requirement and the other in the twist space that represents the relative motion requirement of the task. The constants  $(r_i, \delta_i, c_i)$  that determine shapes of these ellipsoids can be obtained from experiments or from experience with similar tasks. Hence, we need only to store in a library data for the ellipsoids for a set of interesting tasks.

There are also other approaches to develop task ellipsoids. For example, if stiffness control is used for the hand, then the maximum expected positional uncertainties in each of the task directions may be used to scale the axis of  $B_\beta$ . Also, during parts mating, jamming can be avoided if certain constraints on the ratios of the contact forces are satisfied ([Whi82]). Using these constraints on the force ratios to scale the ellipsoid  $A_\alpha$  is another approach.

Generalizing from these examples we will assume that a task is modeled by two generalized ellipsoids,  $A_\alpha$  in the wrench space and  $B_\beta$  in the twist space, of

the form

$$A_\alpha = \left\{ \alpha Ax + c, \text{ such that } x, c \in \mathbb{R}^6, |x| \leq 1, \text{ and } A \in \mathbb{R}^{6 \times 6} \right\} \quad (4.5)$$

and

$$B_\beta = \left\{ \beta Bx + d, \text{ such that } h, d \in \mathbb{R}^6, |x| \leq 1, \text{ and } B \in \mathbb{R}^{6 \times 6} \right\} \quad (4.6)$$

where the structure matrices A, B are given by

$$A = [U_1, \dots, U_6] \text{diag}\{\sigma_1, \dots, \sigma_6\} \begin{bmatrix} U_1 \\ \cdot \\ \cdot \\ U_6 \end{bmatrix} = U \Sigma U^t, U_i \in \mathbb{R}^6, \sigma_i \geq 0, i = 1, \dots, 6; \quad (4.7)$$

and

$$B = [U_1, \dots, U_6] \text{diag}\{\delta_1, \dots, \delta_6\} \begin{bmatrix} U_1 \\ \cdot \\ \cdot \\ U_6 \end{bmatrix} = U \Delta U^t, U_i \in \mathbb{R}^6, i = 1, \dots, 6. \quad (4.8)$$

Here,  $U_i$ , ( $i = 1, \dots, 6$ ), is the task direction;  $\sigma_i$  and  $\delta_i$  are the weights assigned to  $U_i$  in, respectively, the wrench space and the twist space. The constants  $c, d \in \mathbb{R}^6$  are the center positions of the respective task ellipsoids. In the following development, we may assume without loss of generality that  $c = d = 0$ . When the structure matrix, say A, is nonsingular an alternative expression of  $A_\alpha$  would be

$$A_\alpha = \left\{ y \in \mathbb{R}^6, \text{ such that } \langle y - c, \beta^{-2} (AA^t)^{-1} (y - c) \rangle \leq 1 \right\}. \quad (4.9)$$

When stiffness control is used for the hand,  $\sigma_i$  is related to  $\delta_i$  by  $\sigma_i = k_i \cdot \delta_i$ , where  $k_i$  is the desired stiffness in direction  $U_i$ . On the other hand, when hybrid position/force control is used for the hand,  $\sigma_i = 0$  if direction  $U_i$  is position controlled and  $\delta_i = 0$  if direction  $U_i$  is force controlled. Consequently, we see that our approach to task modeling applies to very general tasks.

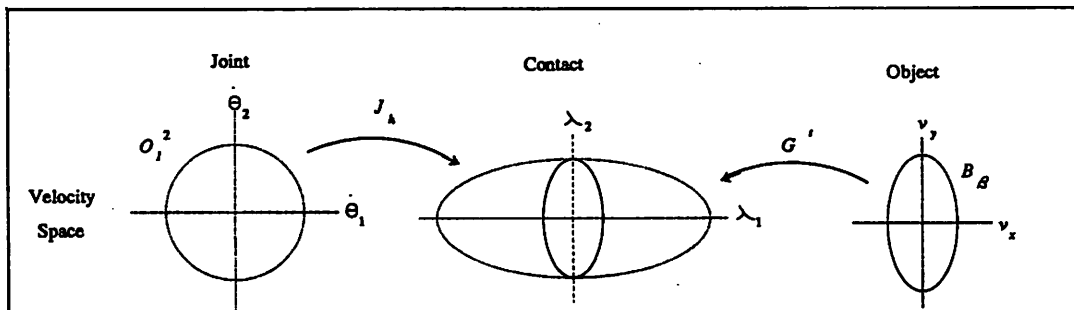


Figure 4.4: A geometrical interpretation of  $\mu_t(\Omega)$

#### 4.2.2 Structured Quality Measures for Grasp Planning

This section combines the task model with the definition of a grasp to develop two quality measures for a grasp.

**Definition 4.1** Consider a grasp  $\Omega = (G, K, J_h)$ . Let  $O_1^m \subset \mathbb{R}^m$  be the unit ball in the finger joint velocity space. We define the structured twist space quality measure  $\mu_t(\Omega)$  of the grasp  $\Omega$  by

$$\mu_t(\Omega) = \sup_{\beta \in \mathbb{R}_+} \left\{ \beta, \text{ such that } J_h(O_1^m) \supset G^t(B_\beta) \right\}. \quad (4.10)$$

**Remark 4.1**  $\mu_t(\Omega)$  has the following geometric interpretation ( see Figure 4.4 ): The unit ball  $O_1^m$  in the finger joint velocity space is mapped into the contact velocity space by  $J_h$ . On the other hand, a task ellipsoid  $B_\beta$  is mapped back into the contact velocity space by  $G^t$ .  $\mu_t(\Omega)$  is then the largest  $\beta$  such that  $G^t(B_\beta)$  is contained in  $J_h(O_1^m)$ . In other words,  $\mu_t(\Omega)$  is the ratio of the structured output ( i.e., the task ellipsoid) to the input ( i.e., the finger joint velocity).  $\square$

**Definition 4.2** Consider a grasp  $\Omega = (G, K, J_h)$ . Let  $O_1^n \subset \mathbb{R}^n$  be the unit ball in the finger wrench space and  $\sigma_{\max}(J_h)$  the maximum singular value of  $J_h$ . We define the structured wrench space quality measure  $\mu_w(\Omega)$  of the grasp  $\Omega$  by

$$\mu_w(\Omega) = \sup_{\alpha \in \mathbb{R}_+} \left\{ \alpha, \text{ such that } G(O_1^n \cap K) \supset A_\alpha \right\} \cdot \sigma_{\max}^{-1}(J_h) \quad (4.11)$$

**Remark 4.2** See Figure 4.5. The first term in the product is the largest  $\alpha$  such that  $A_\alpha$  can be embedded in  $G(O_1^n)$  (the output), and the second term is the largest input torque required to generate the finger wrench  $O_1^n$  ( the input). The structured quality measure is given by the gain factor (output/input).  $\square$

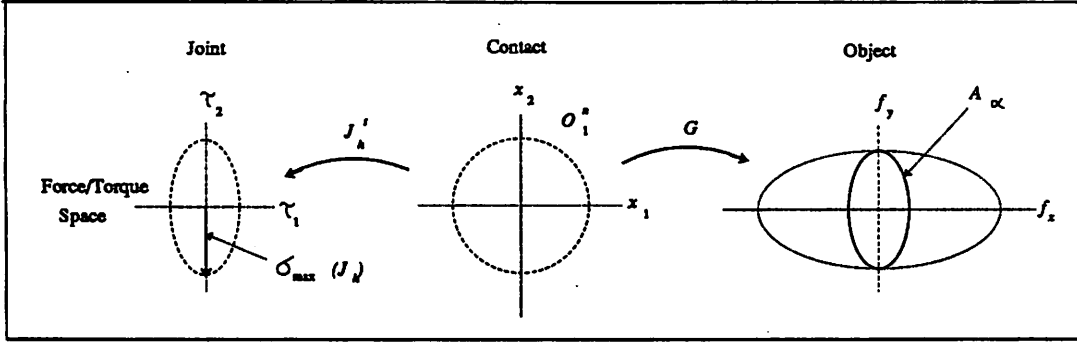


Figure 4.5: A geometrical interpretation of  $\mu_w(\Omega)$

The quality measures defined in (4.10) and (4.11) provide useful characterization of a grasp. Clearly, we can say that a grasp  $\Omega$  is a *good grasp* with respect to a *given task*, modeled by  $A_\alpha$  and  $B_\beta$ , if it has higher structured quality measures  $\mu_t$  and  $\mu_w$  than other candidate grasps. Due to unidirectionality and finite frictional forces, it is, however, not easy to evaluate these measures. In the special case when  $K = \mathbb{R}^n$  we have

**Proposition 4.1** *Assuming that  $K = \mathbb{R}^n$ , then the structured quality measures (4.10) and (4.11) are given by*

$$\mu_t(\Omega) = \sigma_{\max}^{-1/2} \left\{ B^t G (J_h J_h^t)^{-1} G^t B \right\} \quad (4.12)$$

and

$$\mu_w(\Omega) = \sigma_{\max}^{-1/2} \left\{ A^t (G G^t)^{-1} A \right\} \cdot \sigma_{\max}^{-1}(J_h) \quad (4.13)$$

**Proof.** Using the following expressions

$$J_h(O_1^m) = \left\{ y \in \mathbb{R}^n, \langle y, (J_h J_h^t)^{-1} y \rangle \leq 1 \right\}$$

and

$$G^t(B_\beta) = \left\{ \beta G^t B x, x \in \mathbb{R}^6, |x| \leq 1 \right\}$$

in (4.10) and notice that  $G^t(B_\beta) \subset J_h(O_1^m)$  if and only if

$$\langle \beta G^t B x, (J_h J_h^t)^{-1} \beta G^t B x \rangle \leq 1. \quad (4.14)$$

In particular, the above equation must hold for

$$\beta^2 \sup_{|x|=1} \langle G^t B x, (J_h J_h^t)^{-1} G^t B x \rangle = \beta^2 \sup_{|x|=1} \langle x, (G^t B)^t (J_h J_h^t)^{-1} G^t B x \rangle \leq 1$$

which is equivalent to

$$\beta \leq \sigma_{\max}^{-1/2} \{ B^t G (J_h J_h^t)^{-1} G^t B \}$$

By (4.10), we have (4.12).

The proof of (4.13) follows immediately. ■

(4.12) and (4.13) can be easily computed using singular value decomposition. If we also want to consider the manipulability of a grasp in a certain direction, say  $U_i$ , we may simply apply  $U_i$  to (4.14) and obtain that

$$\beta_i = \langle G^t B U_i, (J_h J_h^t)^{-1} G^t B U_i \rangle^{-1/2} = \delta_i^{-1} \langle G^t U_i, (J_h J_h^t)^{-1} G^t U_i \rangle^{-1/2}.$$

Here,  $\beta_i$  measures the effectiveness of the grasp in imparting motion at direction  $U_i$ , and a similar relation holds for the stability measure.

Note that (4.12) and (4.13) exhibit an interesting *dual relation*: Let the task ellipsoids be the unit balls. If we hold  $G$  constant but vary  $J_h$  then  $\mu_t(\Omega)$  is directly proportional to  $\sigma_{\min}(J_h)$  and  $\mu_w(\Omega)$  is inversely proportional to  $\sigma_{\max}(J_h)$ . On the other hand, if we hold  $J_h$  constant but vary  $G$  then  $\mu_w(\Omega)$  is directly proportional to  $\sigma_{\min}(G)$  and  $\mu_t(\Omega)$  is inversely proportional to  $\sigma_{\max}(G)$ . This observation implies that to a certain point it is in general not possible to increase the two quality measures simultaneously by varying  $G$  and  $J_h$ . Namely, increasing one quality measure will sacrifice the other. For instance, if we select a “power grasp” in the scribing task, that is, a grasp with high quality measure in the wrench space, then the grasp will be very poor in imparting motion at the pencil lead. Conversely, if we choose a “dextrous grasp”, that is, a grasp with high quality measure in the twist space, then the grasp will be very poor in rejecting disturbance forces. This also suggests that up to a certain point a compromise has to be made between “dexterity” and “power”. Hence, we propose to use the following function, called the performance measure (PM), as our objective function in the optimization procedure.

$$\text{PM}(\Omega) = [\mu_t(\Omega)]^\gamma \cdot [\mu_w(\Omega)]^{1-\gamma}. \quad (4.15)$$

$\gamma \in [0, 1]$  is called the selection parameter.  $\gamma > 0.5$  indicates that the task is dexterity oriented and  $\gamma < 0.5$  indicates that the task is power oriented. For  $\gamma \in (0, 1)$ , the performance measure is zero if either  $\mu_t(\Omega) = 0$  or  $\mu_w(\Omega) = 0$ . Also, for  $\gamma$  near 0, a grasp that maximizes PM will be a dextrous grasp, and for  $\gamma$  near 1 a

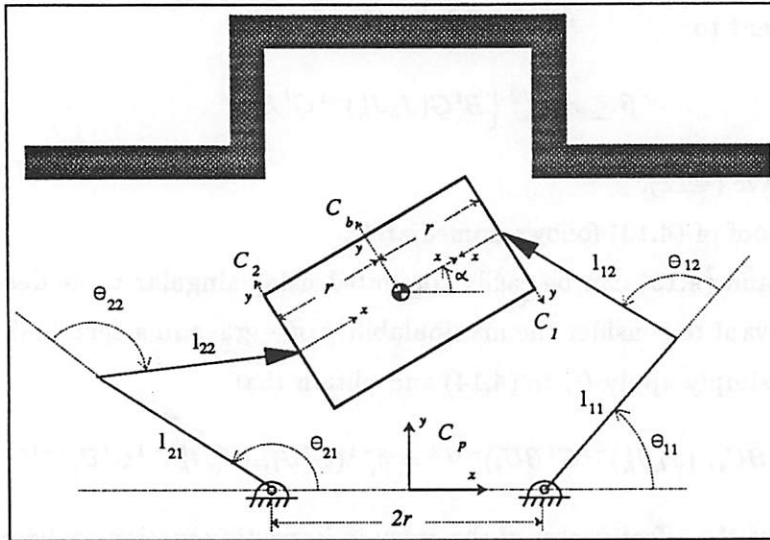


Figure 4.6: Planar peg-in-hole task

grasp that optimizes  $PM$  will be a power grasp. More importantly, for  $\gamma$  near 0.5, a grasp that optimizes  $PM$  will be both stable and manipulable.

An outline of the grasp planning algorithm is given as follows:

**Algorithm 4.1** (*Grasp Planning*)

- Step 1:** Obtain descriptions of the object and the robot hand.
- Step 2:** Write down the expressions of the grip Jacobian and the hand Jacobian.
- Step 3:** Model the task according to Section 4.2.1 and choose the selection parameter  $\gamma$ .
- Step 4:** Formulate the optimization problem using the performance measure as the objective function.
- Step 5:** Solve the optimization problem.

To conclude this section we present a simple example to illustrate the preceding discussions.

**Example 4.3** Consider the planar Peg-in-Hole task, shown in Figure 4.6. For simplicity we assume that the body orientation coincides with the orientation of  $C_p$ . Hence, the task direction matrix  $U$  is given by  $U = I \in \mathbf{R}^{3 \times 3}$ . To execute the task,

stiffness control is used for the hand ([Whi82]) and we assume that the desired stiffness matrix is given by

$$K = \text{diag}(k_x, k_y, k_\theta) = \text{diag}(5, 7, 100). \quad (4.16)$$

From [Whi82] and Example 4.1 we model the task by

$$U = I \in \mathbb{R}^{3 \times 3}, \Sigma = \text{diag}(4, 52), \Delta = \text{diag}(0.8, 0.7, 0.02) = K^{-1} \cdot \Sigma.$$

The objective is to search for grasps that maximize quality measures (4.12) and (4.13).

Assume a frictional point contact and let the block width and the finger spacing be 2. To simplify the problem further we make additional assumptions: G is fixed as in the figure and the object is constrained to move vertically. This leaves the system with a single degree of freedom. Let  $\theta_{11}$  be the generalized coordinate of the system and we study how  $\theta_{11}$  affecting the structured grasp quality measures.

As shown in the figure, the grip Jacobian is given by

$$G = \begin{bmatrix} -1 & 0 & 1 & 0 \\ 0 & -1 & 0 & 1 \\ 0 & -1 & 0 & -1 \end{bmatrix}$$

and the hand Jacobian  $J_h$  is

$$J_h = \text{diag}(J_1, J_2)$$

where

$$J_1 = \begin{bmatrix} \cos \alpha & -\sin \alpha \\ \sin \alpha & \cos \alpha \end{bmatrix} \begin{bmatrix} -\sin \theta_{11} - \sin(\theta_{11} + \theta_{12}) & -\sin(\theta_{11} + \theta_{12}) \\ \cos \theta_{11} + \cos(\theta_{11} + \theta_{12}) & \cos(\theta_{11} + \theta_{12}) \end{bmatrix}$$

and

$$J_2 = \begin{bmatrix} \cos \alpha & \sin \alpha \\ -\sin \alpha & \cos \alpha \end{bmatrix} \begin{bmatrix} \sin \theta_{21} - \sin(\theta_{21} - \theta_{22}) & \sin(\theta_{21} - \theta_{22}) \\ \cos \theta_{21} + \cos(\theta_{21} - \theta_{22}) & -\cos(\theta_{21} + \theta_{22}) \end{bmatrix}$$

where  $\alpha$  is the orientation angle of the object. The previous assumptions impose the following constraints:  $\alpha = 0$ ,  $\theta_{12} = \pi - 2\theta_{11}$ ,  $\theta_{21} = \pi - \theta_{11}$ , and  $\theta_{11} - \theta_{22} = \pi - (\theta_{11} + \theta_{12})$ . Figure 4.7 shows plots of the quality measures and the performance measure ( $\gamma = 0.5$ ) as functions of  $\theta_{11}$ . The structured measure  $\mu_t(\Omega)$  and PM attain their maximum at  $\theta_{11} = 0.475$  radian ( $27^\circ$  degree). Since G is held constant the task structures have no effect on  $\mu_w$ , which is still inversely proportional to  $\sigma_{\max}(J_h)$ . Clearly, the optimal grasp is  $\theta_{11} = 27^\circ$ .  $\square$

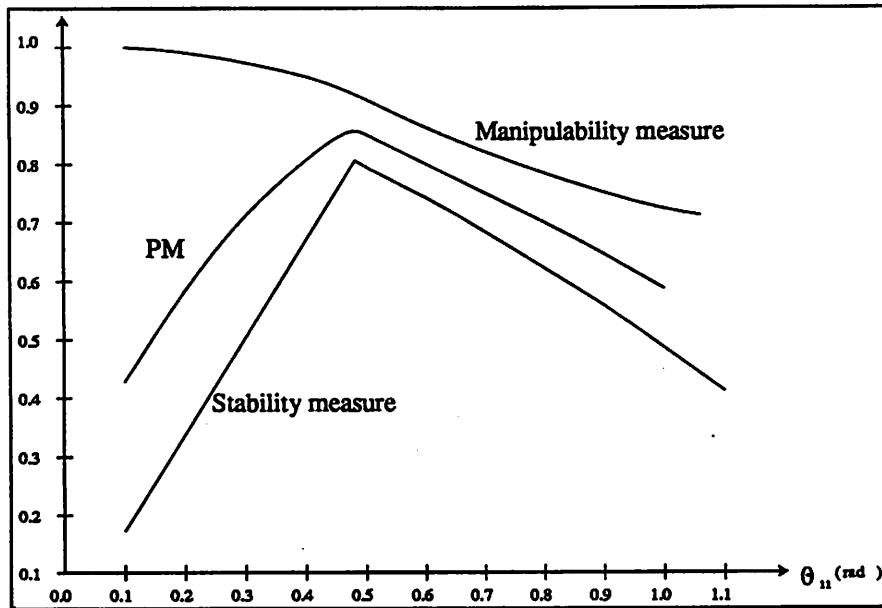


Figure 4.7: Performance measure, grasp quality measures versus  $\theta_{11}$

### 4.3 What Is Dextrous Manipulation?

In the previous section, a performance measure for evaluating a grasp is defined. The optimal grasp, by definition, is then the one that maximizes the performance measure. To execute the task, one would like to stay near the optimal grasp configuration. In practice, however, the optimal grasp may not always be attainable when a robot hand picks up an object subject to a set of initial accessibility constraints. For example, observe a girl performing a scribing task with the pencil initially lying on the desk. She would first pick up the pencil at a stable grasp. Then, she manipulates the pencil within her hand to arrive at a better grasp. Finally, she executes the task near that grasp configuration.

**Definition 4.3** *The act of manipulating an object from one grasp configuration to another without dropping the object is called dextrous manipulation.*

The ability to perform dextrous manipulation is one of the unique features of a dextrous robot hand. Because of this feature a robot hand can grasp objects of various sizes and execute tasks ranging from simple to sophisticated ones.

Dextrous manipulation is a very complex process. Human hands have evolved thousands of years to master this capability. One may observe from the

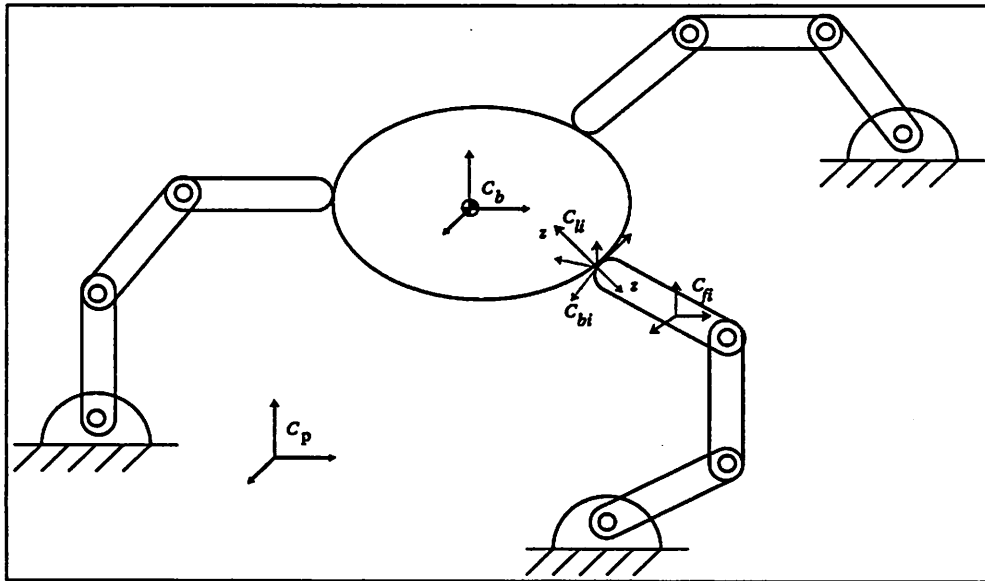


Figure 4.8: A robot hand system.

girl's scribing task, that her finger usually makes rolling contact, sliding contact, as well as fixed point of contact with the object. Sometimes her finger will break contact during one regime and makes new contact during another regime (we call such an act *finger relocation*). Mathematically very little is known about this process. The aim of this section is to formulate the dextrous manipulation problem.

First, we need to re-define a grasp configuration.

Consider the hand manipulation system shown in Figure 4.8. Let  $SE_o(3)$  be a copy of the Euclidean group designated for the configuration space of the object. Similarly, let  $Q_i \subset SE(3)$  be the set of configurations reachable by the last link of finger  $i$ , i.e.,  $Q_i$  is the image of the finger's forward kinematic map. Without loss of generality, we may assume that the forward kinematic map is injective. Thus,  $Q_i$  is in one-to-one correspondence with the finger joint space. Let the object and finger  $i$  be at configurations  $g_o \in SE_o(3)$  and  $g_i \in Q_i$ , respectively, and they are in contact. Clearly the contact points are uniquely determined because the relative curvature form is invertible. Moreover, we conclude from our assumption that there exist unique finger joint angles  $\theta_i$  that give the  $g_i$ . Recall now our early definition of a grasp, which is given by the contact points and the finger joint variables. Thus, the configurations of the object and the fingers suffice to determine a grasp.

**Definition 4.4** *The configuration space,  $P$ , of a robot hand system is given by*

$$P = SE_o(3) \times Q_1 \times \dots \times Q_k,$$

*a point  $z = (g_o, g_1, \dots, g_k) \in P$  is also called a grasp configuration.*

**Remark 4.3** This definition of grasp configuration is more general and more intuitive than the early one. For a given grasp configuration  $z \in P$ , one of the following possibilities exists: (1) none of the fingers contacts the object. Thus,  $\Omega = (G, K, J_h)$  is empty. This is called a null grasp. (2) A subset of the fingers contact the object. This corresponds to finger relocation and the grasp  $\Omega$  is defined by these fingers that are in contact with the object. (3) Every finger contacts the object.  $\square$

It is important to observe that (a) motion of the object is indirectly controlled through contacts with the fingers, and (2) the contact points are unchanged if the grasp configuration  $z \in P$  undergoes a rigid motion. To state these facts in mathematical language, let  $G = SE(3)$  be the group of rigid motion of  $\mathbb{R}^3$ .  $G$  acts on  $P$  by right translation, i.e., there exists a map

$$\Phi : P \times G \longrightarrow P : (z, h) \longmapsto (g_o h, g_1 h, \dots, g_k h).$$

Referring to Figure 4.9, this corresponds to a rigid motion  $h$  on the entire system by the palm where the hand system is attached to. Clearly, for each  $h \neq e$ , the identity element of  $G$ , the map  $\Phi_h : P \longrightarrow P : z \longmapsto \Phi(z, h)$  is one-to-one. This enables us to define an equivalence relation  $\sim$  on  $P$  as follows:  $z_1 \sim z_2$  if there exists a  $h \in G$  such that  $z_2 = z_1 h$ . In other words, two grasp configurations are equivalent if one is related to the other by a rigid motion. We let  $P/G$  denote the space obtained from  $P$  under this equivalence relation. A point  $[z]$  in  $P/G$  is of the form  $[z] = zG$ .  $P/G$  is called the space of shapes ([Mon88]) and there exists a natural projection from  $P$  to  $P/G$ , given by

$$\pi : P \longrightarrow P/G : z \longmapsto zG.$$

The triplet  $(P, G, P/G)$  is called a principal bundle.  $P$  is sometimes called the *total space*,  $P/G$  the *base space* and  $G$  the *structure group*.

**Proposition 4.2** *Let  $M = Q_1 \times \dots \times Q_k$  denote the configuration space of the fingers. Then, the space of shapes,  $P/G$ , is homeomorphic to  $M$ .*

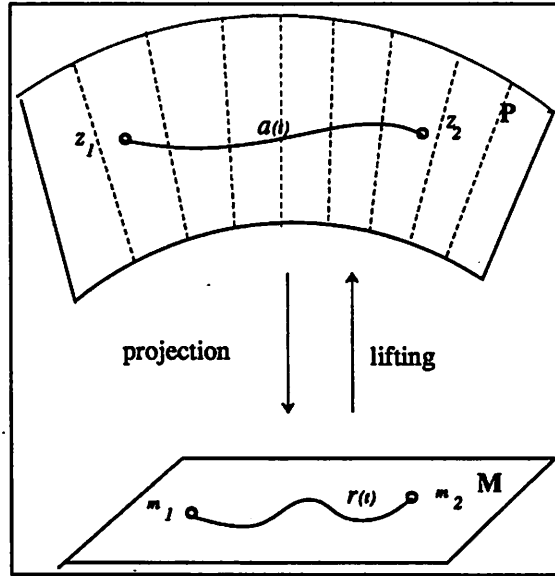


Figure 4.9: A global view of dextrous manipulation

**Proof.** Let  $[z] = zG = (g_0, g_1, \dots, g_k)G$  be an element in  $P/G$ . Then, setting  $h = g_0^{-1}$  we see that  $zG \sim (e, g_1g_0^{-1}, \dots, g_kg_0^{-1})G$ . We call  $[\hat{z}] = (e, g_1, \dots, g_k)G$  the unique representative of  $[z]$ . For if  $[z]$  and  $[z']$  are two different points in  $P/G$ . Then,  $[z] \neq [z']$  if and only if  $[\hat{z}] \neq [\hat{z}']$  if and only if  $(g_1, \dots, g_k) \neq (g'_1, \dots, g'_k)$ . We define the homeomorphism  $f$  by

$$f : P/G \longrightarrow M : zG \longmapsto (g_1, \dots, g_k), \text{ where } zG \sim (e, g_1, \dots, g_k)G.$$

This construction completes the proof. ■

$M$  is also called the *control space* because a trajectory in  $M$  can be controlled using actuators located at the finger joints. On the other hand, if a grasp is both stable and manipulable then the object motion can be effected by the finger motion. Consider now Figure 4.9, where the configuration space is on top of the control space. Starting at an initial grasp configuration,  $z_0$ , we wish to arrive at a final grasp configuration,  $z_f$ , by choosing a proper set of finger trajectories, which can be realized by specifying torque inputs to the motors, and lifting them to the configuration space. Thus, we have

**Problem 4.1 (Dextrous Manipulation)** Given two grasp configurations  $z_0, z_f$  in  $P$ , plan an admissible piecewise continuous curve  $\gamma(t), t \in [0, t_f]$ , in  $M$  such that (1)

$\gamma$  can be lifted to a curve  $\alpha$  in  $P$ , i.e.,  $\pi(\alpha) = \gamma$  and  $\alpha$  connects  $z_0$  to  $z_f$ , i.e.,  $\alpha(0) = z_0$  and  $\alpha(t_f) = z_f$ .

Roughly speaking, a finger trajectory  $\gamma(t) \in M, t \in [0, t_f]$ , is said to be admissible if the object can be held stably by the robot hand (see [LCS89] for more details). We are not sure yet how to construct such a curve. There remain many open questions in this area. What we can do in the next section is to study motion of two objects with rolling contact constraint, and hope that this will provide further insight into this problem.

## 4.4 Motion Planning with Rolling Constraint

In this section, we study motion of two rigid bodies under *rolling constraint*. This problem is a basic ingredient in dextrous manipulation. First, label the two rigid bodies by *obj1* and *obj2*, respectively (see Figure 4.10). *Obj1* may represent the fingertip of a robot hand, and *obj2* the object being manipulated by the robot hand. This problem also has importance of its own. For example, in wheeled mobile robotics ([MN86]), *obj1* may represent the wheel (i.e., 3 degrees of freedom wheel) of a mobile robot and *obj2* the curved surface where the robot travels. In contour following, *obj1* may represent the end-effector of a manipulator and *obj2* the workpiece.

By commanding rolling motion instead of sliding motion, which is known to be holonomic, the advantages gained are: (1) *The problem of wear associated with the contacting bodies is eliminated.* (2) *The associated control problem becomes much simpler.* Recall that in order to control sliding motion, the coefficient of friction has to be known exactly, which is in general difficult. Even the world's best figure skaters have trouble managing controlled sliding. On the other hand, rolling motion can be achieved by exerting forces which are sufficiently close to the center of the friction cone (see Chapter 5). (3) *As we will see soon the set of configurations reachable by rolling is much larger than that reachable by sliding.* This is due to the nonholonomic nature of the constraint.

We address the following two problems in particular.

**Problem 4.2 (The Motion Existence Problem)** *Given two contact configurations, determine whether an admissible path exists between them.*

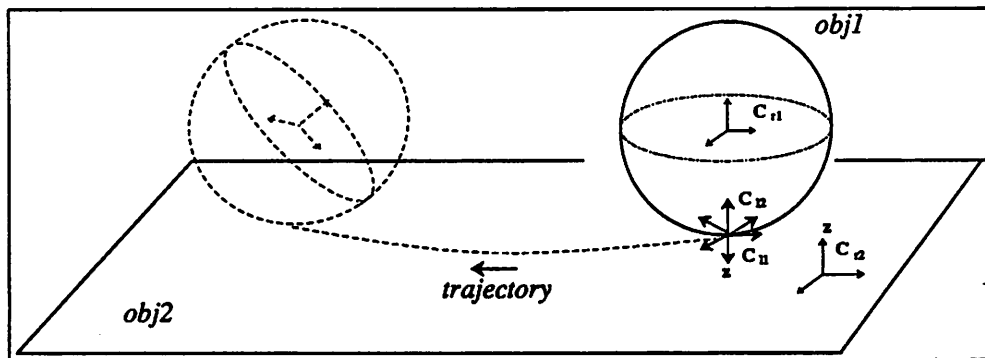


Figure 4.10: Motion of an object with rolling constraints

**Problem 4.3 (The Path Planning Problem)** *Assuming that an admissible path exists (or a motion exists) between two contact configurations, find such a path.*

Motion planning with nonholonomic constraints is fundamentally different from motion planning with holonomic constraints. For the latter, an (semi-) algebraic description of the free space, which a path can be planned, is available. The free space is specified either in terms of a set of equality, or inequality, constraints on the configuration variables ([Can88]) or in terms of a set of integrable differential equations (e.g., sliding). For the former, only a set of nonintegrable differential equations, which a path has to satisfy, is available.

An outline of our approach to these problem is as follows: First, we use the results of Section 3.4 to define the configuration space of contact and derive the system of differential equations for rolling motion. Then we use some known results from differential geometry to determine the existence of a path. Finally we present a simple algorithm that determines a desired path when one of the object is flat.

Consider the contact motion of two objects shown in Figure 4.10.

**Definition 4.5** <sup>1</sup> *The configuration space of contact,  $P$ , is a five dimensional space, which is locally described by the coordinates of contact relative to obj1 and obj2, and the angle of contact, i.e., a contact configuration  $p \in P$  has the form*

$$p = (u_1, v_1, u_2, v_2, \phi)^T,$$

where  $u_1 = (u_1, v_1)^T$ ,  $u_2 = (u_2, v_2)^T$  are the coordinates of contact relative to obj1 and obj2, respectively, and  $\phi$  is the angle of contact.

<sup>1</sup>We assume that the relative curvature form is invertible.

Note that this definition of  $P$  depends on the coordinate systems used for *obj1* and *obj2*. An intrinsic definition of  $P$  is given in [Li89].<sup>2</sup>

#### 4.4.1 Existence of Motion

Along the notation of Section 3.3, let  $(v_x, v_y, v_z)$  be the components of translational velocity of the local contact frame, and  $(w_x, w_y, w_z)$  the components of rotational velocity. Then, rolling contact implies that

$$\begin{bmatrix} v_x \\ v_y \\ v_z \end{bmatrix} = 0 \text{ and } w_z = 0. \quad (4.17)$$

Substitute (4.17) into the contact equations and rearrange the results, we have

$$\dot{p} = X_1(p)w_x + X_2(p)w_y, \quad \dot{p} = \begin{bmatrix} \dot{u}_1 \\ \dot{u}_2 \\ \dot{\phi} \end{bmatrix}, \quad (4.18)$$

where

$$X_1(p) = \begin{bmatrix} M_1^{-1} \\ M_2^{-1} \\ T_1 + T_2 \tilde{R}_\phi \end{bmatrix} (K_1 + \tilde{K}_2)^{-1} \begin{bmatrix} 0 \\ 1 \end{bmatrix}, \quad X_2(p) = \begin{bmatrix} M_1^{-1} \\ M_2^{-1} \\ T_1 + T_2 \tilde{R}_\phi \end{bmatrix} (K_1 + \tilde{K}_2)^{-1} \begin{bmatrix} -1 \\ 0 \end{bmatrix}. \quad (4.19)$$

(4.18) defines a system of differential equations on  $P$ .  $X_1(p)$  and  $X_2(p)$  are the vector fields for the infinitesimal rolling motion.

**Definition 4.6** A path  $p(t) \in P, t \in [0, \infty)$ , is said to be admissible (or conforms with the constraint) if it satisfies the differential equation (4.18) for some piecewise continuous rolling velocity  $(w_x(t), w_y(t)) \in \mathbb{R}^2, t \in [0, \infty)$ .

**Definition 4.7** Let  $p_0 \in P$  be an initial contact configuration. A point  $p_f \in P$  is said to be reachable from  $p_0$  by rolling if there exists an admissible path  $p(t) \in P, t \in [0, t_f]$ , such that  $p(0) = p_0$  and  $p(t_f) = p_f$ .

<sup>2</sup>For readers familiar with differential geometry,  $P$  is defined as follows: Let  $T_oS_1$  be the circle bundle of  $S_1$  and  $T_oS_2$  the circle bundle of  $S_2$ . Form the product space  $(T_oS_1 \times T_oS_2)$  and let  $S^1$ , the circle group, acting on  $T_oS_1$  by left rotation and on  $T_oS_2$  by right rotation (i.e., we have a diagonal action of  $S^1$  on  $(T_oS_1 \times T_oS_2)$ ). Then,  $P$  is the product space quotient the diagonal action, i.e.,  $P = (T_oS_1 \times T_oS_2)/S^1$ . (See [Li89], [Wes81]).

The following is a restatement of the motion existence problem.

**Problem 4.4 (The Motion Existence Problem).** *Given two contact configurations  $p_0, p_f \in P$ , determine the existence of an admissible path that connects  $p_0$  to  $p_f$ .*

Modifying a result from differential geometry, known as the Chow's Theorem ([Cho40]), we arrive at the following algorithm that solves Problem 4.4. A proof of correctness of the algorithm can be found in ([HK77], [Son88a]).

**Algorithm 4.2 (Motion Existence Algorithm)**

**Input:** 1. Coordinate systems  $\{f_{1,i}, U_{1,i}\}_{i=1}^{m_1}$  of obj1, and  $\{f_{2,i}, U_{2,i}\}_{i=1}^{m_2}$  of obj2.  
 2. Geometrical data,  $(M_1, T_1, K_1)$  of obj1 and  $(M_2, T_2, K_2)$  of obj2.  
 3. The coordinates of two contact configurations  $p_0, p_f \in P$ .

**Output:** Determine if  $p_f$  can be reached from  $p_0$  by rolling.

**Step 1:** Compute the coordinate expressions of the vector fields  $X_1(p)$  and  $X_2(p)$  from (4.19).

**Step 2:** Compute the following Lie bracket vector fields (see the remark that follows)

$$\begin{aligned} X_3(p) &= [X_1, X_2] = \frac{\partial X_2}{\partial p_i} X_1 - \frac{\partial X_1}{\partial p_i} X_2, \\ X_4(p) &= [X_1, X_3], \\ X_5(p) &= [X_2, X_3], \end{aligned} \tag{4.20}$$

where  $p = (u_1, v_1, u_2, v_2, \psi)^t$ .

**Step 3:** Form the distribution

$$\nabla(p)^3 = \{X_1, X_2, X_3, X_4, X_5\}. \tag{4.21}$$

For each  $p \in P$ ,  $\nabla(p)$  is a  $5 \times 5$  matrix. Compute the rank of  $\nabla(p)$ .

**Output:** (a) If  $\text{rank}(\nabla(p)) = 5, \forall p \in P$ , then there exists an admissible path between any two contact configurations.<sup>4</sup>

<sup>3</sup>For each  $p \in P$ ,  $\nabla(p)$  is an involutive distribution, known as the Lie algebra generated by  $\{X_1(p), X_2(p)\}$ .

<sup>4</sup>This says that if  $\nabla(p)$  is full rank, then any point in the space can be reached by moving along the integral curves of  $X_1$  and  $X_2$ .

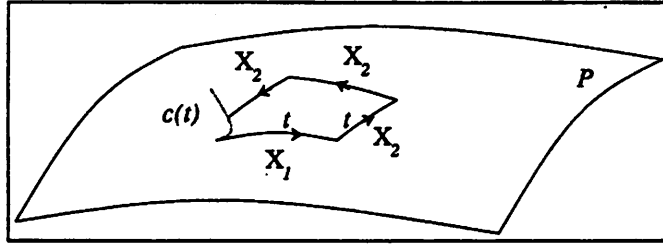


Figure 4.11: An interpretation of  $[X_1, X_2]$ .

- (b) If  $\dim(\nabla(p)) = n < 5, \forall p \in P^5$ , let  $N_{p_0}$  be the maximum integral manifold of  $\nabla$  through  $p_0$ <sup>6</sup>. If  $p_f \in N_{p_0}$ , then an admissible path exists between  $p_0$  and  $p_f$ <sup>7</sup> and  $p_f$ <sup>7</sup>
- (c) Otherwise, no path exists.

**Remark 4.4** 1. The Lie bracket vector field has the following meanings: Let  $X_1$  and  $X_2$  be two vector fields on  $P$ , and  $p \in P$ . Define a curve,  $c$ , on  $P$  as follows. For sufficiently small  $t$ , (1) follow the integral curve of  $X_1$  through  $p$  for time  $t$ ; (2) starting from there, follow the integral curve of  $X_2$  for time  $t$ ; (3) then follow the integral curve of  $X_1$  backwards for time  $t$ ; (4) then follow the integral curve of  $X_2$  backwards for time  $t$  (see Figure 4.11). In other words,

$$c(t) = \Psi_{-t}(\Phi_{-t}(\Psi_t(\Phi_t(p))))$$

where  $\Phi_t, \Psi_t$  are the integral curve of  $X_1$  and  $X_2$ , respectively. Then, it can be shown that

$$\ddot{c}(0) = 2[X_1, X_2](p)$$

2. The previous remark also suggests a way of creating a net motion in the direction  $[X_1, X_2]$  by moving along the directions  $X_1$  and  $X_2$ .
3. Computation of the Lie bracket vector fields, and checking the rank of  $\nabla(p)$  can be done using Macsyma.

□

We now apply the above algorithm to several examples.

<sup>5</sup>For technical reasons we assume that  $\nabla(p)$  has constant rank. Otherwise see ([HK77], [Son88a]).

<sup>6</sup>The existence and uniqueness of  $N_{p_0}$  is guaranteed by Frobenius Theorem.

<sup>7</sup>This condition is rather difficult to check, see [Son88b].

**Example 4.4** Consider a unit ball rolling on the plane, as shown in Figure 4.10. From Example 3.5 and 3.4, the ball has two coordinate systems and the plane one. The curvature form, metric tensor and connection form of the ball and the plane are given by these examples as well.

**Step 1:** On the first coordinate system of  $P$ , the kinematic equations of contact are

$$\begin{bmatrix} \dot{u}_1 \\ \dot{v}_1 \\ \dot{u}_2 \\ \dot{v}_2 \\ \dot{\psi} \end{bmatrix} = \begin{bmatrix} 0 \\ \sec u_1 \\ -\sin \psi \\ -\cos \psi \\ -\tan u_1 \end{bmatrix} w_x + \begin{bmatrix} -1 \\ 0 \\ -\cos \psi \\ \sin \psi \\ 0 \end{bmatrix} w_y \quad (4.22)$$

$$\triangleq X_1(p)w_x + X_2(p)w_y.$$

**Step 2:** Computing the successive Lie brackets of  $X_1(p)$  and  $X_2(p)$ , gives

$$X_3 = [X_1, X_2] = \begin{bmatrix} 0 \\ -\sec u_1 \tan u_1 \\ -\sin \psi \tan u_1 \\ -\cos u_1 \tan u_1 \\ -\sec^2 u_1 \end{bmatrix},$$

$$X_4 = [X_1, X_3] = \begin{bmatrix} 0 \\ 0 \\ -\cos \psi \\ \sin \psi \\ 0 \end{bmatrix},$$

and

$$X_5 = [X_2, X_3] = \begin{bmatrix} 0 \\ (1 + \sin^2 u_1) \sec^3 u_1 \\ 2 \sin \psi \sec^2 u_1 \\ 2 \cos \psi \sec^2 u_1 \\ 2 \sec^2 u_1 \tan u_1 \end{bmatrix}.$$

**Step 3:** Form the distribution

$$\nabla = \{X_1, X_2, X_3, X_4, X_5\}.$$

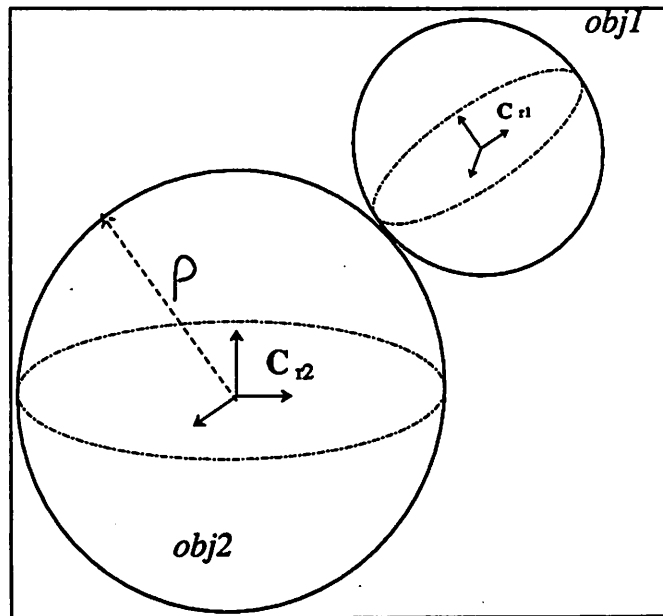


Figure 4.12: Motion of a unit ball over another ball

It is easy to verify that, through elementary row and column operations, the determinant of  $\nabla$  is identically 1.

Steps 1 through 3 are repeated for the second coordinate system of  $P$  and  $\nabla$  is again nonsingular.

**Output:** *It is true that a unit ball can reach any contact configuration on the plane by rolling!*  $\square$

**Example 4.5** The second example consists of a unit ball rolling on another ball of radius  $\rho$  (See Figure 4.12). Clearly,  $P$  has four coordinate systems.

**Step 1:** The kinematic equations of contact in the first coordinate system are

$$\begin{bmatrix} \dot{u}_1 \\ \dot{v}_1 \\ \dot{u}_2 \\ \dot{v}_2 \\ \dot{\psi} \end{bmatrix} = \begin{bmatrix} 0 \\ (1 - \beta) \sec u_1 \\ -\beta \sin \psi \\ -\beta \cos \psi \sec u_2 \\ \beta \tan u_2 \cos \psi - (1 - \beta) \tan u_1 \end{bmatrix} w_x + \begin{bmatrix} -(1 - \beta) \\ 0 \\ -\beta \cos \psi \\ \beta \sin \psi \sec u_2 \\ -\beta \tan u_2 \sin \psi \end{bmatrix} w_y$$

$$\triangleq X_1 w_x + X_2 w_y,$$

where  $\beta = \frac{1}{1+\rho}$ .

**Step 2:** Using Macsyma, the successive Lie brackets of  $X_1$  and  $X_2$  are computed.

$$X_3 = [X_1, X_2] = \begin{bmatrix} 0 \\ (1 - \beta)^2 \sec^2 u_1 \\ \beta(1 - \beta) \sin \psi \sin u_1 \sec u_1 \\ \beta(1 - \beta) \cos \psi \sin u_1 \sec u_1 \sec u_2 \\ X_{3,5} \end{bmatrix},$$

where

$$X_{3,5} = -\frac{\beta(1 - \beta) \cos \psi \cos u_1 \sin u_1 \sin u_2 + \{-\beta^2 \cos^2 u_1 + (\beta - 1)^2\} \cos u_2}{\cos^2 u_1 \cos^2 u_2};$$

$$X_4 = [X_1, X_3] = \begin{bmatrix} 0 \\ 0 \\ \beta(2\beta - 1) \cos \psi \\ -\beta(2\beta - 1) \sin \psi \sin u_2 \sec u_2 \\ \beta(2\beta - 1) \sin \psi \sin u_2 \sec u_2 \end{bmatrix};$$

$$X_5 = [X_2, X_3] = \begin{bmatrix} 0 \\ -\{-(1 - \beta)^3 \cos^2 u_1 + 2(1 - \beta)^3\} \sec^3 u_1 \\ -\{\beta^3 \sin \psi \cos^2 u_1 - 2\beta(1 - \beta)^2 \sin \psi\} \sec^2 u_1 \\ -\{\beta^3 \cos \psi \cos^2 u_1 - 2\beta(1 - \beta)^2 \cos \psi\} \sec^2 u_1 \sec u_2 \\ X_{5,5} \end{bmatrix};$$

where

$$X_{5,5} = \frac{\{\beta^3 \cos \psi \cos^3 u_1 - 2\beta(1 - \beta)^2 \cos \psi \cos u_1\} \sin u_2 + \alpha}{\cos^3 u_1 \cos u_2}$$

and

$$\alpha = \{\beta^2(1 - \beta) \cos^2 u_1 - 2(1 - \beta)^3\} \sin u_1 \cos u_2.$$

**Step 3:** Computing the determinant of

$$\nabla = \{X_1, X_2, X_3, X_4, X_5\}$$

gives

$$\det \nabla = -\frac{(\beta - 1)^2 \beta^2 (2\beta - 1)^3}{\cos u_1 \cos u_2}, \quad \beta = \frac{1}{1 + \rho}.$$

$\nabla$  is singular for the following cases

- $\beta = 1 \rightarrow \rho = 0$  : This corresponds to *obj2* being a single point. Note that the rank of  $\nabla$  is 3 (not 2!). This can also be seen from the multiplicity of the zeros in the determinant.
- $\beta = \frac{1}{2} \rightarrow \rho = 1$ : This corresponds to the case when both objects are balls of identical radius. In fact, counting the multiplicity of the zeros at  $\beta = \frac{1}{2}$ , or computing the rank of  $\nabla$ , the reachable space has dimension 2! This fact can be interpreted using the notion of holonomy angles (See Section 4).
- $\beta = 0 \rightarrow \rho = \infty$ . The result is degenerate because from the previous example we know that a unit ball can reach any contact configuration on the plane by rolling.

Steps 1 through 3 are repeated for the other three coordinate systems and the results are consistent.

**Output:** *It is true that a unit ball can reach any contact configuration by rolling on another ball of radius  $\rho$  if and only if  $\rho$  is not zero or ( $\rho \neq 1$ ).*  $\square$

**Example 4.6 (The classic example re-visited).** Consider again the classic example of a unit disk on the plane. Note that the two rotations are different here from Example 4.4. We get from Example 3.7 the following two vector fields

$$\text{"driving"} = X_1 = \begin{bmatrix} -1 \\ -\cos \psi \\ \sin \psi \\ 0 \end{bmatrix} \quad \text{and "steering"} = X_2 = \begin{bmatrix} 0 \\ 0 \\ 0 \\ 1 \end{bmatrix}.$$

Performing the Lie bracket operation, gives

$$X_3 = [X_1, X_2] = \begin{bmatrix} 0 \\ -\sin \psi \\ -\cos \psi \\ 0 \end{bmatrix},$$

and

$$X_4 = [X_2, X_3] = \begin{bmatrix} 0 \\ -\cos \psi \\ \sin \psi \\ 0 \end{bmatrix}.$$

Note that  $[X_1, X_3] = 0$ .  $X_3$  and  $X_4$  are called the “wriggling” and the “sliding” vector field, respectively. It is then simple to verify that

$$\nabla = \{X_1, X_2, X_3, X_4\}$$

has rank 4, for all points in  $P$ . This shows that a disk can reach any contact configuration by “driving” and “steering”.  $\square$

#### 4.4.2 A Path Planning Algorithm

We now study the path planning problem.

**Problem 4.5 (Path Planning Problem)** *Assuming that an admissible path exists between two contact configurations  $p_0, p_f \in P$ , find one path.*

One approach is to consider it as a *nonlinear control problem*. The *plant equation* is given by (4.18), whereas  $p(t) \in P$  is the state,  $(X_1(p), X_2(p))$  are the control vector fields and  $(w_x, w_y) \in \mathbb{R}^2$  the control inputs. The objective is find a set of control inputs  $(w_x(t), w_y(t)) \in \mathbb{R}^2, t \in [0, t_f]$ , such that the system (4.18), starting from  $p_0$ , reaches  $p_f$  in finite time. Relevant works in nonlinear control literature include ([Son88a], [Bro88], [Bro81], [HK77], [Sus83]). We are currently investigating now about this direction. The solutions are however only approximate.

Making use of the contact constraint, an alternative approach, which gives exact solutions, is presented here. First, from our *driving* experiences, we know that a path relative to the surface of *obj1* (or *obj2*) determines uniquely a path in the configuration space of contact. More precisely, we have

**Proposition 4.3** *Let  $p_0 = \{u_1(0), u_2(0), \psi(0)\} \in P$  be an initial contact configuration. Then, a path  $u_1(t) \in S_1^8, t \in [0, t_f]$ , uniquely determines a path  $p(t) \in P, t \in [0, t_f]$ .*

**Proof.** It suffices to show that  $(u_2(t), \psi(t))$  are uniquely determined by  $u_1(t), t \in [0, t_f]$ . But, from the first contact equation rolling velocity can be expressed in terms of  $\dot{u}_1$  as

$$\begin{bmatrix} -w_y \\ w_x \end{bmatrix} = (K_1 + \tilde{K}_2)M_1 \dot{u}_1. \quad (4.23)$$

---

<sup>8</sup>When the coordinate system in consideration is clear, we shall not distinguish the object surface from its coordinates in order to simplify notation.

Substituting this into the second and third contact equations yields

$$\begin{bmatrix} \dot{\mathbf{u}}_2 \\ \dot{\psi} \end{bmatrix} = \begin{bmatrix} M_2^{-1} \tilde{R}_\psi \\ T_1 + T_2 \tilde{R}_\psi \end{bmatrix} M_1 \dot{\mathbf{u}}_1. \quad (4.24)$$

For given initial conditions  $(\mathbf{u}_2(0), \psi(0))$ , a theorem (the existence and uniqueness theorem) of ODE ensures the existence and uniqueness of the solution to (4.24).

This completes the proof.  $\blacksquare$

We call the solution,  $p(t) = (\mathbf{u}_1(t), \mathbf{u}_2(t), \psi(t))$ ,  $t \in [0, t_f]$ , from (4.24) the lift of the path  $\mathbf{u}_1(t)$  through the point  $p_0$ . Apparently, the lift  $p(t) \in P$  is admissible, or satisfies the rolling constraint.

**Corollary 4.1** *Let  $p_0 \in P$  be an initial contact configuration and  $\mathbf{u}_2(t) \in S_2$ ,  $t \in [0, t_f]$ , a contact trajectory relative to  $\text{obj}2$ . Then, there exists a unique lift  $p(t) \in P$ ,  $t \in [0, t_f]$ , defined by the following ODE.*

$$\begin{bmatrix} \dot{\mathbf{u}}_1 \\ \dot{\psi} \end{bmatrix} = \begin{bmatrix} M_1^{-1} \tilde{R}_\psi \\ T_1 \tilde{R}_\psi + T_2 \end{bmatrix} M_2 \dot{\mathbf{u}}_2. \quad (4.25)$$

The angle of contact,  $\psi$ , whose evolution defined by (4.24), has a useful geometric interpretation when  $\text{obj}2$  is flat, i.e.,  $T_2 = 0$ . Let  $\mathbf{u}_1(t)$ ,  $t \in [t_0, t_1]$ , be a piecewise regular simple closed curve in  $S_1$  representing the contact trajectory of  $\text{obj}1$ , and  $\delta\psi = \psi(t_1) - \psi(t_0)$  denote the net change of contact angle induced by  $\mathbf{u}_1$ .

We have

**Proposition 4.4**  *$-\delta\psi$  is equal to the holonomy angle of the loop  $\mathbf{u}_1$  (See [Tho78] for the definition of holonomy angle). In other words,  $-\delta\psi = \iint_R k dA$ , where  $k$  is the Gaussian curvature of  $S_1$  and  $R$  is the region bounded by  $\mathbf{u}_1$ .*

**Remark 4.5** This is a key result to the path finding algorithm. In order to realize a desired change of contact angle without altering the point of contact relative to  $S_1$ , we may plan a closed curve in  $S_1$  such that the Gaussian curvature integral over the region bounded by the loop is equal to the net angle change.

**Proof.** This follows from Gauss-Bonnet Theorem in differential geometry. For details see ([Tho78], [Kli78] and [Li89]).  $\blacksquare$

Using (4.25), (4.24) and Proposition 4.4, we have the following algorithm that generates a desired path when  $\text{obj}2$  is flat. The example of a unit ball on the plane is used for illustration.

**Algorithm 4.3** (*A Path Finding Algorithm*)

**Input:** 1. Initial and final contact configurations  $p_0 = (u_1^0, u_2^0, \psi^0)$  and  $p_f = (u_1^f, u_2^f, \psi^f)$ .

2. Geometric data of obj1 and obj2: curvature forms  $(K_1, K_2)$ , metric tensors  $(M_1, M_2)$  and connection forms  $(T_1, T_2 = 0)$ .

**Output:** An admissible path that links  $p_0$  to  $p_f$ .

**Step 1:** Find a path  $u_2(t) \in S_2, t \in [0, t_1]$ , such that

$$u_2(0) = u_2^0, \text{ and } u_2(t_1) = u_2^f. \quad (4.26)$$

Let  $u_1(t) \in S_1$  and  $\psi(t), t \in [0, t_1]$ , be the induced trajectory of contact relative to obj1 and the contact angle, respectively (i.e., the solution to (4.25)). At  $t = t_1$ , the contact point of obj1 and the contact angle reach some intermediate values, denoted by

$$\hat{u}_1 = u_1(t_1) \text{ and } \hat{\psi} = \psi(t_1).$$

**Step 2:** Find a closed path  $u_2(t) \in S_2, t \in [t_1, t_2]$ , such that the induced contact trajectory of obj1 has the property

$$u_1(t_1) = \hat{u}_1 \text{ and } u_1(t_2) = u_1^f.$$

Let  $\psi(t), t \in [t_1, t_2]$ , be the induced trajectory of the contact angle. At  $t = t_2$ , the angle of contact reaches some intermediate value denoted by

$$\bar{\psi} = \psi(t_2), \text{ where } \psi(t_1) = \hat{\psi}.$$

**Step 3:** Let  $\delta\psi = \psi^f - \bar{\psi}$  be the desired holonomy angle. Find a closed path  $u_1(t) \in S_1, t \in [t_2, t_f]$ , such that (1) the induced trajectory  $u_2(t) \in S_2, t \in [t_2, t_f]$ , is also closed and (2) the Gaussian curvature integral over the region bounded by  $u_1$  is equal to the desired holonomy angle.

**Output:** Return the path  $(u_1(t), u_2(t), \psi(t)) \in P, t \in [0, t_1, ] \cup [t_1, t_2] \cup [t_2, t_f]$ , which is the union of the paths found in Step 1, 2 and 3.

**Remark 4.6** The desired contact point  $u_2^f$  of obj2 is achieved in Step 1. Then, using a closed curve relative to obj2 in Step 2 the desired contact point  $u_1^f$  of obj1 is realized without sacrificing the desired contact point of obj2. Finally in Step 3,

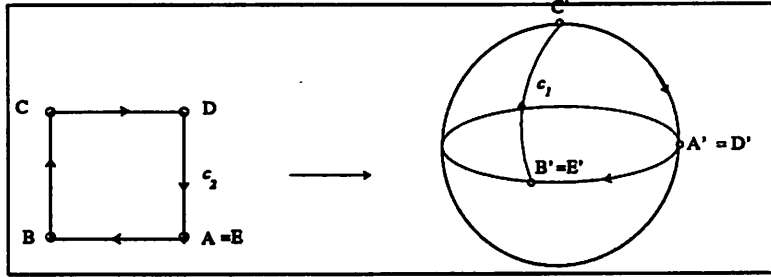


Figure 4.13: A Lie bracket motion

using a closed curve relative to *obj1*, which also induces a closed curve relative to *obj2*, the desired contact angle is realized.

We now use the example of a unit ball on the plane to illustrate the algorithm. Clearly, Step 1 can be easily done using existing techniques in robot motion planning ([Kod87], [Can88]). Step 2 and Step 3 are carried out as follows.

**Step 2A:** Let  $\hat{u}_1$  and  $u_1^f$  be the two contact points of *obj1*. We wish to construct a closed path  $u_2(t)$ ,  $t \in [t_1, t_2]$ , in the plane so that the induced contact trajectory  $u_1(t)$ ,  $t \in [t_1, t_2]$ , of  $S^2$  links  $\hat{u}_1$  to  $u_1^f$ .

**Lemma 4.1** *Let  $\hat{u}_1$  and  $u_1^f$  be exactly  $\pi/2$  distance apart in the unit sphere  $S^2$ . Then, the square of side length  $\pi/2$ , shown in Figure 4.13 will induce a contact trajectory  $u_1$  which links  $\hat{u}_1$  to  $u_1^f$ .*

**Proof.** We need to demonstrate that the square has the desired features. Label the point  $\hat{u}_1$  and  $u_1^f$  in the sphere by  $A'$  and  $B'$ , respectively, as shown in the figure.  $d(A', B') = \pi/2$ . There exists a unique geodesic, i.e., an arc of the great circle, that connects  $A'$  to  $B'$ . The great circle will be called the equator. Let  $A$  denote the initial point of contact in the plane. Thus, tracing the geodesic from  $A'$  to  $B'$  induces a straight line in the plane with end point  $B$ , and  $d(B, A) = \pi/2$  (by arc length constraint). Going from the point  $B$  to the point  $C$  in the plane is equivalent to going from the point  $B'$  to the north pole,  $C'$ , in the sphere. Note that  $\angle(ABC)$  and  $\angle(A'B'C')$  are both right angles. Now, tracing the straight line from  $C$  to  $D$  in the plane induces a curve in the sphere which ends at the starting point  $A'$ . Consequently, by closing the curve in the plane with a straight line joining  $D$  to  $A$ ,

we have arrived at the point  $B'$  in the sphere. This shows that the square indeed induces a curve in the sphere which has a net incremental distance  $\pi/2$ . This is called a Lie bracket motion. ■

We now return to the more general case.

**Step 2B:** By Lemma 4.1, we may assume that  $d(\hat{u}_1, u_1^f) < \pi/2$ . Otherwise, Lemma 4.1 can be applied repeatedly until some intermediate point which is less than  $\pi/2$  distance away from  $u_1^f$  is reached. Let  $l = d(\hat{u}_1, u_1^f) < \pi/2$  be the distance of these two points. We wish to construct a closed curve  $u_2(t), t \in [t_1, t_2]$ , in the plane such that the induced contact trajectory  $u_1(t), t \in [t_1, t_2]$ , has an incremental distance  $l$  along the geodesic connecting  $\hat{u}_1$  to  $u_1^f$ .

We propose to use for  $u_2$  the closed curve  $ABCDE$  shown in Figure 4.14, where  $x = d(A, B)$  is to be determined,  $d(B, C) = d(C, D) = \pi/2$ , and

$$\theta = 2 \tan^{-1} \frac{x}{\pi/2}.$$

We would like to show that for some choice of  $x$ , the closed curve  $ABCDE$  will induce a curve  $u_1(t), t \in [t_1, t_2]$ , in the sphere that links  $\hat{u}_1$  to  $u_1^f$ . First, by tracing the straight line from  $A$  to  $B$  and then to  $C$  induces a curve in the sphere which starts at  $A'$ , passes through  $B'$  and then comes to the north pole,  $C'$ . Note that  $d(B', A') = x$  and  $\angle(A'B'C') = 90^\circ$ . Going down from  $C$  to  $D$  with an angle  $\theta$  and by a distance  $\pi/2$  is equivalent to going down in the sphere from  $C'$  to some point  $D'$  at the equator. Clearly,  $d(B', D') = \theta$ . Now, Connect  $D$  to  $A$  by a straight line, and we claim that (1)  $\angle CDA = 90^\circ$  and (2)  $d(A, D) = x$ . To see this, note that by definition  $\angle ACD = \theta/2$  and  $AC$  is common to both the triangles  $\triangle ABC$  and  $\triangle ACD$ . Thus, they must be congruent triangles and the claim follows.

Thus, by tracing the straight line from  $D$  back to  $A$  in the plane, we have followed the equator from  $D'$  to some point  $E'$ , and  $d(E', D') = x$ . With  $u_2$  being the closed curve  $ABCDE$  for some choice of  $x$ , the induced curve  $u_1$  in the sphere has its starting point  $A'$  and its ending point  $E'$ , where  $d(E', A')$ , the net incremental distance, is a function of  $x$ . Let  $f(x) = d(E', A')$ . It is not hard to see that

$$f(x) = 2x - \theta = 2x - 2 \tan^{-1} \frac{x}{\pi/2}.$$

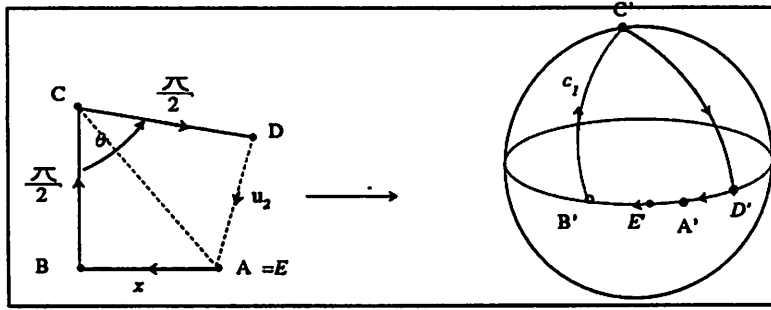


Figure 4.14: A (general) Lie bracket motion

The hope is to find an  $x$ , if possible, that solves the equation

$$f(x) \stackrel{?}{=} l. \quad (4.27)$$

We claim that there exists a unique  $x$  that solves (4.27). To show this, note that  $f(0) = 0$  and  $f(\pi/2) = \pi/2 > l$ . Thus, solutions exist. For the uniqueness part, we compute the derivative of  $f(x)$ , which is given by

$$f'(x) = 2 - 2 \frac{2/\pi}{1 + \frac{4x^2}{\pi^2}} = \frac{2 - 2/\pi + 4x^2/\pi^2}{1 + 4x^2/\pi^2} > 0.$$

Thus,  $f(x)$  is a monotone function and the solution to (4.27), denoted by  $x^*$ , is unique!

Consequently, the curve  $ABCDE$ , with  $d(B, A) = x^*$ , has all the desired features.

**Step 3':** We wish to find a closed path  $u_1(t), t \in [t_2, t_f]$ , in  $S^2$  such that (1) the induced path  $u_2(t), t \in [t_2, t_f]$ , in the plane is also closed and (2)  $u_1$  has a desired holonomy angle  $\delta\psi$ .

We may assume that  $0 < -\delta\psi < 2\pi$ . Consider the latitude circle with  $u_1(t) = u_1(0)$ , and  $v_1(t) = v_1(0) + t, t \in [t_2, t_2 + 2\pi]$ . We claim that (1) the induced trajectory  $u_2$  is also a circle and (2) the holonomy angle of  $u_1$  ranges from 0 to  $2\pi$  for  $0 < u_1(0) < \pi/2$ . To see this, substitute the expression of  $\begin{bmatrix} u_1(t) \\ v_1(t) \end{bmatrix}$  into (4.24) and after some algebra, we get

$$\psi(t) - \psi(0) = -\sin u_1(0)t \triangleq \alpha t, \quad \alpha = -\sin u_1(0),$$

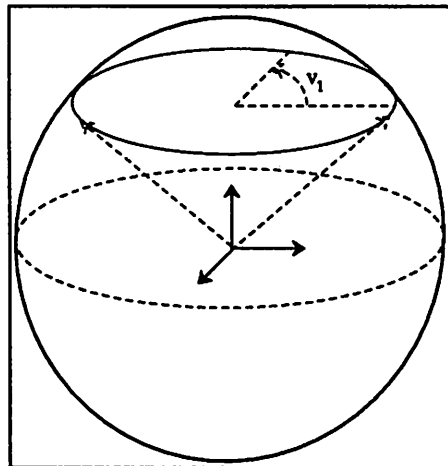


Figure 4.15: Another Lie bracket motion

and

$$u_2(t) = \beta \cos(\alpha t + \psi_0) + \gamma_0, \quad \gamma_0 = u_2(0) - \cos \psi_0 \cos u_1(0)/\alpha,$$

$$v_2(t) = -\beta \sin(\alpha t + \psi_0) + \delta_0, \quad \delta_0 = v_2(0) + \sin \psi_0 \cos u_1(0)/\alpha.$$

Thus, we have

$$(u_2(t) - \gamma_0)^2 + (v_2(t) - \delta_0)^2 = \beta^2.$$

This shows the claim.

## 4.5 Conclusion

This chapter studied three problems related to task planning for a robot hand system.

We have proposed a procedure for task modeling. The task model was used to develop two quality measures for a grasp. We have shown that up to a certain point, as one quality measure goes up the other goes down. Thus, the performance measure which balances the two is the proper objective function to for optimization.

We have not worked out the details for the optimization problem yet, and there remains many open problems in this area.

We have defined precisely the problem of dextrous manipulation. In order to work on motion planning for dextrous manipulation we need to deal with non-

holonomic constraints. The two types of nonholonomic constraints in a robot hand system are: rolling constraint and constraint due to finger relocation. While rolling constraint can be described by differential equations, there is no mathematical model for finger relocation. This is what makes dextrous manipulation difficult.

To gain further insight into dextrous manipulation, we have studied motion of two rigid bodies under rolling constraint. A systematic procedure for deriving the configuration space of contact and the differential equation for the constraint is presented. This approach is applicable to objects of arbitrary shapes and under any contact constraints. For example, one may use this formulation to study motion of two rigid bodies under sliding or a combination of sliding and rolling constraints.

An algorithm that determines the existence of an admissible path between two contact configurations is given. First, the distribution generated by the two constrained vector fields is computed. One then checks to see if the distribution is nonsingular. If so an admissible path exists between any two contact configurations.

It has also been shown that the path finding problem is equivalent to a nonlinear control problem. Thus, existing works in nonlinear control theory can be used. A geometric algorithm that finds a path when one object is flat is presented.

# Bibliography

- [Bro81] R. Brockett. *Control Theory and Singular Riemannian Geometry*, pages 11–27. *New Directions in Applied Mathematics*, Springer-Verlag New York Inc., 1981.
- [Bro88] R. W. Brockett. On the rectification of vibratory motion. In *Proceedings of Microactuators and Micromechanism*, Salt Lake City, Utah, 1988.
- [CAHK87] M. Cutkosky, P. Akella, R. Howe, and I. Kao. *Grasping as a contact of sports*. Technical Report, Department of Mechanical Engineering, Stanford University, 1987.
- [Can88] J.F. Canny. *The complexity of robot motion planning*. MIT Press, 1988.
- [Cho40] W.L. Chow. Ueber systeme von linearen partiellen differentialgleichungen erster ordnung. *Math. Ann.*, 117(No.1):98–105, 1940.
- [Cut86] M. Cutkosky. *Grasping and Fine Manipulation for Automated Manufacturing*. Kulware-Academic Publisher, 1986.
- [HA77] H. Hanafusa and H. Asada. *Stable prehension by a robot hand with elastic fingers*, chapter 5. *Robot Motion: Planning and Control*, MIT Press, 1977.
- [HK77] R. Hermann and A.J. Krener. Nonlinear controllability and observability. *IEEE Transaction on Automatic Control*, 22:728–740, 1977.
- [Kli78] W. Klingenberg. *A course in differential geometry*. Springer-Verlag, 1978.

- [Kod87] D.E. Koditschek. Exact robot navigation by means of potential functions: some topological considerations. In *IEEE International Conference on Robotics and Automation*, pages 1-6, 1987.
- [Lak78] K. Lakshminarayna. Mechanics of form closure. In *ASME Design Engineering Technical Conference*, Minneapolis, Minn., 1978.
- [LCS89] Z.X. Li, J. F. Canny, and S.S. Sastry. On motion planning for dextrous manipulation. In *IEEE International conference on robotics and automation*, 1989.
- [LHS89] Z.X. Li, P. Hsu, and S. Sastry. On grasping and coordinated manipulation by a multifingered robot hand. *International Journal of Robotics Research*, 8:4, 1989.
- [Li89] Z.X. Li. *Motion Planning with Nonholonomic Constraints*. Master's thesis, Mathematics Department, University of California at Berkeley, Berkeley, Ca. 94720 (to appear in *IEEE Transaction on Robotics and Automation*), 1989.
- [Loz82] T. Lozano-Perez. *Task Planning*, chapter 6. *Robot Motion: Planning and Control*, MIT Press, 1982.
- [LS88] Z.X. Li and S. Sastry. Task oriented optimal grasping by multifingered robot hand. *IEEE Journal of Robotics and Automation*, 4(1):32-44, 1988.
- [MN86] Patrick F. Muir and Charles P. Neuman. *Kinematic Modeling of Wheeled Mobile Robots*. Technical Report, Robotics Institute, Carnegie-Mellon University, 1986.
- [Mon88] R. Montgomery. *Shortest loops with a fixed holonomy*. Technical Report, Mathematical Science Research Institute, University of California, Berkeley, 1988.
- [MS85] M.T. Mason and J. K. Salisbury. *Robot Hands and the Mechanics of Manipulation*, chapter 1 - 10. MIT Press, 1985.

- [MSS86] B. Mishra, J.T. Schwartz, and M. Sharir. *On the existence and synthesis of multifinger positive grips*. Technical Report 259, Department of Computer Science, Courant Institute of Mathematical Science, 1986.
- [Ngu86] V. Nguyen. *The synthesis of force-closure grasps*. Master's thesis, Department of Electrical Engineering and Computer Science, MIT, 1986.
- [Reu75] F. Reuleaux. *Theoretische Kinematik*. Translated as Kinematics of Machinery, Dover, New York, 1875.
- [Son88a] Eduardo D. Sontag. *Integrability of certain distributions associated to actions on manifolds and an introduction to Lie-algebra control*. Technical Report, Department of Mathematics, Rutgers University, Report SYCON-88-04, 1988.
- [Son88b] Eduardo D. Sontag. *Some Complexity Questions Regarding Controllability*. Technical Report, Department of Mathematics, Rutgers University, Report SYCON-88-06, 1988.
- [Sus83] H. J. Sussmann. *Lie brackets, real analyticity and geometric control*. Differential Geometric Control Theory, Birkhauser, Boston, 1983.
- [Tho78] J.A. Thorpe. *Elementary topics in differential geometry*. Springer-Verlag, 1978.
- [Tri87] J. Trinkle. *Mechanics and planning of enveloping grasps*. PhD thesis, Department of Computer and Information Science, University of Pennsylvania, 1987.
- [Wes81] C. Von Westenholz. *Differential Forms in Mathematical Physics*. North-Holland Publishing Company, Amsterdam, 1981.
- [Whi82] D.E. Whitney. Quasi static assembly of compliantly supported rigid parts. *Journal of Dynamic Systems, Measurement and Control*, 104:65-77, 1982.

## Chapter 5

# Coordinated Control of Robot Hands

### 5.1 Introduction

Robot hand control, including the control of a multiple-robotic system, has been a topic of active research in the past few years.

C. Alford and S. Belyen ([AB84]) proposed the master-slave scheme for the control of two robot arms manipulating a common object. They assume that each arm *rigidly grips* the object, and one of the arm is assigned as the master and the other the slave. The master arm is position controlled to follow a predetermined path and the slave arm is force controlled to maintain the contact. This scheme is generalized by S. Arimoto ([Ari87]) to a multiple -robotic system. Similar works, including some open-loop control strategies, can also be found in ([NNY87], [TBY86], [ZL85], [MS85] and [CCSS89]). Major drawbacks associated with these approaches are: (1) Restrictive assumptions on the contact models, such as the requirement for rigid contact. (2) A lack of stability proof of the schemes. (3) Ignorance of the dynamical properties of the system.

We present in this chapter a general formulation for the control of a robot hand system The starting assumptions are: *A nominal grasp configuration has been obtained through grasp planning or dextrous manipulation, and the contact constraints are specified. Furthermore, a trajectory of the object is carefully planned (using trajectory planning for coordinated manipulation).*

This formulation provides control laws for the following types of contact constraints: (a) a fixed point of contact, soft-finger contact or rigid contact, and (b) rolling contact. Each control law will ensure that the object can be manipulated to follow the predetermined path and the contact constraint be maintained.

## Control of Robot Manipulators: A Review

First, we will review two strategies for the control of a robot manipulator: the computed-torque method and the Cartesian space control. We will discuss the general philosophy underlying these approaches.

### Control Algorithms for Coordinated Manipulation by Robot Hands

We use the philosophy for the control of a manipulator to formulate the control strategies for a robot hand system. Our approaches consists of three steps. (1) Establish the kinematic constraints; (2) Formulate the dynamics equations of motion for the whole system and (3) apply the kinematic constraints to the dynamics equations of motion and then derive the appropriate control inputs to realize the desired objectives. Finally, we will show simulation results.

## 5.2 Control of Robot Manipulators: A Review

This section presents a review of strategies to the position control of robot manipulators. The objective of each control strategy is to specify a set of torque inputs to motors at the joints so that the end effector of a manipulator follows a prescribed trajectory. A trajectory of the end effector, from Section 2.2, is a curve  $g(t), t \in [0, t_f]$  in the special Euclidean group  $SE(3)$  and has the form

$$g(t) = \begin{bmatrix} R(t) & r(t) \\ 0 & 1 \end{bmatrix}, R(t) \in SO(3), r(t) \in \mathbb{R}^3.$$

But, it would be very inefficient to specify all 9 entries in the rotational matrix  $R(t)$ . The fact that  $SO(3)$  is a 3 dimensional manifold permits us to parameterize it at least locally by three variables  $\phi = (\phi_1, \phi_2, \phi_3)^T \in \mathbb{R}^3$ . Traditional choices of the orientation variables include the Euler angles, roll-pitch-yaw variables and the

exponential coordinates ([Cra86]). Consequently, a desired trajectory of the end effector is represented by a curve  $(r_d(t), \phi_d(t)), t \in [0, t_f]$ , in  $\mathbb{R}^6$ .

The orientation matrix,  $R(\phi)$ , using the roll-pitch-yaw variables,  $\phi = (\phi_1, \phi_2, \phi_3)$ , has the form (see [Cra86]):

$$\begin{bmatrix} \cos \phi_1 \cos \phi_2 & \cos \phi_1 \sin \phi_2 \sin \phi_3 - \sin \phi_1 \cos \phi_3 & \cos \phi_1 \sin \phi_2 \cos \phi_3 + \sin \phi_1 \sin \phi_3 \\ \sin \phi_1 \cos \phi_2 & \sin \phi_1 \sin \phi_2 \sin \phi_3 + \cos \phi_1 \cos \phi_3 & \sin \phi_1 \sin \phi_2 \cos \phi_3 - \cos \phi_1 \sin \phi_3 \\ -\sin \phi_2 & \cos \phi_2 \sin \phi_3 & \cos \phi_2 \cos \phi_3 \end{bmatrix}$$

This enables us to write the angular velocity as a function of  $\dot{\phi}$ ,

$$\begin{bmatrix} w_1 \\ w_2 \\ w_3 \end{bmatrix} = \begin{bmatrix} -\sin \phi_2 & 0 & 1 \\ \cos \phi_2 \sin \phi_3 & \cos \phi_3 & 0 \\ \cos \phi_2 \cos \phi_3 & -\sin \phi_3 & 0 \end{bmatrix} \begin{bmatrix} \dot{\phi}_1 \\ \dot{\phi}_2 \\ \dot{\phi}_3 \end{bmatrix} \triangleq U(\phi)\dot{\phi}. \quad (5.1)$$

$U(\phi)$  has full rank as long as the pitch angle,  $\phi_2$ , remains in the interval  $(-\pi/2, \pi/2)$ . We thus say that the parameterization is locally nonsingular. Note that the Euler angles are singular around any neighborhood of zero.

We assume that (1) *an exact model of the manipulator in terms of its dynamics equations of motion is available* and (2) *there are sensors located at the joints which measure the joint position,  $\theta$  and the joint velocity,  $\dot{\theta}$ .*

With these assumptions, the following control methods specify the joint torque inputs that enables the end effector to follow the desired trajectory.

### 5.2.1 Computed Torque Method

The computed torque method has its roots in ([Pau72], [Mar73] and [Bej74]). It is an example of a class of nonlinear control techniques known as the *exact linearization method* ([Isi85]), which first *linearizes a nonlinear system by state feedback* and then *designs a compensator based on the linearized system*.

The nonlinear dynamics of  $m$  degrees-of-freedom manipulator has the form (see als Section 2.4).

$$M(\theta)\ddot{\theta} + N(\theta, \dot{\theta}) = \tau, \quad (5.2)$$

where  $M(\theta) \in \mathbb{R}^{m \times m}$  is the symmetric, positive definite inertia matrix,  $N(\theta, \dot{\theta}) \in \mathbb{R}^m$  is the vector of Coriolis, centrifugal and gravitational forces, and  $\tau \in \mathbb{R}^m$  is the joint torque inputs.

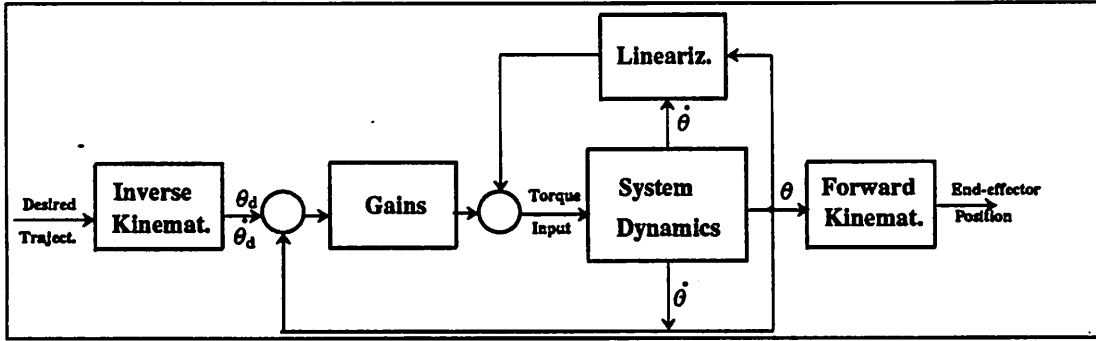


Figure 5.1: A block diagram of the computed torque method.

By the computed torque method, the first step is to obtain the desired joint position trajectory,  $\theta_d(t), t \in [0, t_f]$ , from the desired end-effector trajectory,  $g_d(t), t \in [0, t_f]$ , by solving the inverse kinematics ([Cra86] and [Pad86]). The second step consists of splitting the torque input,  $\tau$ , into two components: The first component linearizes the manipulator dynamics by state feedback and the second component is a compensator based on the linearized dynamics. Overall, the joint torque input has the form

$$\tau = N(\theta, \dot{\theta}) + M(\theta)(\ddot{\theta}_d - K_v \dot{e}_\theta - K_p e_\theta) \quad (5.3)$$

where

$$e_\theta = \theta(t) - \theta_d(t)$$

is the trajectory tracking error,  $K_p, K_v \in \mathbb{R}^{m \times m}$  are the position and velocity gains.

To show the control law given by Eq. (5.3) does the desired job we simply apply it to Eq. (5.2) and after rearrangement of terms, we get

$$M(\theta)(\ddot{e}_\theta + K_v \dot{e}_\theta + K_p e_\theta) = 0. \quad (5.4)$$

Since  $M(\theta)$  is positive definite, we conclude that

$$\ddot{e}_\theta + K_v \dot{e}_\theta + K_p e_\theta = 0. \quad (5.5)$$

and the trajectory tracking error,  $e_\theta$ , goes to zero asymptotically with proper choices of the feedback gains.

A block diagram of the computed torque method is given in Figure 5.1.

### 5.2.2 Cartesian Space Control

A drawback of the computed torque method is the need to calculate the inverse kinematics, which is often computationally intensive. This can be avoided if we define the trajectory error in the Cartesian space, or sometimes called the task space ([Kha87]), and close the control loop at the Cartesian space. This is what so called the Cartesian space control. The philosophy of the Cartesian space control is exactly the same as that of the computed torque method.

The desired trajectory of the end effector has the form

$$x_d(t) \triangleq \begin{bmatrix} r_d(t) \\ \phi_d(t) \end{bmatrix} \in \mathbb{R}^6, t \in [0, t_f].$$

Define the Cartesian space trajectory tracking error,  $e_x$ , by

$$e_x = x(t) - x_d(t).$$

$\dot{x}(t)$  is directly related to the velocity  $(v^T, w^T)^T$  by the formulae

$$\dot{x}(t) = \begin{bmatrix} \dot{r}(t) \\ \dot{\phi}(t) \end{bmatrix} = \begin{bmatrix} R(\phi) & 0 \\ 0 & U^{-1}(\phi) \end{bmatrix} \begin{bmatrix} v \\ w \end{bmatrix}. \quad (5.6)$$

Using the manipulator Jacobian of Section 2.3, we have

$$\dot{x}(t) = J_x \dot{\theta}, \text{ where } J_x = \begin{bmatrix} R(\phi) & 0 \\ 0 & U^{-1}(\phi) \end{bmatrix} J(\theta) \quad (5.7)$$

is called the generalized Jacobian.

Differentiating Eq. (5.7) with respect to time, yields

$$\ddot{x}(t) = J_x \ddot{\theta} + \dot{J}_x \dot{\theta}. \quad (5.8)$$

Consider now the manipulator dynamics equation in the joint space.

$$M(\theta) \ddot{\theta} + N(\theta, \dot{\theta}) = \tau. \quad (5.9)$$

Multiply Eq. (5.9) by  $M^{-1}(\theta)$  and then by  $J_x$  and substitute Eq. (5.8) into the resulting equation, we have

$$\ddot{x} - \dot{J}_x \dot{\theta} + J_x M^{-1}(\theta) N(\theta, \dot{\theta}) = J_x M^{-1}(\theta) \tau. \quad (5.10)$$

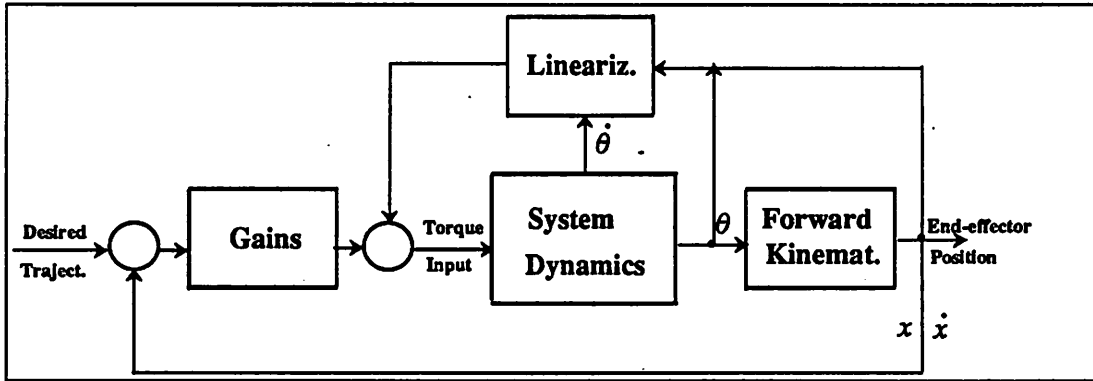


Figure 5.2: A block diagram of the Cartesian space control.

If  $x$  qualifies to be a set of generalized coordinates then Eq. (5.10) will be the dynamical equation of the manipulator in the Cartesian space. Otherwise it has no real physical meaning. We assume that *the manipulator Jacobian and hence the generalized Jacobian is nonsingular*. Under this assumption, it is not difficult to show that the following control law drives the trajectory tracking error,  $e_x$ , to zero asymptotically.

$$\tau = \underbrace{N(\theta, \dot{\theta}) - M(\theta)J_x^{-1}\dot{J}_x\dot{\theta}}_{\tau_1} + \underbrace{MJ_x^{-1}(\ddot{x}_d - K_v\dot{e}_x - K_p e_x)}_{\tau_2}. \quad (5.11)$$

The first component,  $\tau_1$ , of the control linearizes the nonlinear dynamics and the second component,  $\tau_2$ , is a compensator based on the linearized model. A block diagram of the Cartesian space control is shown in Figure 5.2.

### 5.3 Control Algorithms for Coordinated Manipulation by Robot Hands

This section centers on the development of new control algorithms for coordinated manipulation by robot hands. Consider the hand manipulation system shown in Figure 5.3.

The immediate objective of the control task is to *manipulate the object to follow a prescribed trajectory in space, while exert possibly a set of contact forces upon the environment*. During the course of manipulation, the robot fingers may make (1) *fixed frictional point contact* or (2) *rolling contact* (See Section 3.3). Con-

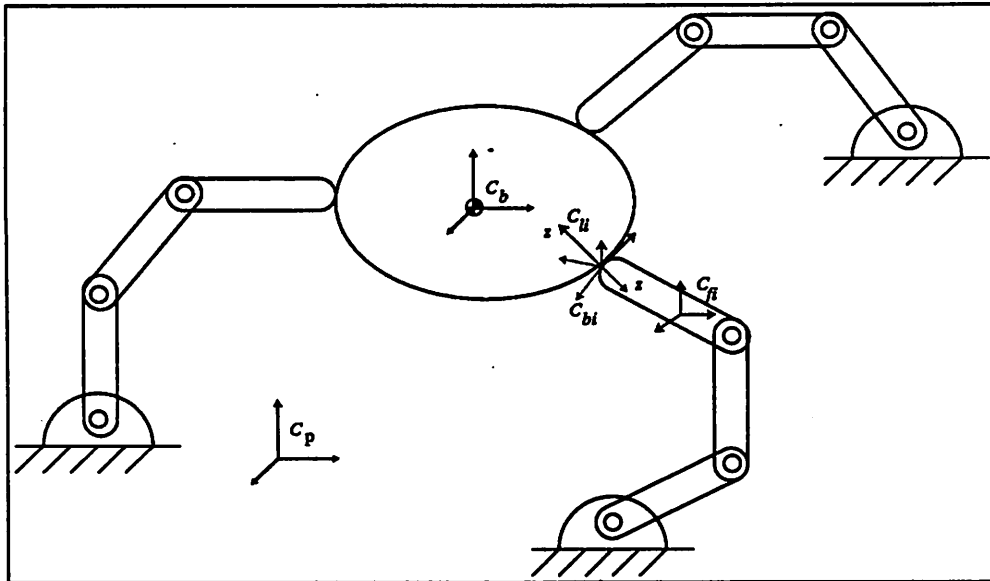


Figure 5.3: A robot hand system.

sequently, the secondary objective of the control is to *ensure that the appropriate contact constraints are maintained or reinforced during the course of manipulation.*

We call the act of manipulating an object with fixed points of contact *coordinated manipulation*, and the act of manipulating an object with rolling contact *rolling motion*. The means of control to achieve coordinated manipulation or rolling motion are the torque inputs to the motors at the finger joints. We develop in the following a set of control laws for coordinated manipulation as well as for rolling motion.

**Assumption 5.1 (a)** *There is available an exact model of the robot hand system, given in terms of the dynamics equations of the object and of the fingers, and the kinematics relations of the robot hand.*

(b) *There are sensors located at the finger joints which measure the joint position and joint velocity, and also there are sensors which measure the object position and velocity.*

(c) *There are tactile-type of sensors located at the fingertips which measure the contact positions and contact forces.*

### 5.3.1 Control Laws for Coordinated Manipulation

We start with the derivation of control laws for coordinated manipulation. The goals of the control are:

- To have the object follow a desired trajectory parameterized by  $(r_{b,p}^d(t), \phi_{b,p}^d(t)) \in \mathbb{R}^6, t \in [0, t_f]$ , where  $\phi_{b,p}^d(t)$  does not go through singularities.
- Reinforce the contact constraint at each point of contact.

From the manipulation experience of human hands, an effective way of maintaining contact constraint is to squeeze the object sufficiently. In terminologies of this thesis this translates to choosing a trajectory of desired internal grasping force and realizing it during the course of manipulation. Recall from Section 3.4 that internal grasping forces are elements of  $\eta(G)$ , the null space of the grip Jacobian, and  $G$  and hence  $\eta(G)$  is constant for fixed points of contact. Thus, the second goal of the control is to ensure that

- A desired trajectory  $x_o^d(t) \in \eta(G), t \in [0, t_f]$ , is realized.

There are many ways to choose  $x_o^d(t)$ , as the degree at which to squeeze an object may vary from person to person, task to task and environment to environment. Trajectory planning for  $x_o^d(t)$  subject to a given task and a given hand is another topic of further research (see also [Ker85] and [NNY87]).

With these two objectives in mind, we use the philosophy of the Cartesian space control to develop a model based control law for coordinated manipulation.

Recall Eq. (5.6), the object velocity can be expressed as a function of

$$\begin{bmatrix} \dot{r}_{b,p} \\ \dot{\phi}_{b,p} \end{bmatrix}.$$

$$\begin{bmatrix} v_{b,p} \\ w_{b,p} \end{bmatrix} = \begin{bmatrix} R^T(\phi) & 0 \\ 0 & U(\phi) \end{bmatrix} \begin{bmatrix} \dot{r}_{b,p} \\ \dot{\phi}_{b,p} \end{bmatrix} \triangleq \hat{U}(\phi) \begin{bmatrix} \dot{r}_{b,p} \\ \dot{\phi}_{b,p} \end{bmatrix} \quad (5.12)$$

$\hat{U}(\phi_{b,p}) \in \mathbb{R}^{6 \times 6}$  is invertible if the parameterization is nonsingular. Differentiating Eq. (5.12) with respect to time  $t$ , yields the acceleration relation

$$\begin{bmatrix} \dot{v}_{b,p} \\ \dot{w}_{b,p} \end{bmatrix} = \hat{U}(\phi_{b,p}) \begin{bmatrix} \ddot{r}_{b,p} \\ \ddot{\phi}_{b,p} \end{bmatrix} + \dot{\hat{U}}(\phi_{b,p}) \begin{bmatrix} \dot{r}_{b,p} \\ \dot{\phi}_{b,p} \end{bmatrix}. \quad (5.13)$$

The kinematic relations of a robot hand system have been summarized in Table 3.1, where the fundamental constraint is given by

$$J_h(\theta)\dot{\theta} = G^t \begin{bmatrix} v_{b,p} \\ w_{b,p} \end{bmatrix} \quad (5.14)$$

$G$  is constant for coordinated manipulation but is time varying for rolling motion. Differentiate Eq. (5.14) with respect to time yields the acceleration constraint between the object and the fingers.

$$J_h(\theta)\ddot{\theta} + \dot{J}_h(\theta)\dot{\theta} = G^t \begin{bmatrix} \dot{v}_{b,p} \\ \dot{w}_{b,p} \end{bmatrix} + \dot{G}^t \begin{bmatrix} v_{b,p} \\ w_{b,p} \end{bmatrix}. \quad (5.15)$$

The second term to the right hand side of Eq. (5.15) disappear for coordinated manipulation.

**Assumption 5.2** *We assume that the grasp  $\Omega \triangleq (G, K, J_h)$  is stable and manipulable through the prescribed trajectory.*

Consequently, we have that  $G$  is onto and  $R(J_h) \supset R(G^T)$ . Without loss of generality we may substitute the manipulability condition by the existence of generalized inverse,  $J^+ = J_h^T (J_h J_h^T)^{-1}$ , to the hand Jacobian.

Under these assumptions, the joint acceleration,  $\ddot{\theta}$ , can be expressed as a function of the object acceleration.

$$\ddot{\theta} = J_h^+ G^t \begin{bmatrix} \dot{v}_{b,p} \\ \dot{w}_{b,p} \end{bmatrix} + J_h^+ \dot{G}^t \begin{bmatrix} v_{b,p} \\ w_{b,p} \end{bmatrix} - J_h^+ \dot{J}_h \dot{\theta} + \ddot{\theta}_o. \quad (5.16)$$

where  $\ddot{\theta}_o \in \eta(J_h)$  is any vector of joint motion not affecting motion of the contact points. The existence of  $\ddot{\theta}_o$  arises from robot fingers having redundant degrees of freedom. For example, a finger with four joints in general position has one redundant degree of freedom under a frictional point contact model. But this redundancy disappears under a soft finger contact model. When every finger has no redundant degrees of freedom  $J_h$  is square and its generalized inverse becomes the usual inverse. Consequently, the last term to the right hand side of Eq. (5.16) vanishes.

**Remark 5.1** Consider again Eq. (5.15). Another possibility is to express the object acceleration in terms of the finger acceleration.

$$\begin{bmatrix} \dot{v}_{b,p} \\ \dot{w}_{b,p} \end{bmatrix} = (G G^t)^{-1} G \left( J_h \ddot{\theta} + \dot{J}_h \dot{\theta} - \dot{G}^t \begin{bmatrix} v_{b,p} \\ w_{b,p} \end{bmatrix} \right)$$

Proceeding along this direction will lead to the development of control laws in the joint space. It would be of interest to examine this alternative.  $\square$

The Newton-Euler equations of motion of the object are

$$\begin{bmatrix} \hat{m} & 0 \\ 0 & \mathcal{I} \end{bmatrix} \begin{bmatrix} \dot{v}_{b,p} \\ \dot{w}_{b,p} \end{bmatrix} + \begin{bmatrix} w_{b,p} \times \hat{m}v_{b,p} \\ w_{b,p} \times \mathcal{I}w_{b,p} \end{bmatrix} = \begin{bmatrix} f_b \\ m_b \end{bmatrix}, \quad (5.17)$$

where  $\hat{m} \in \mathbb{R}^{3 \times 3}$  is the diagonal matrix with the object mass in the diagonal,  $\mathcal{I} \in \mathbb{R}^{3 \times 3}$  is the object inertia matrix with respect to the body coordinates, and  $[f_b^t, m_b^t]^t$  is the applied body wrench in the body coordinates which is also related to the applied finger wrench  $x \in \mathbb{R}^n$  through

$$Gx = \begin{bmatrix} f_b \\ m_b \end{bmatrix}. \quad (5.18)$$

Notice that gravity and interaction forces from the environment can always be added to the right hand side of (5.17), and corresponding contact wrenches will be generated to simply counteract them.

By Assumption 5.2  $G$  is onto and we can write the solution to (5.18) in the form

$$x = G^+ \begin{bmatrix} f_b \\ m_b \end{bmatrix} + x_o, \quad (5.19)$$

where  $G^+ = G^T(GG^T)^{-1}$  is the left inverse of  $G$ , and  $x_o \in \eta(G)$  is the internal grasping force. Remember that the second goal of the control is to steer the internal grasping force  $x_o$  to its desired value  $x_o^d(t)$ .

Combining (5.17) and (5.19) yields

$$x = G^+ \left\{ \begin{bmatrix} \hat{m} & 0 \\ 0 & \mathcal{I} \end{bmatrix} \begin{bmatrix} \dot{v}_{b,p} \\ \dot{w}_{b,p} \end{bmatrix} + \begin{bmatrix} w_{b,p} \times \hat{m}v_{b,p} \\ w_{b,p} \times \mathcal{I}w_{b,p} \end{bmatrix} \right\} + x_o. \quad (5.20)$$

The dynamics of the  $i$ th finger manipulator is given by

$$M_i(\theta_i)\ddot{\theta}_i + N_i(\theta_i, \dot{\theta}_i) = \tau_i - J_i^t(\theta_i)B_i x_i. \quad (5.21)$$

Here again,  $M_i(\theta_i) \in \mathbb{R}^{m_i \times m_i}$  is the moment of inertia matrix of the  $i$ th finger manipulator,  $N_i(\theta_i, \dot{\theta}_i) \in \mathbb{R}^{m_i}$  is the centrifugal, Coriolis and gravitational force

terms,  $\tau_i$  is the vector of joint torque inputs and  $B_i x_i \in \mathbb{R}^6$  the vector of applied finger wrenches. Define

$$M(\theta) = \text{Diag}\{M_1(\theta_1), \dots, M_k(\theta_k)\}, \quad N(\theta, \dot{\theta}) = \begin{bmatrix} N_1(\theta_1, \dot{\theta}_1) \\ \vdots \\ N_k(\theta_k, \dot{\theta}_k) \end{bmatrix} \quad \tau = \begin{bmatrix} \tau_1 \\ \vdots \\ \tau_k \end{bmatrix}. \quad (5.22)$$

Then, the finger dynamics can be grouped to yield

$$M(\theta)\ddot{\theta} + N(\theta, \dot{\theta}) = \tau - J_h^t(\theta)x. \quad (5.23)$$

Eq. (5.23) is the dynamics equation of the robot hand.

The following theorem provides a control law for a robot hand with non-redundant degrees of freedom, i.e.,  $m_i = n_i, i = 1, \dots, k$ .

**Theorem 5.1** *Let Assumption 5.2 hold. Define the position trajectory tracking error,  $e_p \in \mathbb{R}^6$ , and the internal grasping force error,  $e_f \in \mathbb{R}^6$ , by*

$$e_p(t) = \begin{bmatrix} r_{b,p}(t) \\ \phi_{b,p}(t) \end{bmatrix} - \begin{bmatrix} r_{b,p}^d(t) \\ \phi_{b,p}^d(t) \end{bmatrix}; \quad (5.24)$$

and

$$e_f(t) = x_o(t) - x_o^d(t), \quad (5.25)$$

respectively. Then the control law specified by Eq. (5.26) drives  $e_p$  and  $e_f$  asymptotically to zero.

$$\begin{aligned} \tau = & \underbrace{N(\theta, \dot{\theta}) + J_h^T G^+ \begin{bmatrix} w_{b,p} \times \hat{m} v_{b,p} \\ w_{b,p} \times \mathcal{I} w_{b,p} \end{bmatrix}}_{\tau_1} - M(\theta) J_h^{-1} \dot{J}_h \dot{\theta} + M_h \dot{U} \begin{bmatrix} \dot{r}_{b,p} \\ \dot{\phi}_{b,p} \end{bmatrix} \\ & + \underbrace{J_h^t(x_o^d - K_I \int e_f)}_{\tau_2} + M_h \dot{U} \left\{ \underbrace{\begin{bmatrix} \ddot{r}_{b,p}^d \\ \ddot{\phi}_{b,p}^d \end{bmatrix}}_{\tau_3} - K_v \dot{e}_p - K_p e_p \right\}, \end{aligned} \quad (5.26)$$

where

$$M_h = M(\theta) J_h^{-1} G^T + J_h^T G^+ \begin{bmatrix} \hat{m} & 0 \\ 0 & \mathcal{I} \end{bmatrix} \quad (5.27)$$

$K_p, K_v$  are the position and velocity gains in the position loop, and  $K_I$  is the integral gain in the force loop and is chosen so that the null space of  $G$  is  $K_I$ -invariant.

**Remark 5.2** 1.

$$GJ_h^{-T}M_h = GJ_h^{-T}M(\theta)J_h^{-1}G^T + \begin{bmatrix} \hat{m} & 0 \\ 0 & \mathcal{I} \end{bmatrix}$$

is called the generalized inertia matrix of the hand system.

2. The first component,  $\tau_1$ , of the control law linearizes the system dynamics, the second component,  $\tau_2$ , is a compensator in the position loop and the third component,  $\tau_3$ , is a compensator in the internal force loop.
3. As we will see in the proof that the control law decouples the position loop from the force loop. This is one of the unique features of this control law. □

**Proof.** The proof is very procedural and straightforward. First, Eq. (5.16) reads,

$$\ddot{\theta} = J_h^{-1}G^T \begin{bmatrix} \dot{v}_{b,p} \\ \dot{w}_{b,p} \end{bmatrix} - J_h^{-1}j_h\dot{\theta}. \quad (5.28)$$

Substitute Eqs (5.28), (5.20) into (5.23) we have

$$M \left\{ J_h^{-1}G^T \begin{bmatrix} \dot{v}_{b,p} \\ \dot{w}_{b,p} \end{bmatrix} - J_h^{-1}j_h\dot{\theta} \right\} + N = \tau - J_h^T \left\{ G^+ \begin{bmatrix} \hat{m} & 0 \\ 0 & \mathcal{I} \end{bmatrix} \begin{bmatrix} \dot{v}_{b,p} \\ \dot{w}_{b,p} \end{bmatrix} + G^+ \begin{bmatrix} w_{b,p} \times \hat{m}v_{b,p} \\ w_{b,p} \times \mathcal{I}w_{b,p} \end{bmatrix} \right\} - J_h^T x_o. \quad (5.29)$$

Linearize (5.29) with the following control

$$\tau = N(\theta, \dot{\theta}) + J_h^T G^+ \begin{bmatrix} w_{b,p} \times \hat{m}v_{b,p} \\ w_{b,p} \times \mathcal{I}w_{b,p} \end{bmatrix} - M(\theta)J_h^{-1}j_h\dot{\theta} + \tau_1 \quad (5.30)$$

where  $\tau_1$  is to be determined, we have

$$\left\{ M(\theta)J_h^{-1}G^T + J_h^T G^+ \begin{bmatrix} \hat{m} & 0 \\ 0 & \mathcal{I} \end{bmatrix} \right\} \begin{bmatrix} \dot{v}_{b,p} \\ \dot{w}_{b,p} \end{bmatrix} = \hat{\tau}_1 - J_h^T x_o, \quad (5.31)$$

or

$$M_h \begin{bmatrix} \dot{v}_{b,p} \\ \dot{w}_{b,p} \end{bmatrix} = \hat{\tau}_1 - J_h^T x_o.$$

Substituting (5.13) into the above equation yields

$$M_h \left\{ \dot{U} \begin{bmatrix} \ddot{r}_{b,p} \\ \ddot{\phi}_{b,p} \end{bmatrix} + \dot{U} \begin{bmatrix} \dot{r}_{b,p} \\ \dot{\phi}_{b,p} \end{bmatrix} \right\} = \hat{\tau}_1 - J_h^t x_o. \quad (5.32)$$

Finally, let the control input  $\hat{\tau}_1$  be

$$\hat{\tau}_1 = M_h \dot{U} \left\{ \begin{bmatrix} \ddot{r}_{b,p}^d \\ \ddot{\phi}_{b,p}^d \end{bmatrix} - K_v \dot{e}_p - K_p e_p \right\} + M_h \dot{U} \begin{bmatrix} \dot{r}_{b,p} \\ \dot{\phi}_{b,p} \end{bmatrix} + J_h^T \left( x_o^d - K_I \int e_f \right) \quad (5.33)$$

and apply it to (5.32):

$$M_h \dot{U} \{ \ddot{e}_p + K_v \dot{e}_p + K_p e_p \} = -J_h^t (e_f + K_I \int e_f). \quad (5.34)$$

Multiply (5.34) by  $GJ_h^{-T}$ , we obtain the following equation.

$$GJ_h^{-T} M_h \dot{U} \{ \ddot{e}_p + K_v \dot{e}_p + K_p e_p \} = -G(e_f + K_I \int e_f) = 0 \quad (5.35)$$

where we have used the facts that  $\eta(G)$  is constant and the internal grasping forces lie in the null space of  $G$ , i.e.,

$$G(e_f + K_I \int e_f) = 0. \quad (5.36)$$

Since  $GJ_h^{-T} M_h = GJ_h^{-T} M(\theta) J_h^{-1} G^T + \begin{bmatrix} \hat{m} & 0 \\ 0 & \mathcal{I} \end{bmatrix}$  is positive definite and  $\dot{U}$  is nonsingular, (5.35) implies that

$$\ddot{e}_p + K_v \dot{e}_p + K_p e_p = 0. \quad (5.37)$$

Thus, the position trajectory tracking error,  $e_p$ , goes to zero with proper choice of the feedback gain matrices  $K_v$  and  $K_p$ .

We now substitute (5.37) into (5.34) and notice that  $J_h$  is nonsingular.

Thus

$$e_f + K_I \int e_f = 0. \quad (5.38)$$

This shows  $e_f$  goes to zero by choosing  $K_I$ . ■

Quite often in industrial applications several manipulators which usually have more than three degrees of freedom are integrated to maneuver a massive load ([Hsu88]), or to perform a sophisticated task. Under the frictional point contact model the system is redundant. It is therefore desirable to have a control law for such a system. We modify the control law of Theorem 5.1 to give a control law for robot hands with redundant degrees of freedom.

**Theorem 5.2** Consider a robot hand with redundant degrees of freedom, i.e.,  $m_i \geq n_i, i = 1, \dots, k$ . Let Assumption 5.2 hold. Then the control law given by (5.39) drives the object trajectory error and the internal grasp force error to zero.

$$\begin{aligned} \tau = & N(\theta, \dot{\theta}) + J_h^T G^+ \begin{bmatrix} w_{b,p} \times \hat{m} v_{b,p} \\ w_{b,p} \times \mathcal{I} w_{b,p} \end{bmatrix} - M J_h^+ \dot{J}_h \dot{\theta} \\ & + M J_h^+ (J_h M^{-1} J_h^T) M_h \dot{U} \begin{bmatrix} \dot{r}_{b,p} \\ \dot{\phi}_{b,p} \end{bmatrix} + M J_h^+ (J_h M^{-1} J_h^T) (x_o^d - K_I \int e_f) \\ & + M J_h^+ (J_h M^{-1} J_h^T) \hat{M}_h \left\{ \begin{bmatrix} \ddot{r}_{b,p}^d \\ \ddot{\phi}_{b,p}^d \end{bmatrix} - K_v \dot{e}_p - K_p e_p \right\}, \end{aligned} \quad (5.39)$$

where

$$\hat{M}_h = (J_h M^{-1} J_h^T)^{-1} G^T + G^+ \begin{bmatrix} \hat{m} & 0 \\ 0 & \mathcal{I} \end{bmatrix}. \quad (5.40)$$

and  $J_h^+ = J_h^T (J_h J_h^T)^{-1}$ .

**Remark 5.3** The term given by the right hand side of Eq. (5.40) differs from that given by Eq. (5.27).  $\square$

**Proof.** Eq. (5.16) now reads,

$$\ddot{\theta} = J_h^+ G^T \begin{bmatrix} \dot{v}_{b,p} \\ \dot{w}_{b,p} \end{bmatrix} + J_h^+ \dot{G}^T \begin{bmatrix} v_{g,p} \\ w_{b,p} \end{bmatrix} - J_h^+ \dot{J}_h \dot{\theta} + \ddot{\theta}_o, \quad (5.41)$$

where  $\ddot{\theta}_o \in \eta(J_h)$  is any vector of internal motion.

Substitute Eqs. (5.41), (5.20) into the dynamics equation (5.23) and linearize the resulting equation with the following control

$$\tau = N(\theta, \dot{\theta}) + J_h^T G^+ \begin{bmatrix} w_{b,p} \times m v_{b,p} \\ w_{b,p} \times \mathcal{I} w_{b,p} \end{bmatrix} - M J_h^+ \dot{J}_h \dot{\theta} + \tau_1,$$

we have

$$\left\{ M J_h^+ G^T + J_h^T G^+ \begin{bmatrix} m & 0 \\ 0 & \mathcal{I} \end{bmatrix} \right\} \begin{bmatrix} \dot{v}_{b,p} \\ \dot{w}_{b,p} \end{bmatrix} + M \ddot{\theta}_o = \tau_1 - J_h^T x_o.$$

Multiply the above equation by  $J_h M^{-1}$  and realize that  $J_h \ddot{\theta}_o = 0$ , we get

$$\left\{ G^T + J_h M^{-1} J_h^T G^+ \begin{bmatrix} m & 0 \\ 0 & \mathcal{I} \end{bmatrix} \right\} \begin{bmatrix} \dot{v}_{b,p} \\ \dot{w}_{b,p} \end{bmatrix} = J_h M^{-1} \tau_1 - J_h M^{-1} J_h^T x_o.$$

Finally, multiply the above equation by  $(J_h M^{-1} J_h^T)^{-1}$  and use the following control for  $\tau_1$

$$\tau_1 = M J_h^+ (J_h M^{-1} J_h^T) \left\{ M_h \hat{U} \left( \begin{bmatrix} \ddot{r}_{b,p}^d \\ \ddot{\phi}_{b,p}^d \end{bmatrix} - K_v \dot{e}_p - K_p e_p \right) + M_h \dot{U} \begin{bmatrix} \dot{r}_{b,p} \\ \dot{\phi}_{b,p} \end{bmatrix} + (x_o^d - K_I \int e_f) \right\}$$

we have

$$M_h \hat{U} \{ \ddot{e}_p + K_v \dot{e}_p + K_p e_p \} = -(e_f + K_I \int e_f). \quad (5.42)$$

Using the same reasoning for the proof of Theorem 5.1 we conclude from Eq. (5.42) that

$$\ddot{e}_p + K_v \dot{e}_p + K_p e_p = 0,$$

and

$$e_f + K_I \int e_f = 0.$$

This completes the proof. ■

### 5.3.2 Control Laws for Rolling Motion

Finally, we extend the basic formulation of Theorem 5.1 to give a control law for rolling motion. Similar works in this subject include ([CHS89] and [Ker85]).

For rolling motion, the grip Jacobian  $G$  and hence the null space of  $G$  is time varying. The contact coordinates that determine  $G$  evolve according the contact equations of Section 3.3. Let  $V(t) = \eta(G)$  be the null space of  $G$  indexed by time parameter  $t$ . In general  $e_f(t) = x_o(t) - x_o^d(t) \in V(t)$  does not imply  $\int_0^t e_f(\tau) d\tau \in V(t)$ , nor  $\dot{e}_f(t) \in V(t)$ . Thus, we can not introduce dynamic feedback in the force loop, as we have done in Theorem 5.1, to create linear force error equation. Instead we have,

$$G(t)e_f(t) = 0 \text{ implies that } G(t)\dot{e}_f(t) + \dot{G}(t)e_f(t) = 0. \quad (5.43)$$

**Lemma 5.1** *Consider the following differential equation*

$$\dot{x}(t) = A(t)x(t). \quad (5.44)$$

Let  $\mu(A(t)) = \lambda_{\max}(A^*(t) + A(t))/2$  be the matrix measure of  $A(t)$ , where  $\lambda_{\max}$  stands for the maximum eigenvalue value ([Vid78]). Then,

$$\|x(t)\| \leq \|x(t_0)\| \exp \int_{t_0}^t \mu(A(\tau)) d\tau.$$

In other words, if  $\mu(A(t)) < 0, \forall t$ , and  $A(t)$  is sufficiently slow time-varying, then, the system (5.44) is exponentially stable.

**Theorem 5.3** *Let Assumption 5.2 hold for a robot hand with non-redundant degrees of freedom. Then, the following control law, along with the contact equations, realizes both the desired position trajectory and the desired internal grasp force for rolling motion.*

$$\begin{aligned} \tau = & N(\theta, \dot{\theta}) + J_h^T G^+ \begin{bmatrix} w_{b,p} \times \hat{m} v_{b,p} \\ w_{b,p} \times \mathcal{I} w_{b,p} \end{bmatrix} - M(\theta) J_h^{-1} \dot{J}_h \dot{\theta} + M_h \dot{U} \begin{bmatrix} \dot{r}_{b,p} \\ \dot{\phi}_{b,p} \end{bmatrix} + \frac{M(\theta) J_h^{-1} \dot{G}^T \begin{bmatrix} v_{b,p} \\ w_{b,p} \end{bmatrix}}{} \\ & + J_h^T \left( x_o^d - \dot{e}_f / \delta - G^+ \dot{G} e_f / \delta \right) + M_h U \left\{ \begin{bmatrix} \ddot{r}_{b,p}^d \\ \ddot{\phi}_{b,p}^d \end{bmatrix} - K_v \dot{e}_p - K_p e_p \right\}, \end{aligned} \quad (5.45)$$

where

$$M_h = M(\theta) J_h^{-1} G^t + J_h^t G^+ \begin{bmatrix} \hat{m} & 0 \\ 0 & \mathcal{I} \end{bmatrix} \quad (5.46)$$

and  $\delta$  is a sufficiently large number so that the force error equation can be made exponentially stable.

**Proof.** The proof is very similar to that of Theorem 5.1 and we give an outline here. For rolling motion, (5.16) reads

$$\ddot{\theta} = J_h^{-1} G^t \begin{bmatrix} \dot{v}_{b,p} \\ \dot{w}_{b,p} \end{bmatrix} + J_h^{-1} \dot{G}^t \begin{bmatrix} v_{b,p} \\ w_{b,p} \end{bmatrix} - J_h^{-1} \dot{J}_h \dot{\theta}. \quad (5.47)$$

Substitute Eqs. (5.47) and (5.20) into the system dynamic equation (5.23) and linearize the resulting equation with the appropriate terms in the control inputs, we get

$$M_h \begin{bmatrix} \dot{v}_{b,p} \\ \dot{w}_{b,p} \end{bmatrix} = \tau_1 - J_h^T x_o. \quad (5.48)$$

Substituting (5.13) into the above equation and applying the rest of the control inputs yield

$$M_h \{ \ddot{e}_p + K_v \dot{e}_p + K_p e_p \} = -J_h^T \{ e_f + \dot{e}_f / \delta + G^+ \dot{G} e_f / \delta \}. \quad (5.49)$$

Multiply (5.49) by  $G J_h^{-T}$  and notice that because

$$G e_f = 0, \text{ and } (G \dot{e}_f + \dot{G} e_f) / \delta = 0.$$

we have

$$G(e_f + \dot{e}_f/\delta + G^+\dot{G}e_f/\delta) = 0$$

which implies that

$$\ddot{e}_p + K_v\dot{e}_p + K_p e_p = 0. \quad (5.50)$$

This shows that the position error goes to zero. On the other hand, substituting (5.46) into (5.49), and using the fact that  $J_h$  is full rank, we conclude that

$$(\delta I + G^+\dot{G})e_f + \dot{e}_f = 0. \quad (5.51)$$

Let  $A(t) = -(\delta I + G^+\dot{G})$ . It is easy to see that by choosing  $\delta$  sufficiently large,  $\mu(A(t))$  is negative for all  $t \in [t_0, t_f]$ . Consequently, by Lemma 5.1 force error  $e_f$  also goes to zero. ■

One can easily come up with a control law for rolling motion by robot hands with redundant degrees of freedom by combining Theorems 5.2 and 5.3.

### 5.3.3 Simulation

Consider the two-fingered planar manipulation system shown in Figure 5.4, where the fingers are identical. The contact is modeled as frictional point contact. Let the object width and the finger spacing be 2 units. The grip Jacobian and the hand Jacobian are

$$G = \begin{bmatrix} -1 & 0 & 1 & 0 \\ 0 & -1 & 0 & 1 \\ 0 & -1 & 0 & -1 \end{bmatrix}$$

and

$$J_h = \begin{bmatrix} J_1 & 0 \\ 0 & J_2 \end{bmatrix}$$

where

$$J_1 = \begin{bmatrix} \cos \alpha & -\sin \alpha \\ \sin \alpha & \cos \alpha \end{bmatrix} \begin{bmatrix} -\sin \theta_{11} - \sin(\theta_{11} + \theta_{12}) & -\sin(\theta_{11} + \theta_{12}) \\ \cos \theta_{11} + \cos(\theta_{11} + \theta_{12}) & \cos(\theta_{11} + \theta_{12}) \end{bmatrix}$$

and

$$J_2 = \begin{bmatrix} -\cos \alpha & \sin \alpha \\ -\sin \alpha & -\cos \alpha \end{bmatrix} \begin{bmatrix} -\sin \theta_{21} - \sin(\theta_{21} - \theta_{22}) & \sin(\theta_{21} - \theta_{22}) \\ \cos \theta_{21} + \cos(\theta_{21} - \theta_{22}) & -\cos(\theta_{22} + \theta_{22}) \end{bmatrix}.$$

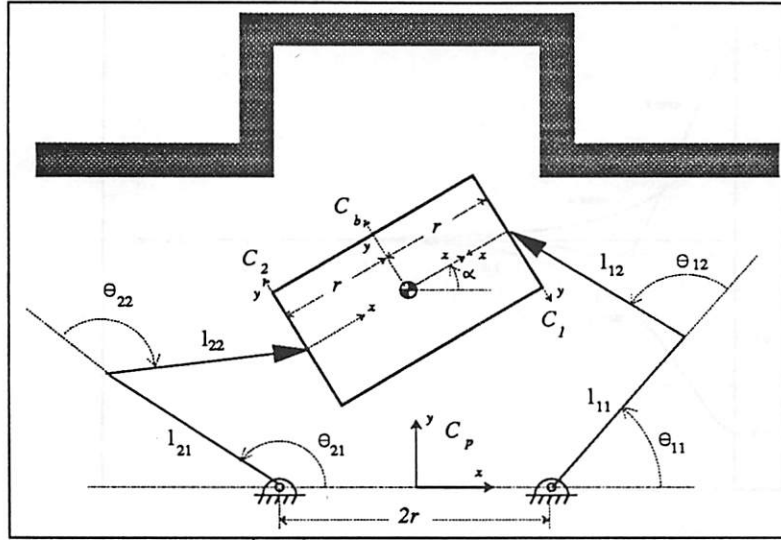


Figure 5.4: A two-fingered planar manipulation system.

The grasp will be stable and manipulable for the object along the following trajectory

$$x(t) = c_1 \sin(t), \quad y(t) = c_2 + c_1 \cos(t), \quad \alpha(t) = c_3 \sin(t).$$

The dynamics of finger  $i, i = 1, 2$ , used in the simulation is

$$M_i = \begin{bmatrix} m_1 h_1^2 + m_1 d_1^2 + m_2 l_1^2 & m_2 l_1 h_2 \cos(\theta_{i,2} - \theta_{i,1}) \\ m_2 l_1 h_2 \cos(\theta_{i,2} - \theta_{i,1}) & m_2 (h_2^2 + d_2^2) \end{bmatrix},$$

$$N_i = \begin{bmatrix} m_2 l_1 h_2 \dot{\theta}_{i,2}^2 \sin(\theta_{i,2} - \theta_{i,1}) + m_1 g l_1 \sin \theta_{i,1} \\ m_2 l_1 h_2 \dot{\theta}_{i,2}^2 \sin(\theta_{i,2} - \theta_{i,1}) + m_2 g h_2 \sin \theta_{i,2} \end{bmatrix}$$

where  $m_j$  = mass of link  $j$ ,  $d_j$  = radii of gyration of link  $j$ ,  $h_j$  = distance between joint  $j$  and the center-of-mass of link  $j$ .

The simulation used a program designed to integrate differential equations with algebraic constraints. Figure 5.4 shows that the initial position error diminishes exponentially as predicted by (5.37).

The simulation was fed to a movie package which shows the continuous motion. Figure 5.6 and Figure 5.7 are sequences of sampled pictures from a typical simulation. In both figures, the line segment at each contact shows the magnitude and the direction of the total force that is exerted to the object by the finger. The desired internal grasping forces are set to 0 and 10 units in Figure 5.6 and 5.7

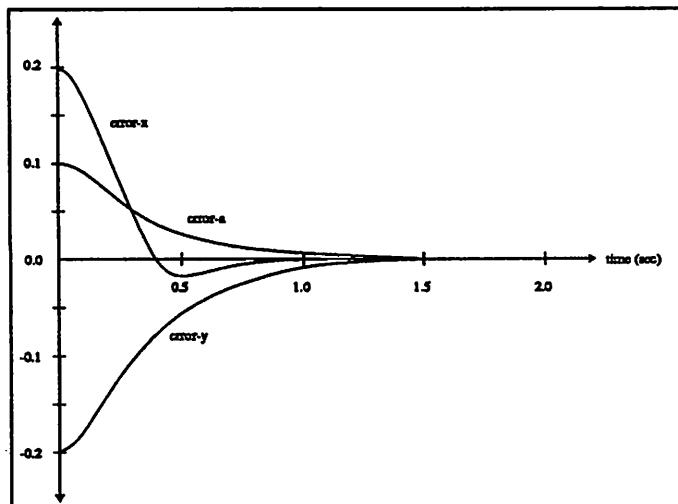


Figure 5.5: Position error from simulation.

respectively. Note that without the internal grasping force (Figure 5.6), the total exerted force may be away from the friction cone and consequently break the contact if this were a real experiment rather than a simulation.

The control laws for coordinated manipulation have been successfully implemented on a two-fingered robot hand system designed by R. Murray ([Mur89]). See [Mur89] for further details.

## 5.4 Conclusions

A general formulation for the control of a robot hand system is presented. This formulation provides control laws for coordinated manipulation with fixed points of contact and with rolling contacts. In each of the control laws, the position loop is decoupled from the internal grasping force loop using the kinematic structures of the system. Convergence proof of these schemes are given. The schemes have been simulated and experimentally verified independently by many others (see [CHS89], [Fie88] and [Mur89]).

The remaining problems are the intensive computations involved in these control schemes. It would be very attractive to investigate possible simplifications of these schemes and study the corresponding robustness issues.

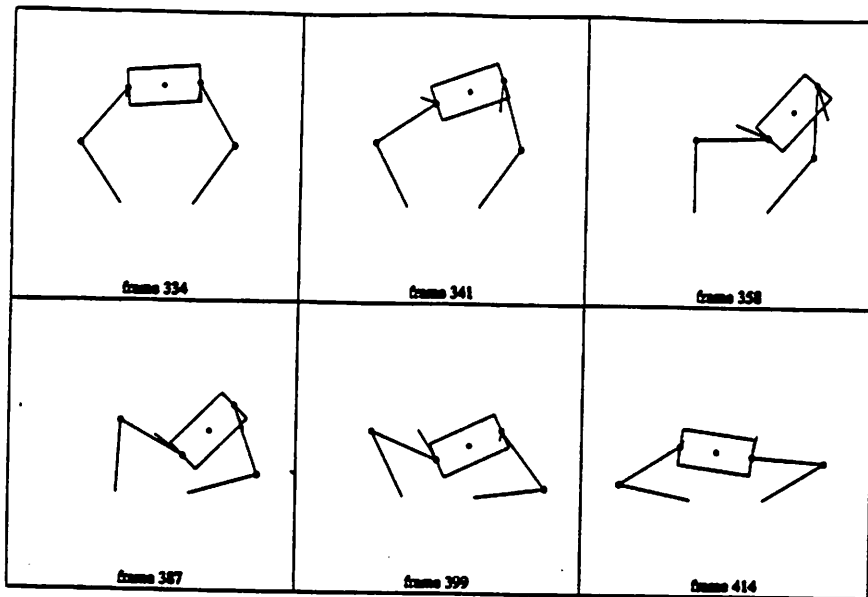


Figure 5.6: Simulation without internal grasping force.

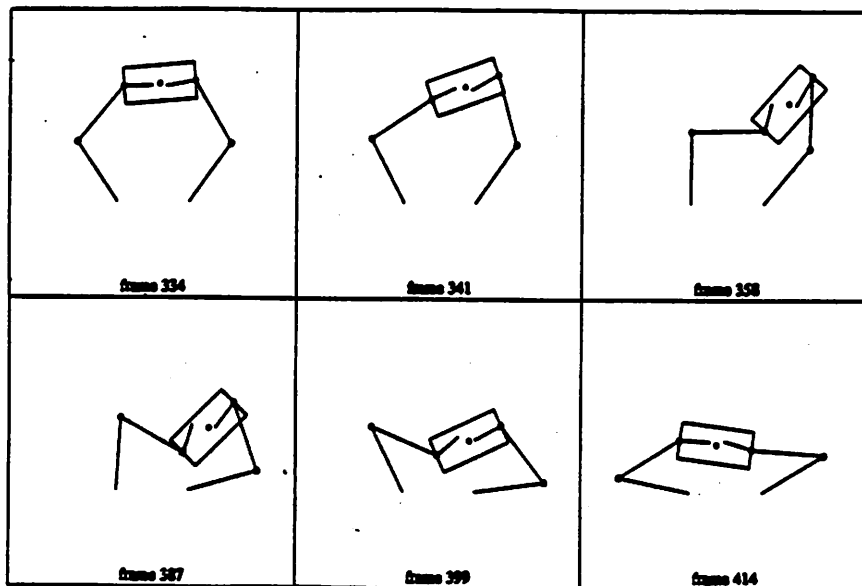


Figure 5.7: Simulation with 10 units of internal grasping force.

# Bibliography

- [AB84] C.O. Alford and S.M. Belyen. Coordinated control two robot arms. In *IEEE International Conference on Robotics and Automation*, pages 468–473, 1984.
- [Ari87] H. Arimoto. Cooperative motion control of multirobot arms or fingers. In *IEEE International Conference on Robotics and Automation*, pages 1407–1412, 1987.
- [Bej74] A.K. Bejczy. *Robot arm dynamics and control*. Technical Report, Jet Propulsion lab. Rep. JPL TM 33-669, 1974.
- [CCSS89] P. Chiacchio, S. Chiarelli, L. Sciaricco, and B. Siciliano. *Dynamic force/motion control of cooperative robot systems*. Technical Report, Preprint, University of Naples, Italy, 1989.
- [CHS89] A. Cole, J. Hauser, and S. Sastry. Kinematics and control of a multifingered robot hand with rolling contact. *IEEE Transaction on Automatic Control*, 34(4), 1989.
- [Cra86] J. Craig. *Introduction to Robotics, Mechanics and Control*. Addison-Wesley Publishing Company, 1986.
- [Fie88] A. J. Fields. *The Dynamics and Control of a Two-Fingered Robot Hand*. Master's thesis, Dept. of Electrical Engineering, Imperial College of Science and Technology, University of London, 1988.
- [Hsu88] P. Hsu. *Control of Mechanical Manipulators*. PhD thesis, EECS Dept, University of California at Berkeley, 1988.

- [Isi85] A. Isidori. *Nonlinear control systems: An introduction. Lecture notes in control and information sciences*, Springer-Verlag, 1985.
- [Ker85] J. Kerr. *An analysis of multifingered hand*. PhD thesis, Department of Mechanical Engineering, Stanford University, 1985.
- [Kha87] O. Khatib. The operational space formulation in robot manipulator control. *IEEE Journal of Robotics and Automation*, RA-3(1), 1987.
- [Mar73] B. R. Markiewicz. *Analysis of the computed torque drive method and comparison with conventional position al servo for a computer-controlled manipulator*. Technical Report, Jet Propulsion Lab. Rep. JPL TM 33-601, 1973.
- [MS85] M.T. Mason and J. K. Salisbury. *Robot Hands and the Mechanics of Manipulation*, chapter 1 - 10. MIT Press, 1985.
- [Mur89] R. Murray. *Control Experiments in Planar Manipulation and Grasping*. Technical Report, University of California at Berkeley, ERL Memo. No. UCB/ERL M89/3, 1989.
- [NNY87] Y. Nakamura, K. Nagai, and T. Yoshikawa. Mechanics of coordinative manipulation by multiple robotic mechanisms. In *IEEE International Conference on Robotics and Automation*, pages 991-998, 1987.
- [Pad86] B. Paden. *Kinematics and control of robot manipulators*. PhD thesis, Department of Electrical Engineering and Computer Science, University of California, Berkeley, 1986.
- [Pau72] R. C. Paul. *Modeling, trajectory calculation and servoing of a computer controlled arm*. Technical Report, Stanford AI Lab, Stanford University, 1972.
- [TBY86] T. Tarn, A. Bejczy, and X. Yuan. Control of two coordinated robots. In *IEEE International Conference on Robotics and Automation*, pages 1193-1202, 1986.
- [Vid78] M. Vidyasagar. *Nonlinear System Analysis*. Prentice-Hall, Inc., 1978.

- [ZL85] Y.F. Zheng and J.Y.S. Luh. Control of two coordinated robots in motion.  
In *24th Control and Decision Conference*, pages 1761–1766, 1985.

# Chapter 6

## Conclusions

### 6.1 Review

This thesis has been intended to provide a rigorous and general analysis of dextrous robot hands: from two-fingered gripper to multi-fingered multi-jointed hands.

The work covers three different areas: hand kinematics, planning and coordinated control.

The configuration space of a rigid body is identified with the Euclidean group. Differentiable structure in the Euclidean group allows us to define the velocity of a rigid body by left translation. The transformation relation for velocity and force under changes of coordinate frame are given by the adjoint map and the dual adjoint map, respectively, of  $SE(3)$ .

The forward kinematic map of a general  $n$  degrees-of-freedom manipulation is expressed as a product of exponentials, where the exponents are twists representing the joint axes. Each column of the manipulator Jacobian is the twist representing the corresponding joint axis relative to the end-effector frame. The exponential formula is applied to derive the recursive relations for velocity and acceleration of the links of a manipulator. Finally, the joint torques required for the Newton-Euler equations of motion are calculated using inward iterations. The Lagrangian equations of motion for a three-linked manipulator are calculated in closed-form.

The geometry of a surface in  $\mathbb{R}^3$  is reviewed. After coordinatizing the surface, the local properties such as metric tensor, curvature form and connection

form, are examined. The holonomy angle of a path in the surface is related to the path integral of the connection form and this notion is used in the path finding algorithm for changing the angle of contact.

Using the basic properties of a surface, the contact equations for motion of two rigid bodies are derived. The coordinates of contact involve as a function of the instantaneous contact velocity and the contact geometry. The contact equations for an unit disk moving in a plane are presented.

The kinematics of contact gives one of the three kinematic relations within a robot hand system. The other two are the grip Jacobian and the hand Jacobian, all of which can be constructed given the contact locations and the joint angles of the fingers. The hand Jacobian relates the joint velocity to the contact velocity at the fingertips and the transpose of the grip Jacobian relates the velocity of the object to the contact velocity. Thus, in order to maintain the grasp, the contact velocity determined by the hand Jacobian and the contact velocity determined by the transpose of the grip Jacobian have to equal. The net force exerted on the object in response to applied finger force is given by the grip Jacobian. The null space of the grip Jacobian represents the internal grasp force. On the other hand, the required joint torque in the presence of finger force is given by the transpose of the hand Jacobian. When rolling contacts are present, the parameters determining the hand Jacobian and the grip Jacobian involve according to contact equations. In order to impart fine motion to the grasped object, one has to solve two inverse problems.

Grasp planning is carefully examined. We argued that task requirement should be the primary considerations in the choice of a grasp. For this, a task is modeled using one ellipsoid in the twist space and another ellipsoid in the wrench space. Shapes of these ellipsoids reflect the task requirement. The task model is then used to define two grasp quality measures, one in wrench space and the other in the twist space. It is shown that up to a certain point the two quality measures have to be balanced, and this gives rise to the performance measure. The performance measure is used to formulate an optimization problem for grasp planning.

The problem of dextrous manipulation is formulated. This leaves many open problems in this area. To gain further insight of dextrous manipulation, we studied motion of two rigid bodies under rolling constraint. First, the configuration

space of contact was defined. Then, the differential equations governing rolling motion were derived. Chow's theorem is invoked to determine the existence of an admissible path between two contact configurations. Finally, some geometric techniques were used to find a path when one of the objects is connection free.

Finally, we studied coordinated controls for a robot hand system. Starting with a review of control strategies for a manipulator, we have developed two control laws, one for coordinated manipulation with fixed points of contact and another for rolling motion. Each of the control laws realizes the desired trajectory of the grasped object while simultaneously maintaining the contact constraint. Simulation results have shown consistency of the control laws.

## 6.2 Future Work

The analyses in this thesis have made only a minor dent in the overall work needed before dextrous robot hands can be used in a productive manner. While observation of the human hand reveals some of the capabilities of hands, it also points out the vast complexity required to realize these capabilities.

We list here a few open problems in hand research. Solving these problems will speed up our understanding of dextrous robot hands.

- Geometric/computer tools for object modeling. These tools can be used for grasp planning and motion planning for dextrous manipulation and the generation of robot hand kinematics and dynamics.
- Efficient algorithms that generate the kinematics and dynamics of a robot hand system in perhaps symbolical forms. The dynamics will be used for the determination of control laws and the kinematics will be used for task planning.
- Using the procedure outlined in Section 4.2 to develop an expert system for task modeling. The results should be stored in a database.
- Using the task model and the kinematics of a robot hand system to formulate the optimization problem for grasp planning. Then, develop efficient algorithms (see [Pol71] and [Hau86] and the references therein for some optimization techniques) to solve the problem.

- Motion planning for dextrous manipulation is perhaps one of the most complex and least understood problems in hand research. First, we need to solve the reachability problem for a nonlinear system of the form

$$\dot{x} = B(x)u \quad (6.1)$$

where  $x \in M$ , an  $m$ -dimensional manifold,  $u \in \mathbb{R}^n$ ,  $n \leq m$ , are the control inputs and  $B(x) \in \mathbb{R}^{m \times n}$  are the control vector fields. Recent works in nonlinear control theory (see [Bro81], [Mon88] and the references therein) and in motion planning (see [Can88], [KR88] and the references therein) can be possibly applied. Second, we need to further study finger relocation and understand how anholonomy is introduced through finger relocation. Third, develop techniques that can solve motion planning for both holonomic, nonholonomic and unidirectional constraints.

- Implementation of the control algorithms presented in this thesis on a general robot hand, and hopefully this will reveal some problems that can't be predicted through simulation.
- When a robot hand is used for space applications, e.g., repairing a satellite or grasping a free-flying object, finger motion can have significant effect on motion of the base where the hand is attached to, because of appropriate conservation laws. Understanding (relative) stability of the overall system due to motion of the fingers is another challenging problem. The reader is referred to [Mon88], [MR89] and [Sre87] for further details.

# Bibliography

- [Bro81] R. Brockett. *Control Theory and Singular Riemannian Geometry*, pages 11–27. *New Directions in Applied Mathematics*, Springer-Verlag New York Inc., 1981.
- [Can88] J.F. Canny. *The complexity of robot motion planning*. MIT Press, 1988.
- [Hau86] J. Hauser. *Proximity algorithms: implementation and applications*. Technical Report ERL Memo. No. UCB/ERL M86/53, Electronics Research Laboratory, University of California, Berkeley, 1986.
- [KR88] D. E. Koditschek and E. Rimon. Robot navigation functions on manifolds with boundary. *Advances in applied mathematics (to appear)*, 1988.
- [Mon88] R. Montgomery. *Shortest loops with a fixed holonomy*. Technical Report, Mathematical Science Research Institute, University of California, Berkeley, 1988.
- [MR89] J. Marsden and T. Ratiu. *Mechanics and Symmetry*. University of California at Berkeley, 1989.
- [Pol71] E. Polak. *Computational Methods in Optimization: A Unified Approach*. New York: Academic Press, 1971.
- [Sre87] N. Sreenath. *Modeling and Control of Multibody Systems*. PhD thesis, Dept. of Electrical Engineering, University of Maryland, 1987.